1.11 Short-Lived Radionuclides and Early Solar System Chronology

AM Davis, University of Chicago, Chicago, IL, USA
KD McKeegan, University of California, Los Angeles, CA, USA

1.11.1 Introduction

1.11.1.1 Chondritic Meteorites as Probes of Early Solar System Evolution

The evolutionary sequence involved in the formation of relatively low-mass stars, such as the Sun, has been delineated in recent years through impressive advances in astronomical observations at a variety of wavelengths, combined with improved numerical and theoretical models of the physical processes thought to occur during each stage. From the models and the observational statistics, it is possible to infer in a general way how the solar system ought to have evolved through the various stages from gravitational collapse of a fragment of a molecular cloud to the accretion of planetary-sized bodies (e.g., Adams, 2010; Alexander et al., 2001; André et al., 2000; Cameron, 1995; Shu et al., 1987; Williams and Cieza, 2011; see **Chapters 2.3**, **2.4**, and **2.8**). However, the details of these processes remain obscured, literally, from an astronomical perspective, and the

 http://dx.doi.org/10.1016/B978-0-08-095975-7.00113-3

dependence of such models on various parameters requires data to constrain the specific case of the solar system's origin.

Fortunately, the chondritic meteorites sample aspects of this evolution. The term 'chondrite' (or chondritic) was originally applied to meteorites bearing chondrules, which are approximately millimeter-sized solidified melt droplets consisting largely of mafic silicate minerals and glass commonly with included metal or sulfide. However, the meaning of chondritic has been expanded to encompass all extraterrestrial materials that are 'primitive,' that is, undifferentiated samples having nearly solar elemental composition. Thus, the chondrites represent a type of cosmic sediment, and to a first approximation can be thought of as 'hand samples' of the condensable portion of the solar nebula. The latter is a general term referring to the phase(s) of solar system evolution intermediate between molecular cloud collapse and rocky planet formation. During the nebular phase, the still-forming Sun was an embedded young stellar object (YSO) enshrouded by gas and dust, which was distributed first in an extended envelope that later evolved into an accretion disk that ultimately defined the ecliptic plane. The chondrites agglomerated within this accretion disk, most likely close to the position of the present asteroid belt from whence meteorites are currently derived. In addition to chondrules, an important component of some chondrites are inclusions containing refractory oxide and silicate minerals, so-called calcium, aluminum-rich inclusions (CAIs) that also formed as free-floating objects within the solar nebula (see **Chapter 1.3**). These constituents are bound together by a 'matrix' of chondrule fragments and fine-grained dust (which includes a tiny fraction of dust grains that predate the solar nebula; see **Chapter 1.4**). It is important to realize that, although these materials accreted together at a specific time in some planetesimal, the individual components of a given chondrite can, and probably do, sample different places and/or times during the nebular phase of solar system formation. Thus, each grain in one of these cosmic sedimentary rocks potentially has a story to tell regarding aspects of the early evolution of the solar system.

Time is a crucial parameter in constructing any story. Understanding of relative ages allows placing events in their proper sequence, and measures of the duration of events are critical to developing an understanding of process. If disparate observations can be related temporally, then structure (at any one time) and evolution of the solar system can be better modeled, or, if a rapid succession of events can be inferred, it can dictate a cause and effect relationship. This chapter is concerned with understanding the timing of different physical and chemical processes that occurred in the solar nebula and possibly on early accreted planetesimals that existed during the nebula stage. These events are 'remembered' by the components of chondrites and recorded in the chemical and, especially, isotopic compositions of the host mineral assemblages; the goal is to decide which events were witnessed by these ancient messengers and to decipher those memories recorded long ago.

1.11.1.2 Short-Lived Radioactivity at the Origin of the Solar System

The elements of the chondritic meteorites, and hence of the terrestrial planets, were formed in previous generations of stars. Their relative abundances represent the result of the general chemical evolution of the galaxy, possibly enhanced by recent local additions from one or more specific sources just prior to collapse of the solar nebula ~4.56 Ga ago. A volumetrically minor but nevertheless highly significant part of this chemical inventory is comprised of radioactive elements, from which this age estimate is derived. The familiar long-lived radionuclides, such as ^{238}U, ^{235}U, ^{232}Th, ^{187}Re, ^{176}Lu, ^{147}Sm, ^{87}Rb, and ^{40}K, provide the basis for geochronology and the study of large-scale differentiation among geochemical reservoirs over time (see **Chapter 1.12**). The long-lived radioactive isotopes of uranium, thorium, and potassium also provide a major heat source to drive chemical differentiation on a planetary scale (e.g., terrestrial plate tectonics).

A number of short-lived radionuclides also existed at the time that the Sun and the rocky bits of the solar system were forming (**Table 1**). These nuclides are sufficiently long-lived that they could exist in appreciable quantities in the earliest solar system rocks, but their mean lives are short enough that they are now completely decayed from their primordial abundances. In this sense, they are referred to as extinct nuclides. Although less familiar than the still-extant radionuclides, these short-lived isotopes potentially play similar roles: their relative abundances can, in principle, form the basis of various chronometers that constrain the timing of early chemical fractionations, and the more abundant radioisotopes can possibly provide sufficient heat to drive differentiation (i.e., melting) of early accreted planetesimals. The very rapid rate of decay of the short-lived isotopes, however, means that inferred isotopic differences translate into relatively short amounts of time, that is, these potential chronometers have inherently high precision (temporal resolution). The realization of these possibilities is predicated upon understanding the origin(s) and distributions of the now-extinct radioactivity. While this is a comparatively easy task for the long-lived, still existing radionuclides, it poses a significant challenge for studies of the early solar system. However, this represents the best chance at developing a quantitative high-resolution chronology for events in the solar nebula, and, moreover, the question of the origins of the short-lived radioactivity has profound implications for the mechanisms of formation of the solar system (as being, possibly, quite different from that for solar-mass stars in general).

1.11.1.3 A Brief History and the Scope of the Present Review

That short-lived radioactive isotopes existed in the early solar system has been known since the 1960s, when ^{129}Xe excesses were first shown to be correlated with the relative abundance of iodine, implicating the former presence of its parent nuclide, ^{129}I (Jeffery and Reynolds, 1961). Because the half-life of ^{129}I (~16 Ma) is not so short, its presence in the solar system can be understood as primarily a result of the ambient, quasi-steady-state abundance of this nuclide in the parental molecular cloud due to continuous *r*-process nucleosynthesis in the galaxy (Wasserburg, 1985). The situation changed dramatically in the mid-1970s when it was discovered that CAIs from the Allende meteorite exhibited apparent excesses of ^{26}Mg (Gray and Compston, 1974; Lee and Papanastassiou, 1974) and that the degree of excess ^{26}Mg correlated with Al/Mg in CAI mineral

Table 1 Short-lived radioactive nuclides once existing in solar system objects

Fractionation[a]	*Parent nuclide*	*Half-life*[b]	*Daughter nuclide*	*Estimated initial solar system abundance*	*Objects found in*	*References*
Neb	^{7}Be	53.1 d	^{7}Li	$(6.1 \pm 1.3) \times 10^{-3} \times {}^{9}$Be	CAIs	(1)
Neb	^{41}Ca	0.102 Ma	^{41}K	$4 \times 10^{-9} \times {}^{40}$Ca	CAIs	(2)
Plan	^{36}Cl	0.301 Ma	^{36}S, ^{36}Ar	$1.8 \times 10^{-5} \times {}^{35}$Cl	CAIs, chondrites	(3)
Neb	^{26}Al	0.717 Ma	^{26}Mg	$(5.23 \pm 0.13) \times 10^{-5} \times {}^{27}$Al	CAIs, chondrules, achondrite	(4)
Neb	^{10}Be	1.387 Ma[c]	^{10}B	$(8.8 \pm 0.6) \times 10^{-4} \times {}^{9}$Be	CAIs	(1)
Neb	^{135}Cs	2.3 Ma	^{135}Ba	$4.8 \times 10^{-4} \times {}^{133}$Cs	CAIs, chondrites	(5)
Neb,Plan	^{60}Fe	2.62 Ma	^{60}Ni	$(7.1 \pm 2.3) \times 10^{-9} \times {}^{56}$Fe	achondrites, chondrites	(6)
Neb, Plan	^{53}Mn	3.74 Ma	^{53}Cr	$(6.71 \pm 0.56) \times 10^{-6} \times {}^{55}$Mn	CAIs, chondrules, carbonates, achondrites	(7)
Plan	^{107}Pd	6.5 Ma	^{107}Ag	$(5.9 \pm 2.2) \times 10^{-5} \times {}^{108}$Pd	iron meteorites, pallasites	(8)
Plan	^{182}Hf	8.90 Ma	^{182}W	$(9.81 \pm 0.41) \times 10^{-5} \times {}^{180}$Hf	CAIs, planetary differentiates	(9)
Neb	^{247}Cm	15.6 Ma	^{235}U	$(1.1–2.4) \times 10^{-3} \times {}^{235}$U	CAIs	(10)
Plan	^{129}I	15.7 Ma	^{129}Xe	$10^{-4} \times {}^{127}$I	chondrules, secondary minerals	(11)
Plan	^{205}Pb	17.3 Ma	^{205}Tl	$10^{-3} \times {}^{204}$Pb	iron meteorites	(12)
Plan	^{92}Nb	34.7 Ma	^{92}Zr	$10^{-5} \times {}^{93}$Nb	chondrites, mesosiderites	(13)
Plan	^{146}Sm	68 Ma[d]	^{142}Nd	$(9.4 \pm 0.5) \times 10^{-3} \times {}^{144}$Sm	planetary differentiates	(14)
Plan	^{244}Pu	80.0 Ma	Fission products	$7 \times 10^{-3} \times {}^{238}$U	CAIs, chondrites	(15)

References: (1) Chaussidon et al. (2006); (2) Iso et al. (2006); Liu et al. (2012b); (3) Jacobsen et al. (2011); (4) Jacobsen et al. (2008); (5) Hidaka et al. (2001); (6) Tang and Dauphas (2012); (7) this work; (8) Schönbächler et al., 2008; (9) Burkhardt et al. (2012); (10) Brennecka et al. (2010); (11) Jeffery and Reynolds (1961); (12) Baker et al. (2010); (13) Schönbächler et al. (2002); (14) Lugmair et al. (1983), Boyet et al. (2010), Kinoshita et al. (2012); (15) Hudson et al. (1988).

[a]Environment in which most significant parent–daughter fractionation processes occur: Neb–nebular; Plan–planetary.

[b]Half-lives from National Nuclear Data Center, Brookhaven National Laboratory (http://www.nndc.bnl.gov), except as noted.

[c]Korschinek et al., 2010; Chmeleff et al., 2010.

[d]Kinoshita et al. (2012).

separates (Lee et al., 1976) in a manner indicative of the in situ decay of ^{26}Al ($t_{1/2} = 0.717$ Ma).

The high abundance inferred for this short-lived isotope ($\sim 5 \times 10^{-5} \times {}^{27}Al$) demanded that it had been produced within a few million years of CAI formation, possibly in a single stellar source, which 'contaminated' the nascent solar system with freshly synthesized nuclides (Wasserburg and Papanastassiou, 1982). Because of the close time constraints, an attractively parsimonious idea arose, whereby the very same dying star that threw out new radioactivity into the interstellar medium may also have served to initiate gravitational collapse of the molecular cloud fragment that would become the solar system, through the shock wave created by its expanding ejecta (Cameron and Truran, 1977). An alternative possibility that the new radioactive elements were produced 'locally' through nuclear reactions between energetic solar particles and the surrounding nebular material was also quickly recognized (Clayton et al., 1977; Heymann and Dziczkaniec, 1976; Lee, 1978; Lee et al., 1998). However, many of the early models were unable to produce sufficient amounts of ^{26}Al by irradiation within the constraints of locally available energy sources and the lack of correlated isotopic effects in other elements (see discussion in Wadhwa and Russell, 2000). Almost by default, 'external seeding' scenarios and the implied supernova trigger became the preferred class of models for explaining the presence of ^{26}Al and its distribution in chondritic materials. The details of this seeding continue to be debated; this subject will be dealt with later.

In the intervening decades since the discovery that the solar system contained ^{26}Al, many other short-lived isotopes have been found to have existed in early solar system materials (**Table 1**). Several of these have been discovered in recent years, and the record of the distribution of ^{26}Al and other nuclides in a variety of primitive and evolved materials has been documented with much greater clarity. Significant progress has been made since the last edition of this chapter was written. It now seems that both stellar and local productions are necessary to explain the full range of short-lived radionuclide abundances. In part due to improvements in mass spectrometry, new data are being generated at an increasing pace, and in some cases, interpretations that seemed solid only a short time ago are now being revised. For further details, the reader is directed to several excellent reviews (Dauphas and Chaussidon, 2011; Kita et al., 2005; Krot et al., 2009; Nyquist et al., 2009; Podosek and Nichols, 1997; Russell et al., 2006; Wadhwa et al., 2006a,b; Wasserburg, 1985).

Development of a quantitative understanding of the source, or sources, of now-extinct radionuclides is important for constraining the distribution of these radioactive species throughout the early solar system and, thus, is critical for chronology. For the major part of this review, the prevailing point of view has been adopted, namely, that external seeding for the short-lived isotopes most important for chronology dominates over possible local additions from nuclear reactions with energetic particles associated with the accreting Sun. This approach permits examination of timescales for self-consistency with respect to major chemical or physical 'events' in the evolution of the solar system; the issues of the scale of possible isotopic heterogeneity within the nebula and assessment of local irradiation effects will be explicitly addressed following an examination of the preserved record.

1.11.2 Dating with Ancient Radioactivity

In 'normal' radioactive dating, the chemical fractionation of a parent isotope from its radiogenic daughter results, after some decay of the parent, in a linear correlation of excesses of the daughter isotope with the relative abundance of the parent. For a cogenetic assemblage, individual minerals or components plot along a straight line on a diagram of daughter isotope excess versus parent/daughter ratio. This line is referred to as an isochron, and its slope permits the calculation of the time since the attainment of isotopic closure, that is, since all relative transport of parent or daughter isotopes effectively ceased. If the fractionation event is magmatic and the rock quickly cooled, then this time corresponds to an absolute crystallization age.

In a manner similar to dating by long-lived radioisotopes, the former presence of short-lived radioactivity in a sample is demonstrated by excesses of the radiogenic daughter isotope that correlate with the inferred concentration of the parent. However, because the parent isotope is extinct, a stable isotope of the respective parent element must serve as a surrogate with the same geochemical behavior (e.g., stable ^{27}Al serves as a surrogate for short-lived ^{26}Al). The correlation line yields the initial concentration of radioactive parent relative to its stable counterpart and may represent an isochron; however, its interpretation in terms of 'age' for one sample relative to another requires an additional assumption. The initial concentrations of a short-lived radionuclide among a suite of samples can correspond to relative ages only if the samples are all derived from a reservoir that at one time had a uniform concentration of the radionuclide. Under these conditions, differences in concentration correspond to differences in time only. As before, if the fractionation event corresponds to mineral formation and isotopic closure is rapidly achieved and maintained, then relative crystallization ages are obtained.

One further complication potentially arises that is unique to the now-extinct nuclides. In principle, excesses of a radiogenic daughter isotope could be 'inherited' from an interstellar (grain) component, in a manner similar to what is known to have occurred for some stable isotope anomalies in CAIs and, to a smaller extent, in bulk meteorites (e.g., Begemann, 1980; Burkhardt et al., 2011; Carlson et al., 2007; Dauphas et al., 2002; Fahey et al., 1987; Niederer et al., 1980; Niemeyer and Lugmair, 1981; Qin et al., 2011; Trinquier et al., 2009; Zhang et al., 2012). In such a case, the correlation of excess daughter isotope with radioactive parent would represent a mixing line rather than in situ decay from the time of last chemical fractionation. Such 'fossil' anomalies (in magnesium, from ^{26}Al decay; in calcium, from ^{44}Ti decay; in potassium, from ^{41}Ca decay, etc.) have, in fact, been documented in bona fide presolar grains (Zinner, 1998; see **Chapter 1.4**). These grains of SiC, graphite, corundum, hibonite, silicate, and Si_3N_4 crystallized in the outflows or explosion ejecta of evolved stars, incorporating very high abundances of newly synthesized radioactivities with $^{26}Al/^{27}Al$ sometimes approaching unity. However, because these grains did not form in the solar nebula from a uniform isotopic reservoir, there is no chronological constraint that can be derived. Probably, the radioactivity in such grains decayed during interstellar transit and hence arrived in the solar nebula as a 'fossil.'

Even before the discovery of presolar materials, Clayton championed a fossil origin for the magnesium isotope anomalies in CAIs in a series of papers (e.g., Clayton, 1982, 1986). A significant motivation for proposing a fossil origin was, in fact, to obviate chronological constraints derived from ^{26}Al–^{26}Mg systematics in CAIs that apparently required a late injection and fast collapse timescales along with a long (several Ma) duration of small dust grains in the nebula. Although some level of inheritance may be present and can possibly even be the dominant signal in a few rare samples or for specific isotopes (discussed in the succeeding text), for the vast majority of early solar system materials, it appears that most of the inventory of short-lived isotopes did indeed decay following mineral formation in the solar nebula. MacPherson et al. (1995) summarized the arguments against a fossil origin for the ^{26}Mg excesses in their comprehensive review of the ^{26}Al–^{26}Mg systematics in early solar system materials. In addition to the evidence regarding chemical partitioning during igneous processing of CAIs, must now be added the number of short-lived isotopes known (**Table 1**) and a general chronological consistency of the isotopic records in a wide variety of samples. The new observations buttress the previous conclusions of MacPherson et al. (1995), such that the overwhelming consensus of current opinion is that correlation lines indicative of the former presence of now-extinct isotopes are truly isochrons representing in situ radioactive decay. This is a necessary, but not sufficient, condition for developing a chronology based on these systems.

1.11.3 'Absolute' and 'Relative' Timescales

In order to tie high-resolution relative ages to an 'absolute' chronology, a correlation must be established between the short-lived and long-lived chronometers, that is, the ratio of the extinct nuclide to its stable partner isotope must be established at some known time (while it was still alive). This time could correspond to the 'origin of the solar system,' which, more precisely defined, means the crystallization age of the first rocks to have formed in the solar system, or it could refer to some subsequent well-defined fractionation event, for example, large-scale isotopic homogenization and fractionation occurring during planetary melting and differentiation. Both approaches for reconciling relative and absolute chronologies have been investigated in recent years, for example, utilizing the ^{26}Al–^{26}Mg and Pb–Pb systems in CAIs and chondrules for constraining the timing and duration of events in the nebula, and the ^{26}Al–^{26}Mg, ^{53}Mn–^{53}Cr, and Pb–Pb systems in differentiated meteorites to pin the timing of early planetary melting. The consistency of the deduced chronologies may be evaluated to give confidence (or not) that the assumptions necessary for a temporal interpretation of the record of short-lived radioactivity are, indeed, fulfilled.

1.11.3.1 An Absolute Timescale for Solar System Formation

The early evolution of the solar system is characterized by significant thermal processing of original presolar materials. This processing typically results in chemical fractionation that may potentially be dated by isotopic means in appropriate samples, for example, nebular events such as condensation or evaporation fractionate parent and daughter elements according to differing volatility. Likewise, chemical differentiation during melting and segregation leads to unequal rates of radiogenic ingrowth in different planetary reservoirs (e.g., crust, mantle, and core) that can constrain the nature and timing of early planetary differentiation. Several long-lived and now-extinct radioisotope systems have been utilized to delineate these various nebular and parent-body processes; however, it is only the U–Pb system that has sufficiently high precision to record the absolute ages of the earliest volatility-controlled fractionation events that correspond to the formation of the first refractory minerals, as well as the timing of melt generation on early planetesimals, and provide a quantitative link to the short-lived isotope systems.

The U–Pb system represents the premier geochronometer because it inherently contains two long-lived isotopic clocks that run at different rates: ^{238}U decays to ^{206}Pb with a half-life of 4468 Ma, and ^{235}U decays to ^{207}Pb with a much shorter half-life of 704 Ma. This unique circumstance provides a method for checking for isotopic disturbance (by either gain or loss of uranium or lead) that is revealed by discordance in the ages derived from the two independent isotopic clocks with the same geochemical behavior (Tera and Wasserburg, 1972; Wetherill, 1956). Such an approach is commonly used in evaluating the ages of magmatic or metamorphic events in terrestrial samples.

For obtaining the highest-precision ages of volatility-controlled fractionation events in the solar nebula, the U–Pb concordance approach is of limited utility, however, and instead one utilizes ^{207}Pb/^{206}Pb and ^{204}Pb/^{206}Pb variations in a suite of cogenetic samples to evaluate crystallization ages (the Pb–Pb method). The method has a significant analytical advantage since only isotope ratios need to be determined in the mass spectrometer, but equally important is the high probability that the age obtained represents a true crystallization age, because the system is relatively insensitive to recent gain or loss of lead (or, more generally, recent fractionation of U/Pb). This age is traditionally based on the isotopic evolution of uranium, a refractory element whose isotopic composition was thought to be invariant throughout the solar system (Chen and Wasserburg, 1980, 1981). The high precision for old materials comes from the rapid evolution radiogenic ^{207}Pb/^{206}Pb 4.5 Ga ago because of the relatively short half-life of ^{235}U. In principle, ancient lead loss or redistribution (e.g., due to early metamorphic or aqueous activity on asteroids, the parent bodies of meteorites) can confound the interpretation of lead isotopic ages as magmatic ages, but such closure effects are usually considered to be insignificant for the most primitive meteorite samples. Whether or not this is a valid assumption is an issue that is open to experimental assessment and interpretation (see discussions in Amelin, 2006; Amelin et al., 2009; Tera and Carlson, 1999; Tilton, 1988). The Pb–Pb method can have precisions of 0.1–1.0 Ma in favorable cases using the most advanced current techniques (Amelin, 2006; Connelly et al., 2012). There are uncertainties in the decay constants of the uranium isotopes that give an uncertainty of 9.3 Ma for early solar system ages. These uncertainties are not included when Pb–Pb ages are quoted. This is not a problem when comparing relative chronologies determined by Pb–Pb with those from short-lived chronometers, but needs to be considered when comparing absolute Pb–Pb ages with those determined from other long-lived chronometers (Amelin, 2006).

One further potential complication of the U–Pb system is the recent discovery that $^{235}U/^{238}U$ ratios can vary on Earth (Weyer et al., 2008) due to redox effects. It turns out that the variations in $^{235}U/^{238}U$ in CAIs are even larger than those in terrestrial rocks and point to the possible presence of extinct ^{247}Cm in the early solar system (Brennecka et al., 2010). This isotope decays to ^{235}U by three α- and two β-decays. Pb–Pb ages can be perturbed by up to 5 Ma for the observed range in $^{235}U/^{238}U$ in CAIs (**Figure 1(a)**). Fortunately for the purposes of early solar system chronology, fine-grained CAIs have the largest enhancements in $^{235}U/^{238}U$ (Brennecka et al., 2010), but are not often used for Pb–Pb chronology. Measurement of the $^{235}U/^{238}U$ is now a requirement for accurate Pb–Pb dating of early solar system materials. There is, however, a difficulty in that uranium is a very low-abundance element and many CAIs that would otherwise be suitable for Pb–Pb dating do not contain enough uranium for an accurate measurement of $^{235}U/^{238}U$. Brennecka et al. (2010) have shown that there is a correlation between $^{235}U/^{238}U$ and Nd/U and Th/U, so that one of the latter ratios can potentially be used as a proxy for $^{247}Cm/^{238}U$. Both proxies show some scatter in their correlations with $^{235}U/^{238}U$, so a direct measurement is highly desirable. Another issue is that until 2010, most workers used the average present-day solar system $^{238}U/^{235}U$ ratio of 137.88. However, recent measurements of terrestrial uranium standards are somewhat variable but generally lower than the old value of 137.88 (Condon et al., 2010; Richter et al., 2010); new measurements of angrite meteorites, which should have relatively unfractionated uranium isotope ratios, give a ratio of 137.78 (Brennecka and Wadhwa, 2012). This shift corresponds to a shift of 1 Ma in Pb–Pb ages, and even if constant uranium isotopic composition was assumed, one must note which standard was used when a Pb–Pb age is reported.

Absolute crystallization ages have been calculated for refractory samples, CAIs that formed with very high depletions

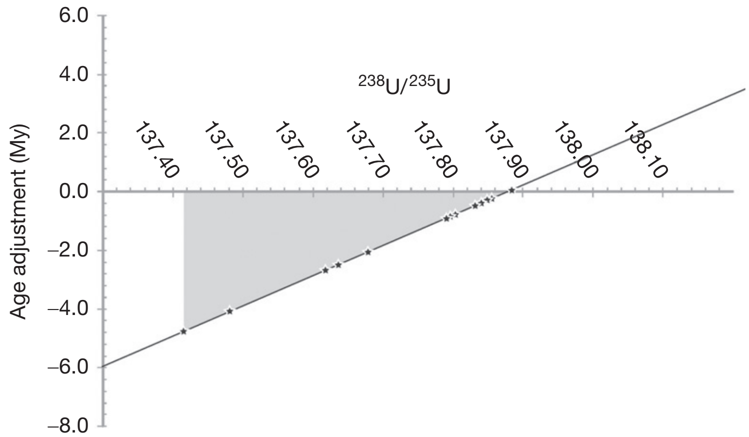

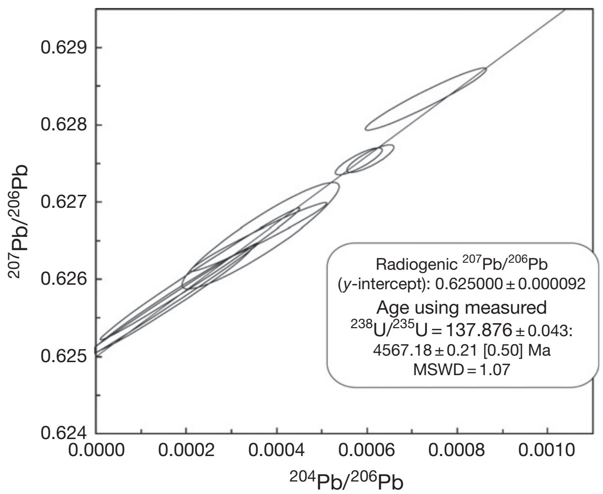

Figure 1 (a) The effect of $^{238}U/^{235}U$ isotope ratio on Pb–Pb isochron ages. The gray-shaded area shows the range observed in CAIs. Reproduced from Brennecka GA, Weyer S, Wadhwa M, Janney PE, Zipfel J, and Anbar AD (2010) $^{238}U/^{235}U$ variations in meteorites: Extant ^{247}Cm and implications for Pb–Pb dating. *Science* 327: 449–451. Reprinted with permission from AAAS. (b) Pb–Pb isochron for acid-washed fractions of CAI SJ101 from the Allende CV3 chondrite. This is the only CAI for which both a Pb–Pb isochron and the uranium isotopic composition have been measured. Reproduced from Amelin Y, Kaltenbach A, Iizuka T, et al. (2010) U–Pb chronology of the solar system's oldest solids with variable $^{238}U/^{235}U$. *Earth and Planetary Science Letters* 300: 343–350.

of volatile lead, by modeling the evolution of $^{207}Pb/^{206}Pb$ from primordial common (i.e., unradiogenic) lead found in early-formed sulfides from iron meteorites. Such 'model ages' can be determined with good precision (typically a few Ma), but accuracy depends on the correctness of the assumption of the isotopic composition of initial lead. Sensitivity to this correction is relatively small for highly radiogenic samples, such as CAIs, where almost all the lead is due to in situ decay, nevertheless, depending on the details of data reduction and sample selection, even the best early estimates of Pb–Pb model ages for CAI formation ranged over $\sim$15 Ma, from 4553 to 4568 Ma, with typical uncertainties in the range of 4–5 Ma (see discussions in Tera and Carlson, 1999; Tilton, 1988). By progressively leaching samples to remove contaminating lead (probably introduced from the meteorite matrix), Allègre et al. (1995) were able to produce highly radiogenic ($^{206}Pb/^{204}Pb > 150$) fractions from four CAIs from the Allende CV3 chondrite, which yielded Pb–Pb model ages of 4566 ± 2 Ma. Accuracy problems associated with initial lead corrections can also be addressed by an isochron approach where no particular composition of common lead need be assumed, only that a suite of samples are cogenetic and incorporated varying amounts of the same initial lead on crystallization (Tera and Carlson, 1999). Utilizing this approach, Tera and Carlson (1999) reinterpreted previous lead isotopic data obtained on nine Allende coarse-grained CAIs that had indicated a spread of ages (Chen and Wasserburg, 1981) to instead fit a single lead isochron of age equal to 4566 ± 8 Ma which, however, is evolved from an initial lead isotopic composition that is unique to CAIs. Amelin et al. (2002) used the isochron method to determine absolute ages of formation of two CAIs from the Efremovka CV3 carbonaceous chondrite. Both samples are consistent with a mean age of 4567.2 ± 0.6 Ma. Connelly et al. (2008a) investigated Pb–Pb ages of CAIs from the CV3 chondrite Allende, finding that leached residues of two CAIs, composed mainly of melilite and pyroxene, could be fit by a single isochron passing through primordial lead with an age corresponding to 4567.7 ± 0.9 Ma. Amelin et al. (2006) reported further isotopic analyses on one of the two Efremovka CAIs, E60, refining the age to 4567.11 ± 0.16 Ma, which is the most precise absolute age obtained on a CAI prior to the discovery of $^{235}U/^{238}U$ variations. The Pb–Pb data available since this discovery are limited. Amelin et al. (2010) measured lead and uranium isotopes in the unusual forsterite-bearing Allende CAI SJ101 (Petaev and Jacobsen, 2009) and obtained an age of 4567.18 ± 0.50 Ma. Connelly et al. (2012) reported lead and uranium isotope data of three Efremovka CAIs that give ages in agreement with SJ101, 4567.35 ± 0.28, 4567.23 ± 0.29, and 4567.38 ± 0.31 Ma. Bouvier and Wadhwa (2010) measured lead isotopes and inferred the uranium isotope ratio using the Th/U proxy in a type B CAI from the North African meteorite NWA 2364 and obtained an age of $4568.2^{+0.2}_{-0.4}$, 0.9 Ma older than the weighted mean age SJ101 and the three Efremovka CAIs.

As all SJ101 and the three Efremovka CAIs are the only ones with measured uranium and lead isotopic compositions and they give the same age within error, the weighted average of these ages given by Connelly et al. (2012), 4567.30 ± 0.16 Ma is adopted here as the best estimate for the absolute formation age for coarse-grained (igneous) CAIs from CV chondrites. There remains a concern that ^{26}Al–^{26}Mg systematics suggest that melting of these kinds of CAIs extended over as much as 0.6 Ma (MacPherson et al., 2012), that ^{26}Al–^{26}Mg studies have not been reported for SJ101 or the three Efremovka CAIs, and that secondary processing has the potential to shift ages to younger values. To the extent that the high precision, high accuracy results of Amelin et al. (2010) and Connelly et al. (2012) represent the absolute age of crystallization of CAIs generally, they provide a measure of the age of formation of the solar system, since several lines of evidence, in addition to the absolute Pb–Pb ages, indicate that CAIs are the first solid materials to have formed in the solar nebula (for a review, see Podosek and Swindle, 1988). In fact, it is the relative abundances of the short-lived radionuclides, especially ^{26}Al, which provides the primary indication that CAIs are indeed these first local materials. Other evidence is more circumstantial, for example, the prevalence of large stable isotope anomalies in CAIs compared to other material of solar system origin (see **Chapter 1.3**). The issue of antiquity of CAIs will be considered further when the distribution of short-lived isotopes among different CAI types is examined.

Other volatility-controlled long-lived parent–daughter isotope systems (e.g., Rb–Sr) yield absolute ages that are compatible with the coupled U–Pb systems, albeit with poorer precision. Because the chondrites are unequilibrated assemblages of components that may not share a common history, whole-rock or even mineral separate 'ages' are not meaningful for providing a very useful constraint on accretion timescales. High-precision age determinations, approaching 1 Ma resolution, can, in principle, be obtained from initial $^{87}Sr/^{86}Sr$ in low Rb/Sr phases, such as CAIs (e.g., Podosek et al., 1991). However, such ages depend on deriving an accurate model of the strontium isotopic evolution of the reservoir from which these materials formed. The latter is a very difficult requirement because it is not likely that a strictly chondritic Rb/Sr ratio was always maintained in the nebular regions from which the precursor materials that ultimately formed CAIs, chondrules, and other meteoritic components condensed. Thus, initial strontium 'ages,' while highly precise, may be of little use in terms of quantitatively constraining absolute ages of formation of individual nebular objects and are best interpreted as only providing a qualitative measure of antiquity (Podosek et al., 1991). It is possible that initial $^{87}Sr/^{86}Sr$ ratios of similar nebular components, for example, type B CAIs, could provide relative formation ages under the assumption that such objects share a common long-term Rb/Sr heritage; however, this has not yet been demonstrated. Finally, recent indications of strontium isotopic heterogeneity within solar system materials casts further uncertainty on the utility of initial $^{87}Sr/^{86}Sr$ as a chronometer (Moynier et al., 2012).

1.11.3.2 An Absolute Timescale for Chondrule Formation

Although chondrule formation is thought to be one of the most significant thermal processes to have occurred in the solar nebula, in the sense of affecting the majority of planetary materials in the inner solar system (see **Chapter 1.2**), the mechanism(s) responsible remains hotly debated after many years of investigation. Similarly, it has long been recognized that obtaining good measurements of chondrule ages would be extremely useful for possibly constraining formation mechanisms and environments, as well as setting important limits on the duration of the solar nebula and, thus, on accretion timescales. However, determination of crystallization ages of chondrules is very difficult because their mineralogy is typically not amenable to large parent–daughter fractionation. Several short-lived isotope systems (discussed in the succeeding text) have been explored in recent years in order to try to delimit relative formation times for chondrules, for example, compared to CAIs, but high-precision absolute Pb–Pb data are very limited. Amelin et al. (2002) used aggressive acid washing of a suite of chondrules from the unequilibrated CR chondrite Acfer 059 to remove unradiogenic lead (from both meteorite matrix and terrestrial contamination). Isochron ages ranged from 4563 to nearly 4565 Ma, with a preferred value of 4564.7 ± 0.6 Ma for six of the most radiogenic samples (^{206}Pb/^{204}Pb > 395). Amelin and Krot (2007) reported a Pb–Pb age of 4566.6 ± 1.0 Ma for internal residue-leachate isochrons for eight Allende chondrules, which overlaps within error the Pb–Pb ages of Allende and Efremovka CAIs (see preceding text). Connelly and Bizzarro (2009) reported Pb–Pb age of 4565.3 ± 0.8 Ma from selected leaching steps from an aggregate of chondrules from Allende. Connelly et al. (2012) measured uranium isotopes in three chondrules from the Allende CV3 chondrite and found that they had the same values as bulk meteorites. They used this uranium isotope ratio and Pb–Pb data on five individual chondrules to obtain ages ranging from 4564.71 ± 0.30 to 4567.32 ± 0.42 Ma. Taken together, the available Pb–Pb data suggest that chondrules are ∼0–3 Ma younger than CAIs from the same meteorite group (CV3 chondrites). Krot et al. (2005) reported Pb–Pb ages for chondrules from the CB_a chondrite Gujba (4562.7 ± 0.5 Ma) and CB_b chondrite Hammadah al Hamra 257 (4562.8 ± 0.9 Ma). These ages are ∼5 Ma younger than CAIs. Krot et al. (2005) argued that this time difference was too great for nebular processes and suggested that CB chondrite chondrules were formed in a giant impact between planetary embryos.

1.11.3.3 An Absolute Timescale for Early Differentiation of Planetesimals

Time markers for tying short-lived chronometers to an absolute timescale can potentially be provided by early planetary differentiated samples. The basic requirements are that appropriately ancient samples would have to have evolved from a reservoir (magma) that had achieved isotopic equilibrium with respect to daughter elements of both long-lived (Pb–Pb) and short-lived systems (^{182}Hf–^{182}W, ^{53}Mn–^{53}Cr, or ^{26}Al–^{26}Mg), then cooled rapidly following crystallization and remained isotopically closed until analysis in the laboratory. In practice, the latter requirement means that samples should be undisturbed by shock and free of terrestrial contamination. No sample is perfect in all these respects, but the angrites are considered to be nearly ideal (the major problem being terrestrial lead contamination). By careful cleaning, Lugmair and Galer (1992) determined high-precision Pb–Pb model ages for the plutonic angrites Lewis Cliff 86010 (LEW) and Angra dos Reis (AdoR). The results are concordant in U/Pb and with other isotopic systems as well as with each other and provide an absolute crystallization age of 4557.8 ± 0.5 Ma for these angrites (Lugmair and Galer, 1992). This is a significant time marker ('event') because angrite mineralogy also provides large Mn/Cr fractionation that is useful for accurate ^{53}Mn/^{55}Mn determination. Baker et al. (2005) reported a highly precise and ancient Pb–Pb age for the quenched volcanic angrite Sahara 99555 of 4566.2 ± 0.1 Ma, indicating crystallization of basalt on the surface of the angrite parent body only 1 Ma after formation of CAIs. However, further work on Sahara 99555 showed some disturbance of the U–Pb system and careful leaching experiments led to revised ages of 4564.86 ± 0.38 Ma (Amelin, 2008b) and 4564.58 ± 0.14 Ma (Connelly et al., 2008b). Another quenched volcanic angrite, D'Orbigny, has proven to be a more robust time marker, with evidence for ^{26}Al decay (Spivak-Birndorf et al., 2009) and well-behaved Pb–Pb systematics. Amelin (2008a) reported high-precision Pb–Pb ages for AdoR (4557.65 ± 0.13 Ma), LEW (4558.55 ± 0.15 Ma), and D'Orbigny (4564.42 ± 0.12 Ma). One other differentiated meteorite that has proven useful for tying together short- and long-lived chronometers is the unique basaltic achondrite NWA2976, which has a Pb–Pb age of 4562.89 ± 0.59 Ma (Bouvier et al., 2011). Brennecka and Wadhwa (2012) measured uranium isotope ratios in several angrites. They found that all angrites have the same uranium isotope ratio, but the ^{238}U/^{235}U ratio is slightly lower than the value previously assumed. The corrected ages for D'Orbigny and AdoR are 4563.37 ± 0.25 and 4556.60 ± 0.26 Ma, respectively. There is a significant spread in ages among angrites with D'Orbigny being significantly older than other angrites, thus assuming particular importance as an anchor for short-lived radionuclide chronometers.

The eucrites are highly differentiated (basaltic) achondrites that, along with the related howardites and diogenites, may have originated from the asteroid 4 Vesta (Binzel and Xu, 1993; see **Chapter 1.6**). Unfortunately, the U/Pb systematics of eucrites appear to be disturbed, yielding Pb–Pb ages up to ∼220 Ma younger than angrites (Galer and Lugmair, 1996). This compromises the utility of the eucrites as providing independent tie points between long- and short-lived chronometers.

Evidence for an extended thermal history of equilibrated ordinary chondrites is provided by U–Pb analyses of phosphates (Göpel et al., 1994). The phosphates merrillite and apatite are metamorphic minerals produced by the oxidation of phosphorus originally present in metal grains. Phosphate mineral separates obtained from chondrites of metamorphic grade 4 and greater have Pb–Pb model ages (Göpel et al., 1994) from 4563 Ma (for Ste. Marguerite, an H4) to 4502 Ma (for Guareña, an H6). The oldest ages are nearly equivalent to Pb–Pb ages from CR chondrules (Amelin et al., 2002) and only a few million years younger than CAIs, indicating that accretion and thermal processing was rapid for the H4 chondrite parent body. The relatively long time interval of ∼60 Ma has implications for the nature of the H chondrite parent body and the heat sources responsible for long-lived metamorphism (Göpel et al., 1994).

1.11.4 The Record of Short-Lived Radionuclides in Early Solar System Materials

Here, the evidence for the prior existence of now-extinct isotopes in meteoritic materials is discussed and, in the better-studied cases, the distribution of some isotopes in the early solar system are explored. **Table 1** summarizes the basic facts regarding those short-lived radioisotopes that are inferred to have existed as live radioactivity in rocks formed in the early solar system and provides an estimate of their initial abundances compared to a reference isotope. The table is organized in order of increasing half-life and according to the main environment for parent–daughter chemical fractionation. The latter property indicates what types of events can potentially be dated and largely dictates what types of samples record evidence that a certain radioisotope once existed. Note that there is only a small degree of overlap demonstrated thus far for a few of the isotope systems. For example, it is well documented that the ^{53}Mn–^{53}Cr and ^{182}Hf–^{182}W systems are sensitive to fractionation in both nebular and parent-body environments, and, as can be seen in the succeeding text, new high-precision magnesium isotopic measurements are making possible application of the ^{26}Al–^{26}Mg system to parent-body processes, but other systems that might similarly provide linkages from the nebula through accretion to early differentiation have not been fully developed as chronometers due to low parent abundances (e.g., ^{60}Fe–^{60}Ni) and/or difficulties in constraining mineral hosts and closure effects (e.g., ^{129}I–^{129}Xe and ^{244}Pu). The initial abundances refer to the origin of the solar system, which, as discussed previously, means the time of CAI formation, and hence, these can only be measured directly in nebular samples. The initial abundances of those isotopes that are found only in differentiated meteorites also refer back to the time of CAI formation, but such a calculation necessarily requires a chronological framework and is underpinned by the absolute time markers provided by the Pb–Pb system.

In order of increasing half-life, short-lived radionuclides will be described whose presence has been searched for and, in most cases, confirmed in the early solar system.

1.11.4.1 Beryllium-7

Beryllium-7 decays by electron capture to ^{7}Li with a half-life of 53.3 days. Chaussidon et al. (2006a) found variations of about 25% in ^{7}Li/^{6}Li ratios within an Allende CAI and suggested that they may be due to in situ decay of ^{7}Be. Boron isotopes were also measured in this CAI and show a well-defined ^{10}Be–^{10}B isochron with a slope corresponding to an initial ^{10}Be/^{9}Be ratio of $(8.8 \pm 0.6) \times 10^{-4}$ (see **Section 1.11.4.5**). There are significant difficulties associated with lithium isotopic measurements in CAIs, in that lithium can be introduced by secondary alteration processes long after decay of short-lived ^{7}Be. Chaussidon et al. (2006a) rejected analyses that did not plot along trajectories expected for closed system crystal fractionation on a Be versus Li concentration plot. There are further difficulties caused by the fact that lithium diffuses very rapidly and can mass fractionate during diffusion (Richter et al., 2003). Corrections also had to be made for spallation production of lithium isotopes by galactic cosmic rays. After correction for these effects and rejection of 'contaminated' analyses, Chaussidon et al. (2006a) concluded that ^{7}Be was possibly present and calculated an initial ^{7}Be/^{9}Be ratio of 0.0061 ± 0.0013 for Allende CAI 3529-41. The possible presence of ^{7}Be in CAIs remains controversial: after the Chaussidon et al. (2006a) paper was published, there was a comment by Desch and Ouellette (2006) and a reply by Chaussidon et al. (2006b). If ^{7}Be was present, it has profound importance for short-lived radionuclide production within the early solar system. The half-life is so short that it cannot have been produced elsewhere.

1.11.4.2 Calcium-41

Calcium-41 decays by electron capture to ^{41}K with a half-life of only 0.102 Ma. It has the distinction of being the shortest-lived isotope for which evidence exists in multiple early solar system refractory materials, and this fact makes it key for constraining the timescale of last nucleosynthetic addition to solar system matter (in the external seeding scenario). It also makes ^{41}Ca exceedingly difficult to detect experimentally, because it can only be found to have existed in the oldest materials and then in only very small concentrations. Fortunately, its daughter potassium is rather volatile and calcium is concentrated in refractory minerals (the 'C' in CAI) leading to large fractionations. Hutcheon et al. (1984) were the first to find hints for ^{41}Ca in Allende refractory inclusions, but they could not clearly resolve ^{41}K excesses above measurement uncertainties.

The first evidence of live ^{41}Ca came with the demonstration of excesses of ^{41}K/^{39}K correlated with Ca/K in Efremovka CAIs by Srinivasan et al. (1994, 1996). The ^{41}Ca–^{41}K systematics in the discovery CAI, Efremovka E44, was confirmed later by Liu et al. (2008). Subsequent measurements have established that ^{41}Ca was also present in some hibonite grains from CM and CV chondrites (Sahijpal et al., 1998, 2000). The CM hibonite grains are generally too small to permit enough multiple measurements to define an isochron on individual objects, even by ion probe; however, hibonite crystals from Allende CAIs show good correlation lines (Sahijpal et al., 2000) consistent with that found for Efremovka and indicating that ^{41}Ca decayed in situ. Most of the isolated CM hibonite grains also show ^{41}K/^{39}K excesses that are consistent with the isochrons obtained on silicate minerals of CAIs, except $\sim 1/3$ of the hibonite grains appear to have crystallized with 'dead' calcium (i.e., they have normal ^{41}K/^{39}K compositions). The ensemble isochron for hibonite yields an initial value of $^{41}\text{Ca}/^{40}\text{Ca} = 1.4 \times 10^{-8}$ with a formal error of $\sim 10\%$ relative and a statistical scatter that is commensurate with the measurement uncertainties. Such a small uncertainty would correspond to a very tight timescale (~ 15 ka) for the duration of formation of these objects; however, possible systematic uncertainties in the mass spectrometry may increase this interval somewhat. The hibonite grains that contain no excess ^{41}K/^{39}K are unlikely to have lost that signal and, thus, must either have formed after the other samples, or else they never incorporated live ^{41}Ca during their crystallization. An important clue is that these same grains also never contained ^{26}Al (Liu et al., 2008; Sahijpal and Goswami, 1998; Sahijpal et al., 1998, 2000).

Some recent progress suggests a lower ^{41}Ca/^{40}Ca ratio. Ito et al. (2006) determined a ^{41}Ca–^{41}K isochron for the Allende CAI EGG3, which yielded $^{41}\text{Ca}/^{40}\text{Ca} = (4.1 \pm 2.0) \times 10^{-9}$, less than half the value of Sahijpal et al. (2000). This CAI has a canonical ^{26}Al/^{27}Al ratio of $(5.29 \pm 0.39) \times 10^{-5}$ (Wasserburg et al., 2011), so there is no need for a decay correction. Liu et al. (2012b) have remeasured two of the original Efremovka CAIs for which ^{41}Ca–^{41}K studies were done in the 1990s. Correcting their inferred ^{41}Ca/^{40}Ca values back in time to the canonical

$^{26}Al/^{27}Al$ ratio, they suggested that the early solar system $^{41}Ca/^{40}Ca$ was $\sim 4.2 \times 10^{-9}$, in good agreement with Ito et al. (2006). A value of 4×10^{-9} has been adopted, as only one significant figure seems justified at this time.

1.11.4.3 Chlorine-36

Chlorine-36 has a half-life of 0.30 Ma and decays by β^--decay (98.1%) to ^{36}Ar and by electron capture and positron emission (1.9%) to ^{36}S. Murty et al. (1997) reported ^{36}Ar in the matrix of the Efremovka CV chondrite in excess of the amount expected from trapped and cosmogenic components and attributed it to in situ decay of ^{36}Cl. They inferred an initial $^{36}Cl/^{35}Cl$ ratio of $(1.4 \pm 0.2) \times 10^{-6}$. Lin et al. (2005) used an ion microprobe to measure sulfur isotopes in sodalite, a chlorine-bearing mineral commonly found as a secondary alteration product in CAIs and matrix in CV chondrites. They found well-defined isochrons in four sodalite-rich regions in a CAI from the Ningqiang CV chondrite, leading to inferred initial $^{36}Cl/^{35}Cl$ ratios of $(5–11) \times 10^{-6}$. From the fact that these areas had $^{26}Al/^{27}Al$ of $<5 \times 10^{-6}$, they inferred an initial solar system $^{36}Cl/^{35}Cl$ ratio of $\geq 1.6 \times 10^{-4}$. Hsu et al. (2006) reported a combined $^{36}Cl–^{36}S$ and $^{26}Al–^{26}Mg$ study of an altered Allende CAI named the Pink Angel. From the inferred $^{36}Cl/^{35}Cl$ ratio and the upper limit on $^{26}Al/^{27}Al$, they calculated an early solar system $^{36}Cl/^{35}Cl$ ratio of $>10^{-3}$. It is not plausible to produce this level of ^{36}Cl in supernovae or asymptotic giant branch (AGB) stars, so Hsu et al. (2006) concluded that ^{36}Cl must have been produced by a late episode of particle bombardment within the solar system. A new mineral, wadalite ($Ca_6Al_5Si_2O_{16}Cl_3$), was recently discovered in type B CAIs from the Allende CV chondrite (Ishii et al., 2010). Wadalite contains has an inferred $^{36}Cl/^{35}Cl$ ratio of $(1.81 \pm 0.13) \times 10^{-6}$ (Jacobsen et al., 2011). Coexisting grossular, another secondary mineral commonly found in CAIs, contains no evidence of ^{26}Al decay ($^{26}Al/^{27}Al$ $<3.9 \times 10^{-6}$), which led Jacobsen et al. (2011) to conclude that ^{36}Cl was made by solar energetic particle irradiation late in the history of the protoplanetary disk and that its production was unrelated to production of ^{26}Al, ^{10}Be, and ^{53}Mn.

1.11.4.4 Aluminum-26

Aluminum-26 decays by positron emission and electron capture to ^{26}Mg with a half-life of 0.717 Ma. The discovery circumstances of ^{26}Al have already been discussed (**Section 1.11.1.3**), and since those early measurements, a large body of data has grown to include analyses of CAIs from all major meteorite classes (carbonaceous, ordinary, and enstatite) as well as important groups within these classes (e.g., CM, CV, CH, CR, and CO); a growing body of data also exists for aluminum-rich phases from several differentiated meteorites and in chondrules. Data obtained prior to 1995 were the subject of a comprehensive review by MacPherson et al. (1995); for the most part, their analysis relied heavily on the extensive record in the large, abundant CAIs from CV chondrites, although significant numbers of refractory phases from other carbonaceous chondrite groups were also considered. Between that time and the first edition of this chapter, work generally concentrated on extending the database to include smaller CAIs from underrepresented meteorite groups and, especially, chondrules (mostly from ordinary chondrites). Most measurements were performed by ion microprobe, because of the need to localize analysis on mineral phases with high Al/Mg ratios in order to detect the addition of radiogenic ^{26}Mg; this capability was particularly important for revealing internal $^{26}Al–^{26}Mg$ isochrons in chondrules by examining small regions of trapped melt or glassy mesostasis in between the larger ferromagnesian minerals that dominate chondrules (Kita et al., 2000; McKeegan et al., 2000b; Mostefaoui et al., 2002; Russell et al., 1996). There have been two significant technical developments in the past few years that have profoundly changed understanding of the $^{26}Al–^{26}Mg$ system, both of which resulted in much higher-precision magnesium isotopic analyses: (1) high-precision isotopic analysis by multicollector inductively coupled plasma mass spectrometry (MC-ICPMS), both on dissolved samples and using laser ablation sampling devices for spot analyses, and (2) multicollector development on large-radius ion microprobes. With these new capabilities came measurements suggesting that the early solar system $^{26}Al/^{27}Al$ ratio might be higher than the canonical early solar system value considered by MacPherson et al. (1995), $\sim 5 \times 10^{-5}$, perhaps as high at 6 or 7×10^{-5} (Bizzarro et al., 2004, 2005a; Galy et al., 2004; Thrane et al., 2006; Young et al., 2005). More recently, analyses have now settled down to a widely, but not universally, accepted 'canonical' value of 5.2×10^{-5} (Jacobsen et al., 2008; Larsen et al., 2011; MacPherson et al., 2010, 2012).

In order for the $^{26}Al–^{26}Mg$ system to be used as a chronometer for solar system objects, ^{26}Al must be uniformly distributed within the solar system. The picture that seems to be emerging is that some rare CAIs with large isotope anomalies of nucleosynthetic origin may have formed early in solar system history, before ^{26}Al was introduced, but by the time the large CAIs found in CV chondrites formed, ^{26}Al was well mixed in the solar system and remained so through the formation of chondrules and the parent bodies of the differentiated meteorites.

1.11.4.4.1 Bulk and internal isochrons and the solar system initial $^{26}Al/^{27}Al$

It is important to consider what event is being recorded by an $^{26}Al–^{26}Mg$ isochron. An internal isochron, in which magnesium isotopic data and Al/Mg ratios are measured on individual minerals, records the $^{26}Al/^{27}Al$ ratio at the last time the sample crystallized and magnesium became immobile. **Figure 2** shows a high-precision internal isochron obtained for a CAI from the Leoville CV chondrite by Kita et al. (2012), using a multicollector ion microprobe for analyses of individual minerals. Kita et al. (2012) concluded that this CAI was remelted ~ 50 ka after an initial Al/Mg fractionation event, based on the difference in slope between the Leoville CAI and the bulk CAI isochrons of Jacobsen et al. (2008) and Larsen et al. (2011). The isotopic composition of most spinel is slightly below the isochron, and some fassaite is slightly above the isochron, suggesting that spinel remained unmelted during partial melting and fassaite and anorthite crystallized from a partial melt. The timing of the initial Al/Mg fractionation event in the solar system is believed to be recorded in bulk CAIs whose precursor materials formed as condensates from a gas of solar composition (Grossman et al., 2000; **Chapter 1.10**). The coarse-grained igneous CAIs were subsequently melted and crystallized in relatively short-lived heating

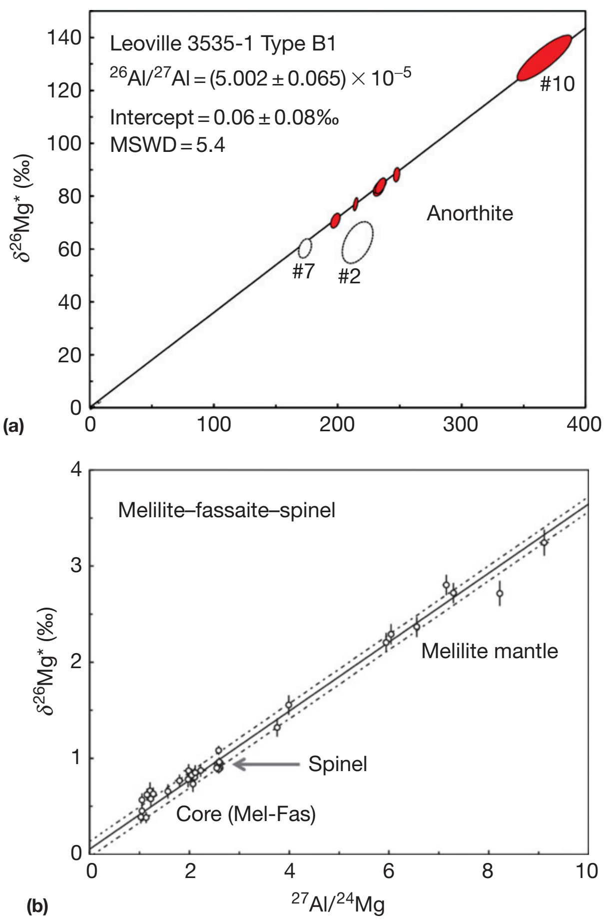

Figure 2 ^{26}Al–^{26}Mg isochron diagrams for the Type B1 CAI 3535-1, from the Leoville CV3 chondrite, demonstrating the high precision that can be achieved with modern SIMS instruments. All data are shown in (a) and low-Mg phases are shown in (b). Anorthite points #2 and #7 were excluded from the isochron regression because SEM imaging showed that the ion probe beam spot intersected cracks. Error bounds are 2σ. Reproduced from Kita NT, Ushikubo T, Knight KB, et al. (2012) Internal ^{26}Al–^{26}Mg isotope systematics of a Type B CAI: Remelting of refractory precursor solids. *Geochimica et Cosmochimica Acta* 86: 37–51.

events during which some magnesium was lost by evaporation, increasing the bulk Al/Mg ratio and generating enrichment in the heavy isotopes of magnesium (Richter et al., 2002, 2007). In principle, this magnesium loss and Al/Mg fractionation could occur any time between the initial condensation event and the last melting event. In practice, recent high-precision data on CAIs suggest that evaporative Al/Mg fractionation occurred early, essentially at the same time as condensation (MacPherson et al., 2012). Thus, measuring magnesium isotopes and Al/Mg ratios in a variety of bulk CAIs and plotting them on an isochron diagram gives the ^{26}Al/^{27}Al ratio at the time of Al/Mg fractionation, regardless of later melting events (as long as no magnesium loss or exchange occurs during those later events).

Galy et al. (2004) made MC-ICPMS measurements of a number of bulk CAIs, which gave an isochron with a slope corresponding to $(6.85 \pm 0.85) \times 10^{-5}$. This work suggested the possibility that nebular fractionation established the bulk Al/Mg ratios of CAIs at a high value, but that internal isochrons (determined mostly by ion microprobe) recorded later remelting events. Bizzarro et al. (2004) measured a suite of bulk Allende CAIs and amoeboid olivine aggregates (AOAs) and reported a slope corresponding to $(^{26}\text{Al}/^{27}\text{Al})_0 = (5.25 \pm 0.10) \times 10^{-5}$, but they published a corrigendum (Bizzarro et al., 2005a) revising their Al/Mg ratio data and recalculating the $(^{26}\text{Al}/^{27}\text{Al})_0$ ratio to $(5.83 \pm 0.11) \times 10^{-5}$. The same group measured additional CAIs and AOAs and reported a slope for all of their CAI–AOA data corresponding to $(^{26}\text{Al}/^{27}\text{Al})_0 = (5.85 \pm 0.05) \times 10^{-5}$ (Thrane et al., 2006). Young et al. (2005) reported about 300 spot analyses of phases in eight CAIs by laser ablation multicollector ICPMS. Some of these analyses imply $(^{26}\text{Al}/^{27}\text{Al})_0$ values as high as 7×10^{-5}, which led Young et al., to propose that early solar system ^{26}Al/^{27}Al ratio was 'supracanonical.'

With further work, the case for a supracanonical early solar system ^{26}Al/^{27}Al ratio has weakened. The Young et al. (2005) data points could be explained by postcrystallization metamorphic effects, which Podosek et al. (1991) showed could produce supracanonical data points from a CAI that crystallized with the canonical ^{26}Al/^{27}Al ratio. Simon and Young (2011) explored ways in which supracanonical CAIs could appear to be canonical, but did not explore how canonical CAIs could appear to be supracanonical. Jacobsen et al. (2008) essentially repeated the Bizzarro group experiment with a new suite of Allende CAIs, putting a substantial effort into accurately measuring Al/Mg ratios. They reported a new bulk isochron, as well as internal isochrons for three of the CAIs. The bulk CAI isochron yielded a slope corresponding to $(^{26}\text{Al}/^{27}\text{Al})_0 = (5.23 \pm 0.13) \times 10^{-5}$. Larsen et al. (2011) reported a bulk isochron from several CAIs and AOAs from the Efremovka CV chondrite with a slope corresponding to $(^{26}\text{Al}/^{27}\text{Al})_0 = (5.252 \pm 0.019) \times 10^{-5}$. They also reported a well-defined but puzzling correlation between the mass-fractionation corrected ^{26}Mg excess and ^{54}Cr isotope anomalies among CAIs, bulk chondrites, achondrites, and Martian samples, which led them to suggest that either ^{26}Al/^{27}Al or initial magnesium isotopic composition (fractionation-corrected initial ^{26}Mg/^{24}Mg) was not well mixed in the solar system.

The Jacobsen et al. (2008) value of $(5.23 \pm 0.13) \times 10^{-5}$ is adopted here as the initial solar system ^{26}Al/^{27}Al ratio, since Larsen et al. (2011) included AOAs, which may not have formed at the same time as CAIs, in their isochron. MacPherson et al. (2010) did laser ablation MC-ICPMS and multicollector ion microprobe measurements of a fine-grained CAI from the Leoville CV3 chondrite, which they argued had never experienced a melting event. They found $(^{26}\text{Al}/^{27}\text{Al})_0 = (5.27 \pm 0.17) \times 10^{-5}$, in agreement with the Jacobsen et al. (2008) bulk isochron. Careful SIMS (secondary ion mass spectrometry, another name for ion microprobe) and ICPMS measurements on CAIs from CV and CR chondrites have failed to find any CAI internal isochrons implying $(^{26}\text{Al}/^{27}\text{Al})_0$ in excess of $\sim 5.2 \times 10^{-5}$ (Bouvier and Wadhwa, 2010; Jacobsen et al., 2008; Kita et al., 2012; MacPherson et al., 2010, 2012; Makide et al., 2009).

1.11.4.4.2 Mass fractionation correction

With the new level of precision of magnesium isotopic analyses, additional care must be taken in treating the data. Magnesium has three stable isotopes, ^{24}Mg, ^{25}Mg, and ^{26}Mg. Isotopic mass fractionation of magnesium can occur in nature, during chemical separation of magnesium from samples, and in mass spectrometers. During mass fractionation, the $^{26}Mg/^{24}Mg$ ratio varies by about twice as much as the $^{25}Mg/^{24}Mg$ ratio. When magnesium isotopic compositions were measured with precision of $\sim 1‰$ or worse, the exact relationship between $^{26}Mg/^{24}Mg$ fractionation and $^{25}Mg/^{24}Mg$ fractionation did not matter much when determining the amount of radiogenic ^{26}Mg. However, in more recent results with precisions of 0.1‰ or better on samples with low Al/Mg, the fractionation law used becomes important in determining the amount of radiogenic ^{26}Mg present. Isotopic mass fractionation during laboratory chemical separation is minimized by ensuring that chemical yields are high; fractionation during mass spectrometry can be corrected for using standards of known isotopic composition such that the instrumental mass fractionation law is well calibrated; however, mass fractionation in nature can be significant. Normal CAIs frequently show mass-dependent fractionation of magnesium in the range of -2 to $+10‰\,amu^{-1}$ and the famed fractionated and unknown nuclear isotopic effect (FUN) CAIs with isotopic anomalies in many elements can be enriched in the heavy isotopes of magnesium by more than $30‰\,amu^{-1}$.

Magnesium isotopic compositions are usually expressed in delta notation, that is, $\delta^{25}Mg = [(^{25}Mg/^{24}Mg)_{sample}/(^{25}Mg/^{24}Mg)_{standard} - 1] \times 1000$. On a plot of $\delta^{25}Mg$ versus $\delta^{26}Mg$, mass fractionation due to equilibrium fractionation or kinetic effects lie along lines that have a slope of ~ 0.5. Although these relationships appear to be linear over a narrow range of mass fractionation, in fact they are curves. Since most mass fractionation mechanisms are exponential processes, it is convenient to express isotope ratios as another related quantity, $1000 \times \ln[(^{25}Mg/^{24}Mg)_{sample}/(^{25}Mg/^{24}Mg)_{standard} - 1]$, which is usually denoted as $\delta^{25}Mg'$ (Young and Galy, 2004). On a plot of $\delta^{25}Mg'$ versus $\delta^{26}Mg'$, the different mass fractionation processes plot as straight lines but with differing slopes depending on the nature of the fractionation process. Fractionation due to the kinetic isotope effect gives a slope of 0.5110 and that due to equilibrium isotope partitioning gives 0.5210 (Davis et al., 2005; Young et al., 2002).

Most CAIs have magnesium that is mass fractionated by a few ‰ amu^{-1} (see **Chapter 1.10**). The mass fractionation in CAIs is believed to have been caused by a kinetic isotope effect during high-temperature evaporation in the solar nebula. Davis et al. (2005) evaporated melts of CAIs in vacuum and measured magnesium isotopic compositions by MC-ICPMS. On a plot of $\delta^{25}Mg'$ versus $\delta^{26}Mg'$, their data give a slope of 0.514; additional unpublished data have refined this slope to 0.5133 ± 0.0006. Several papers have been published with high-precision magnesium isotopic data, using different slopes to correct for mass fractionation. Values used include 0.521, the ‘equilibrium’ value (Young et al., 2002); 0.511, the ‘exponential law’ (Young et al., 2002); and 0.514, which was a preliminary experimental value determined by Davis et al. (2005). As an example of the effect of these different fractionation laws, consider a spinel grain, with $^{27}Al/^{24}Mg = 2.53$, a typical degree of mass fractionation for a CAI, $\delta^{25}Mg = 5‰$, and an initial $^{26}Al/^{27}Al$ value of 5.2×10^{-5}. Excesses or deficits in ^{26}Mg due to ^{26}Al decay are usually expressed as $\delta^{26}Mg^*$. In this example, $\delta^{26}Mg^*$ should be 0 before decay and grow to 0.944‰ after complete decay of ^{26}Al. If this is the value obtained with the slope that has been adopted, 0.5133, recalculating with the kinetic value, 0.511, gives 0.900‰, and the equilibrium value, 0.521, gives 1.089‰. These shifts may seem small, but for an isochron passing through the origin and the spinel in the example, the two extreme slopes would imply initial $^{26}Al/^{27}Al$ values of 4.96×10^{-5} and 6.00×10^{-5}, a range of 17% that corresponds to a time difference of 197 ka. The effect of the $\delta^{25}Mg'$ versus $\delta^{26}Mg'$ slope on $\delta^{26}Mg^*$ depends only on the degree of mass fractionation, not on the Al/Mg ratio. It has only become important recently with the development of high-precision magnesium isotopic methods applied to low-Al/Mg samples.

1.11.4.4.3 Magnesium isotopic evolution in the early solar system

Useful chronological information can be derived not only from the slope, but also from the intercept of an isochron plot. This technique has long been used for strontium (Gray et al., 1973; Papanastassiou and Wasserburg, 1969; Podosek et al., 1991). With the advent of high-precision multicollector mass spectrometry techniques, it has become possible to study the evolution of magnesium isotopic composition in early solar system history. The Earth has a present-day $\delta^{26}Mg^*$ value of 0, by definition. If the solar system formed with an $^{26}Al/^{27}Al$ value of 5.2×10^{-5} and the Earth has a chondritic Al/Mg ratio (actually, this is currently not precisely known), the $\delta^{26}Mg^*$ before ^{26}Al decayed must have been $-0.038‰$. The intercept determined for a suite of Allende CAIs by Jacobsen et al. (2008) is $-0.040 \pm 0.029‰$, which is within error of this value.

Villeneuve et al. (2009) used high-precision multicollector SIMS measurements of chondrules from the Semarkona unequilibrated ordinary chondrite to study magnesium isotopic evolution in the early solar system. They found that the slopes of the ^{26}Al–^{26}Mg internal isochrons of individual chondrules were consistent with chondrule formation 1.2–4 Ma after CAIs, and the intercepts of the chondrules, which were determined with 0.005‰ precision in olivine, lie along the solar system magnesium isotopic evolution diagram (**Figure 3**). Villeneuve et al. (2009) argued that this internal consistency demonstrates that $^{26}Al/^{27}Al$ was uniformly distributed in (at least) the inner solar system.

Minerals that have very low Al/Mg ratios, such as olivine, preserve the magnesium isotopic composition of the reservoir from which they crystallize, as the amount of aluminum in these minerals is too low to allow any change in magnesium isotopic composition from ^{26}Al decay. If the Al/Mg ratio of the reservoir from which such minerals crystallized can be inferred, the magnesium isotopic composition can be used to obtain chronological information by reading off the time on a magnesium isotope evolution diagram (**Figure 3**). Villeneuve et al. (2011) used this approach to conclude that isolated olivines and olivines in Type I (magnesium-rich) chondrules from the Allende meteorite formed in reservoirs before complete decay of ^{26}Al and that the Eagle Station pallasite experience differentiation as early as $0.15^{+0.29}_{-0.23}$ Ma after CAIs. Schiller et al. (2011) used high-precision magnesium isotopic data on bulk diogenites to conclude that they formed as cumulates from a magma ocean on the howardite–eucrite–diogenite (HED) parent body (presumably Vesta) starting $0.6^{+0.5}_{-0.4}$ Ma after CAIs and continuing for ~ 3 Ma. However, this estimate depends on their

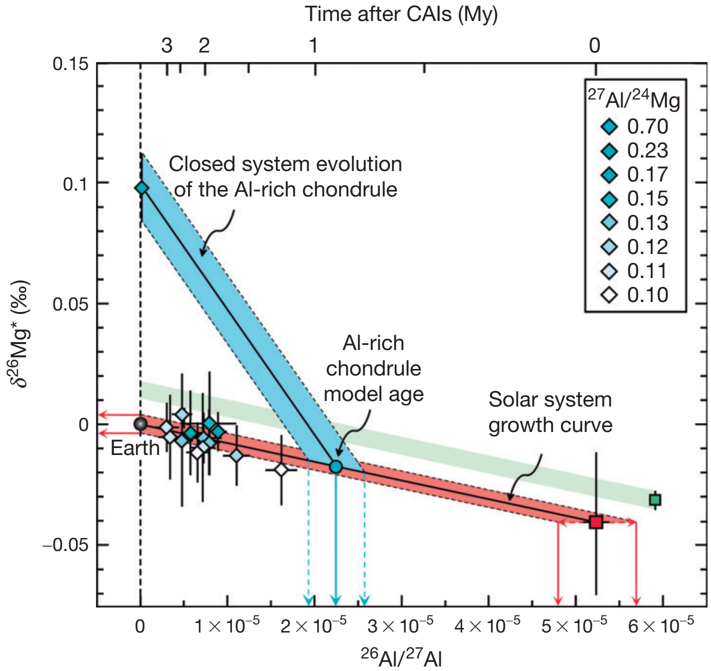

Figure 3 Magnesium isotopic evolution diagram for the ^{26}Al–^{26}Mg system. Initial δ^{26}Mg* versus ^{26}Al/^{27}Al for CAIs and chondrules. Each data point is derived from the slope and intercept of an isochron diagram for a single chondrule. The Earth is defined as having δ^{26}Mg* = 0‰. A line with a slope defined by the bulk solar system Al/Mg ratio is extrapolated back in time to the ^{26}Al/^{27}Al ratio for CAIs derived by Jacobsen et al. (2008), 5.23×10^{-5}, which gives a δ^{26}Mg* value of −0.038‰. The fact that chondrules lie along this line is used to show that ^{26}Al/^{27}Al was uniformly distributed in the early solar system to a precision of 10%. The red square is derived from the bulk CAI isochron of Jacobsen et al. (2008) and the green square from the bulk CAI isochron of Thrane et al. (2006). The Jacobsen et al. (2008) isochron is compatible with the chondrule evolution line and the Thrane et al. (2006) isochron is not. Reproduced from Villeneuve J, Chaussidon M, and Libourel G (2009) Homogeneous distribution of ^{26}Al in the solar system from the Mg isotopic composition of chondrules. *Science* 325: 985–988. Reprinted with permission from AAAS.

inference, based on the correlation between fractionation-corrected ^{26}Mg excess and nucleosynthetic ^{54}Cr anomalies among bulk meteorites (Larsen et al., 2011), that the initial ^{26}Al/^{27}Al value of the HED parent body was $(1.6 \pm 0.3) \times 10^{-5}$. Based on magnesium isotopic data on olivine from main group pallasites and ureilites, Baker et al. (2012) inferred that their parent bodies differentiated $1.24^{+0.40}_{-0.28}$ and $1.9^{+2.2}_{-0.7}$ Ma after CAIs, respectively.

1.11.4.4.4 ^{26}Al–^{26}Mg systematics in CAIs

As delineated by MacPherson et al. (1995), the large data set existing prior to the recent high-precision measurements shows clearly that the distribution of inferred initial ^{26}Al/^{27}Al in CAIs is bimodal, with the dominant peak at the so-called canonical value of $\sim 5 \times 10^{-5}$ and a second large peak at 'dead' aluminum (i.e., ^{26}Al/^{27}Al = 0). MacPherson et al. (1995) demonstrated that this pattern applied to all classes of carbonaceous chondrites, although the relative heights of the two peaks varied among different meteorites (mostly reflecting a difference in CAI types; see **Chapter 1.3**). The dispersion of the canonical peak (amounting to $\sim 1 \times 10^{-5}$, FWHM) was considered to represent a convolution of measurement error and geologic noise; there were no robust data indicating that any CAIs formed with $(^{26}\mathrm{Al}/^{27}\mathrm{Al})_0$ significantly above the canonical ratio.

Relatively few CAIs have been studied using the multicollector SIMS methods capable of giving high-precision data. MacPherson et al. (2012) reported internal isochrons for several CAIs from the Vigarano CV3 chondrite measured by multicollector SIMS and summarized other recent high-precision CAI isochrons reported by Jacobsen et al. (2008), Bouvier and Wadhwa (2010), MacPherson et al. (2010), and Kita et al. (2012). Makide et al. (2009) reported isochrons for a number of CAIs from CR chondrites. Despite data being available for only about 20 CAIs, a clear picture seems to be emerging: CAIs that formed as condensates have ^{26}Al/^{27}Al value that agree with the canonical early solar system ^{26}Al/^{27}Al value of 5.23×10^{-5} within small uncertainties, whereas CAIs that show clear petrologic evidence for melting have a range of ^{26}Al/^{27}Al values from the canonical value down to $\sim 3 \times 10^{-5}$ (**Figure 4**). The intercepts of ^{26}Al–^{26}Mg isochrons can also provide useful chronological information. MacPherson et al. (2012) used a variant of the methods pioneered by Villeneuve et al. (2009) (**Section 1.11.4.4.3**) to conclude that the Al/Mg ratios of the CAIs they studied were established at the time of canonical early solar system ^{26}Al/^{27}Al, regardless of whether the final melting and crystallization occurred at that time or a later time.

A number of CAIs contained little or no ^{26}Al at their time of formation, including the so-called FUN inclusions (e.g., Lee et al., 1977, 1980), some micrometer-sized corundum grains in carbonaceous chondrites (Makide et al., 2011), and the platelet hibonite crystals (PLACs), which are extremely refractory grains from CM chondrites that are characterized by huge isotopic anomalies in the neutron-rich isotopes of titanium and calcium (Fahey et al., 1987; Ireland, 1988; Liu et al., 2009). Also present in CM chondrites are spinel-hibonite CAIs, sometimes called SHIBs. It is not possible to obtain internal isochrons on PLACs, because they consist of a single mineral, hibonite, with a high Al/Mg ratio, or on SHIBs, because they are too fine-grained to allow analysis of hibonite or spinel alone. For these CAIs, it is necessary to calculate so-called 'model' isochrons, in which it is assumed that their initial magnesium isotopic composition was isotopically normal. This approach fails for some PLACs, because they can have deficits, rather than excesses, in mass-fractionation corrected ^{26}Mg, for which a model isochron calculation gives a negative ^{26}Al/^{27}Al, which is clearly impossible. Both PLACs and FUN CAIs typically have low or undetectable excess ^{26}Mg, implying that little (or no) ^{26}Al was present when they formed. Two explanations are possible: these objects formed after ^{26}Al decayed or before ^{26}Al was introduced into the solar system. As pointed out by MacPherson et al. (1995), many of the inclusions with low $(^{26}\mathrm{Al}/^{27}\mathrm{Al})_0$ are not mineralogically altered, which argues against late metamorphism. Moreover, the PLACs and FUN inclusions are typically hosts for large isotopic anomalies in a variety of elements, which argues strongly for their antiquity. Because of their preservation of extreme stable isotope anomalies, these refractory phases are best understood as having formed at an early time in the nebula, but from an isotopic reservoir (or precursor minerals) that was missing the ^{26}Al inventory sampled by other 'normal' refractory materials (Sahijpal and Goswami, 1998). The scope of this heterogeneity, both spatially and temporally, is the focus of much conjecture and research, as this is a key issue for the utility of ^{26}Al as a high-resolution chronometer for nebular events. Of course, the key measurement, which has not been made at this writing, is an absolute Pb–Pb age of a FUN CAI, which would settle the issue of whether these objects are older or younger than normal CAIs.

1.11.4.4.5 ^{26}Al–^{26}Mg systematics in chondrules

The duration of high-temperature processes in the solar nebula is closely related to the age difference between CAIs and chondrules, and it is in this area that some of the most significant new data have been developed in recent years. The first evidence for radiogenic ^{26}Mg* in non-CAI material was found in a plagioclase-bearing chondrule from the highly unequilibrated ordinary chondrite Semarkona (Hutcheon and Hutchison, 1989); the isochron implies an initial abundance of $(^{26}\mathrm{Al}/^{27}\mathrm{Al})_0 = (7.7 \pm 2.1) \times 10^{-6}$. In most cases, however, only upper limits on ^{26}Al abundances could be determined in a handful of plagioclase grains from chondrules in ordinary chondrites (Hutcheon and Jones, 1995; Hutcheon et al., 1994). Today, initial ^{26}Al/^{27}Al ratios have been determined in over 100 chondrules from several unequilibrated ordinary and carbonaceous chondrites. Chondrules with abundant aluminum-rich minerals (plagioclase-rich chondrules) and those with 'normal' ferromagnesian mineralogy have been analyzed. Chondrules have distinctly lower $(^{26}\mathrm{Al}/^{27}\mathrm{Al})_0$ than CAIs, most by a factor of 5 or more (Figure 5). In this figure, only the

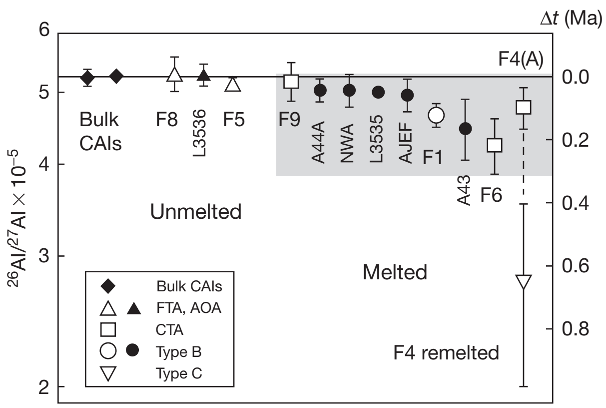

Figure 4 Isochrons defined by several bulk CAIs from Jacobsen et al. (2008) and Larsen et al. (2011) as well as internal isochrons from unmelted CAIs are consistent with $^{26}\mathrm{Al}/^{27}\mathrm{Al} = \sim 5.2 \times 10^{-5}$. Melted CAIs can have the same or lower ^{26}Al/^{27}Al, implying that remelting of CAIs occurred up to 600 ka after initial CAI formation. Reproduced from MacPherson GJ, Kita NT, Ushikubo T, Bullock ES, and Davis AM (2012) Well-resolved variations in the formation ages for Ca–Al-rich inclusions in the early solar system. *Earth and Planetary Science Letters* 331–332: 43–54.

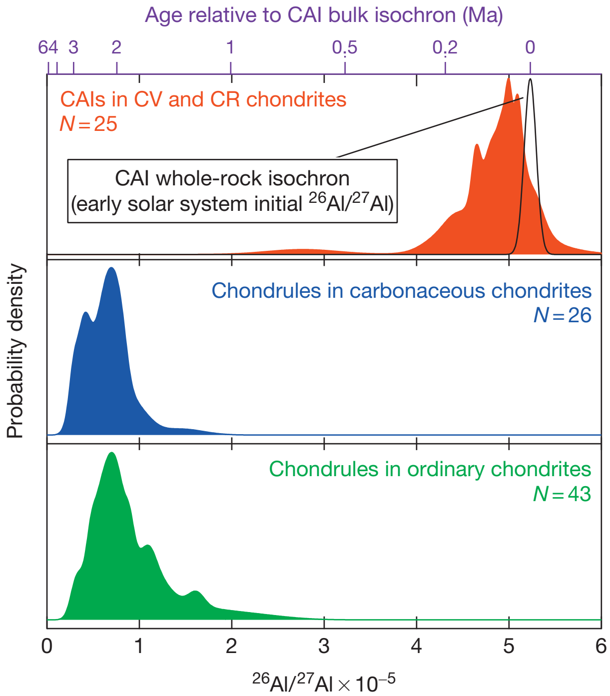

Figure 5 Probability density plots of ^{26}Al/^{27}Al ratios determined from high-quality internal isochrons for CAIs and chondrules. The CAI whole-rock curve is based on the data of Jacobsen et al. (2008). Data sources are as follows: CAIs (Bouvier and Wadhwa, 2010; Jacobsen et al., 2008; Kita et al., 2012; MacPherson et al., 2010, 2012; Makide et al., 2009), carbonaceous chondrite chondrules (Hsu et al., 2003; Hutcheon et al., 2009; Kunihiro et al., 2004; Kurahashi et al., 2008; Sugiura and Krot, 2007; Yurimoto and Wasson, 2002), and ordinary chondrite chondrules (Hutcheon and Hutchison, 1989; Kita et al., 2000; Mishra et al., 2010; Mostefaoui et al., 2002; Rudraswami and Goswami, 2007; Rudraswami et al., 2008; Villeneuve et al., 2009). The tail of the CAI curve extends to values above the canonical initial ^{26}Al/^{27}Al ratio $\sim 5.2 \times 10^{-5}$, but this only reflects uncertainties in individual internal isochrons. No internal isochron show ^{26}Al/^{27}Al ratio in excess of 5.2×10^{-5}. Chondrule data have several peaks that might indicate several distinct episodes of chondrule formation (Villeneuve et al., 2009). Most chondrule formation occurred 2–3 Ma after CAI formation.

69 chondrules with well-defined internal isochrons are plotted, and the data were restricted to those chondrules whose 1σ uncertainty is less than 50% of the $(^{26}Al/^{27}Al)_0$ value. The distribution of $(^{26}Al/^{27}Al)_0$ values in carbonaceous and unequilibrated ordinary chondrites appear to have several peaks (**Figure 5**). Both distributions have peaks at $(^{26}Al/^{27}Al)_0$ $\sim 7\times10^{-6}$; ordinary chondrites show peaks at 1.1×10^{-5} and 1.6×10^{-5} and carbonaceous chondrites have a peak at 4×10^{-6}. Villeneuve et al. (2009) identified five peaks in the distribution of $(^{26}Al/^{27}Al)_0$ values of Semarkona (L3.0) chondrules, but not all of these peaks are apparent in **Figure 5**. They attributed these peaks to discrete chondrule forming events in the solar nebula occurring 1.5–3 Ma after CAI formation. The largest peak in the distribution of $(^{26}Al/^{27}Al)_0$ values in carbonaceous and ordinary chondrite chondrules occurs at a value corresponding to 2 Ma after CAI formation, but some chondrules appear to have formed as late as 3.5 Ma after CAIs.

1.11.4.4.6 ^{26}Al–^{26}Mg systematics in achondrites

Recent technical advances in magnesium isotopic measurements have led to the application of the ^{26}Al–^{26}Mg system to achondrites. Early searches (e.g., Schramm et al., 1970) were unable to detect radiogenic ^{26}Mg. The first success was that of Srinivasan et al. (1999), who showed that plagioclase crystals in the eucrite Piplia Kalan have significant excess ^{26}Mg; however, the correlation of $^{26}Mg^*$ with Al/Mg in the plagioclase is poor, indicating that the system has suffered partial reequilibration of magnesium isotopes following crystallization. A best-fit correlation through plagioclase and pyroxene yields an apparent $(^{26}Al/^{27}Al)_0=(7.5\pm0.9)\times10^{-7}$, which would correspond to $\sim$4 Ma after the CAI canonical value.

With the development of high-precision techniques for magnesium isotopes, progress has been significant in applying the ^{26}Al–^{26}Mg system to achondrites. Bizzarro et al. (2005b) reported magnesium isotopic compositions and Al/Mg ratios in bulk eucrites, angrites, and mesosiderite silicates. They calculated model isochrons, assuming that ^{26}Al was uniform in the solar system, and concluded that initiation of basaltic magmatism on the mesosiderite, eucrite, and angrite parent bodies occurred at $2.56^{-0.15}_{+0.18}$, $3.05^{-0.13}_{+0.15}$, and $3.31^{-0.14}_{+0.16}$ Ma after CAI formation, respectively. Several groups reported internal isochrons in achondrites in abstracts in the early 2000s, but the first internal isochrons in the refereed literature did not appear for nearly 10 years. Wadhwa et al. (2009) reported that the unique basaltic achondrite Asuka 881394 showed some evidence of isotopic disturbance, but most of the data lie on an internal isochron corresponding to $(^{26}Al/^{27}Al)_0=(1.28\pm0.07)\times10^{-6}$. Spivak-Birndorf et al. (2009) reported that internal isochrons for two angrites, D'Orbigny and Sahara 99555, show initial values of $^{26}Al/^{27}Al$ of $(5.10\pm0.55)\times10^{-7}$ and $(5.13\pm1.90)\times10^{-7}$, respectively, corresponding to crystallization $\sim$4.8 Ma after CAIs. Sahara 99555 shows disturbances in some systems, but D'Orbigny apparently crystallized rapidly and is free of later disturbance, so it is key to anchoring several short- and long-lived chronometers. Schiller et al. (2010) remeasured magnesium isotopes and Al/Mg ratios in many of the bulk achondrites analyzed by Bizzarro et al. (2005b) and reported internal isochrons for Sahara 99555, D'Orbigny, and the unique basaltic achondrite NWA 2976 of $(4.45\pm0.56)\times10^{-7}$, $(3.88\pm0.27)\times10^{-7}$, and $(4.91\pm0.46)\times10^{-7}$, respectively. The angrite data are of higher precision but in agreement with the data of Spivak-Birndorf et al. (2009). Bouvier et al. (2011) reported Pb–Pb and ^{26}Al–^{26}Mg systematics of NWA 2976. An internal isochron for this meteorite gives a $^{26}Al/^{27}Al$ value of $(3.94\pm0.16)\times10^{-7}$, which corresponds to formation 0.26 Ma after the D'Orbigny angrite. The uranium-isotope-corrected Pb–Pb ages of NWA2976 and D'Orbigny are consistent with this time difference. Goodrich et al. (2010) reported ion microprobe data for a feldspathic clast in the DaG 319 ureilite, which gave an initial $^{26}Al/^{27}Al$ value of $(3.0\pm1.1)\times10^{-7}$, implying formation $\sim$5.4 Ma after CAIs. As mentioned earlier, Baker et al. (2012) used high-precision magnesium isotopic data on olivine from Eagle Station pallasites, main group pallasites, and ureilites to infer that their parent bodies differentiated $0.15^{+0.29}_{-0.23}$, $1.24^{+0.40}_{-0.28}$, and $1.9^{+2.2}_{-0.7}$ Ma after CAIs, respectively. The latter age is earlier than the differentiation age inferred by Goodrich et al. (2010) for ureilites and may imply that feldspathic clasts date later crustal processing rather than parent-body differentiation. Gounelle et al. (2009) reported that a basaltic micrometeorite has no excess ^{26}Mg in plagioclase with high Al/Mg ratios, giving an upper limit for the $^{26}Al/^{27}Al$ at the time of formation of $<2.8\times10^{-7}$, implying formation more that 7.9 Ma after CAI formation.

1.11.4.5 Beryllium-10

Beryllium-10 β^--decays to ^{10}B with a half-life of 1.387 Ma (Chmeleff et al., 2010; Korschinek et al., 2010). Evidence for its former existence in the solar system is provided by excesses of $^{10}B/^{11}B$ correlated with Be/B ratio, first found within coarse-grained (type B) CAIs from Allende (McKeegan et al., 2000a). From the slope of the correlation line, McKeegan et al. calculated an initial $^{10}Be/^{9}Be=(9.5\pm1.9)\times10^{-4}$ at the time corresponding to isotopic closure of the Be–B system. Chaussidon et al. (2006a) reported further measurements on the same CAI and refined the initial $^{10}Be/^{9}Be$ value to $(8.8\pm0.6)\times10^{-4}$ (**Figure 6**). This discovery was confirmed and extended by analyses of a variety of CAIs of types A and B and a FUN inclusion from various CV3 chondrites, including Allende, Efremovka, Vigarano, Leoville, and Axtell (Chaussidon et al., 2006a,b; MacPherson et al., 2003; Sugiura et al., 2001; Wielandt et al., 2012). Of the nearly 29 CAIs from CV chondrites that have been examined so far, in every case for which high Be/B ratios could be found in a sample (i.e., except where boron contamination is prevalent), excesses of $^{10}B/^{11}B$ are measured, implying that the existence of live ^{10}Be was rather widespread in the solar nebula, at least at the locale of CAI formation. Some spread in initial $^{10}Be/^{9}Be$ ratios is clear: calculated initial $^{10}Be/^{9}Be$ ratios for 'normal' CV CAIs range over a factor of 2 from $(\sim4.5–8.8)\times10^{-4}$, with no difference seen between type B CAIs (mean of 9, $^{10}Be/^{9}Be=(6.0\pm0.5)\times10^{-4}$) and type A CAIs (mean of 8, $^{10}Be/^{9}Be=(6.4\pm0.3)\times10^{-4}$). Two FUN inclusions have been measured, a type A from Axtell (MacPherson et al., 2003; Wielandt et al., 2012) and a type B2 from NWA 779 (Wielandt et al., 2012), which have lower initial $^{10}Be/^{9}Be$ values of $(2.75\pm0.24)\times10^{-4}$ and $(3.37\pm0.20)\times10^{-4}$, respectively. The data of Wielandt et al. (2012) imply heterogeneity in $^{10}Be/^{9}Be$ even among CAIs with similar $^{26}Al/^{27}Al$ ratios.

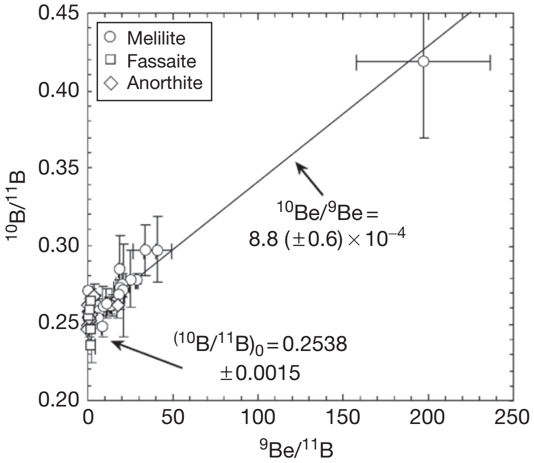

Figure 6 ^{10}Be–^{10}B isochron diagram for the Type B1 CAI 3529-41, from the Allende CV3 chondrite. Adapted from Chaussidon M, Robert F, and McKeegan KD (2006a) Li and B isotopic variations in an Allende CAI: Evidence for the in situ decay of short-lived ^{10}Be and for the possible presence of the short-lived nuclide ^{7}Be in the early solar system. *Geochimica et Cosmochimica Acta* 70: 224–245.

The former presence of ^{10}Be was extended to another important class of refractory objects, hibonite from the CM2 Murchison meteorite (Liu et al., 2009; Marhas et al., 2002). Hibonite [$CaAl_{12-2x}(Mg_xTi_x)O_{19}$] is one of the most refractory minerals calculated to condense from a gas of solar composition and is known to host numerous isotopic anomalies, especially in the heavy isotopes of calcium and titanium (Fahey et al., 1987; Ireland et al., 1985; Zinner et al., 1986). Curiously, when these anomalies are of an exceptionally large magnitude (in the approximately several to 10% range), the PLAC hibonite grains show a distinct lack of evidence for having formed with ^{26}Al (e.g., Ireland, 1988, 1990) or ^{41}Ca (Sahijpal et al., 1998, 2000). Marhas et al. (2002) found excesses of $^{10}B/^{11}B$ in three such hibonite grains that are each devoid of either $^{26}Mg^*$ or $^{41}K^*$ from the decay of ^{26}Al and ^{41}Ca, respectively. Collectively, the Be–B data imply $^{10}Be/^{9}Be = (5.2 \pm 2.8) \times 10^{-4}$ when these hibonites formed. This initial $^{10}Be/^{9}Be$ is in the same range as for other refractory inclusions and indicates that existence of ^{10}Be is decoupled from the other two short-lived nuclides that partition into refractory objects, namely, ^{26}Al and ^{41}Ca. Even more striking evidence for decoupling of the ^{26}Al–^{26}Mg and ^{10}Be–^{10}B systems came with the report of Marhas and Goswami (2003) that hibonite in the well-known FUN CAI HAL had an initial $^{10}Be/^{9}Be$ ratio in the same range as other CAIs, yet had an initial $^{26}Al/^{27}Al$ ratio three orders of magnitude lower than the canonical early solar system ratio (Fahey et al., 1987). The significance of this lack of correlation, for both chronology and source of radionuclides, is discussed further in the succeeding text. More PLAC hibonite grains were analyzed by Liu et al. (2009) and Liu et al. (2010), for which the combined data are consistent with single inferred $^{10}Be/^{9}Be$ ratios of $(5.3 \pm 1.0) \times 10^{-4}$.

Convincing evidence of live ^{10}Be has so far only been found in refractory inclusions because these samples exhibit large volatility-controlled Be/B fractionation and high Be concentrations (since beryllium is a refractory element). It is of great interest to extend the ^{10}Be–^{10}B system to chondrules in order to further explore irradiation events in the early solar system.

1.11.4.6 Cesium-135

Cesium-135 β^--decays to ^{135}Ba with a half-life of 2.3 Ma. This system is difficult to work with because cesium is a volatile element and is easily transported during aqueous alteration, whereas barium is refractory and immobile. Hidaka et al. (2001) presented the first evidence suggesting the presence of ^{135}Cs in the early solar system. They found that acid leachates from CAI from the Allende CV3 chondrite have high Cs/Ba ratios that were correlated with excess ^{135}Ba, consistent with $^{135}Cs/^{133}Cs = (4.82 \pm 0.79) \times 10^{-4}$, which they suggested as the early solar system ratio. However, they also found variations of ^{135}Ba and ^{137}Ba of nucleosynthetic origin in CAIs and had to correct for this effect. Given the mobility of cesium, it is unclear whether the $^{135}Cs/^{133}Cs$ value recorded by CAIs is the early solar system ratio or the result of later events, such as parent-body aqueous activity. Hidaka et al. (2001) also performed leaching experiments on Beardsley, an H5 chondrite with high $^{87}Sr/^{86}Sr$ and high a Rb concentration, and Zag, an H3–6 chondrite that contains halite. The leachates had high Cs/Ba and excess ^{135}Ba, leading to inferred $^{135}Cs/^{133}Cs$ ratios of $(1.34 \pm 0.20) \times 10^{-5}$ and $(2.4 \pm 1.0) \times 10^{-6}$ for Beardsley and Zag, implying aqueous activity 12 and 18 Ma after CAI formation, respectively. Hidaka et al. (2003) performed leaching experiments on the CM2 chondrites Murchison and Sayama finding an inferred $^{135}Cs/^{133}Cs$ ratio of $(6.5 \pm 5.0) \times 10^{-5}$. Hidaka and Yoneda (2011) performed leaching experiments on several bulk carbonaceous chondrites, revealing several components of nucleosynthetic origin. Only the Mighei CM2 chondrite showed evidence for ^{135}Cs decay ($^{135}Cs/^{133}Cs = (2.7 \pm 1.6) \times 10^{-4}$). The strongest evidence for presence of live ^{135}Cs in the early solar system remains the data from the Beardsley and Zag meteorites. For the leaching data on CAIs and bulk carbonaceous chondrites, it is difficult to separate the effect of nucleosynthetic anomalies in ^{135}Ba from ^{135}Ba due to ^{135}Cs decay. The early solar system value listed in **Table 1**, 4.8×10^{-4}, is derived from CAI leaching experiments of Hidaka et al. (2001) but must be considered as highly uncertain.

1.11.4.7 Iron-60

Iron-60 β^--decays to ^{60}Ni with a half-life of 2.62 Ma (Rugel et al., 2009). Unlike the other short-lived nuclides with half-lives of a few million years or less, and in particular contrast to ^{10}Be, ^{60}Fe is not produced by spallation because there are no suitable target elements, and therefore all of its solar system inventory must reflect stellar nucleosynthesis. The first plausible evidence for the existence of ^{60}Fe in the solar system was provided by ^{60}Ni excesses found in bulk samples of the eucrites Chervony Kut and Juvinas (Shukolyukov and Lugmair, 1993a,b). These are basaltic achondrites, the result of planetary-scale melting and differentiation (possibly on the asteroid Vesta; see **Chapters 1.6** and **2.14**) that fractionated nickel into the core. Thus, the excess ^{60}Ni cannot represent nucleogenetic isotope anomalies of the iron-group elements, as is seen in CAIs, and its presence in such a large volume of material indicates wide-scale occurrence of ^{60}Fe in the solar system (Shukolyukov and Lugmair, 1993a). However, internal mineral isochrons could not be obtained on the eucrite samples because of element redistribution after the decay of ^{60}Fe (Shukolyukov and Lugmair, 1993b). Moreover, the inferred initial $^{60}Fe/^{56}Fe$ differs by an order a magnitude between these eucrites for which other isotopic systems (e.g., ^{53}Mn–^{53}Cr) indicate a similar formation age (Lugmair and Shukolyukov, 1998). These inconsistencies point out problems with interpreting eucrite $^{60}Fe/^{56}Fe$ abundances in chronologic terms and indicate that estimates of a solar system initial $^{60}Fe/^{56}Fe$ based on an absolute age of eucrite formation are likely subject to large systematic uncertainties.

Subsequent work has revealed that the ^{60}Fe–^{60}Ni system is technically very challenging and estimates of the early solar system $^{60}Fe/^{56}Fe$ have varied by more than an order of magnitude. One of the major difficulties is that iron is not a refractory element and the small amount of iron present in most CAIs is essentially entirely introduced during secondary processing in the solar nebula or, more likely, on meteorite parent bodies at an unknown time. Because primary iron-rich condensates are generally lacking, measurements in iron-rich minerals found in chondrites and achondrites must be extrapolated in time to solar system formation by using other short-lived radionuclides. Interest in the ^{60}Fe–^{60}Ni system was revived by the development of SIMS techniques for nickel isotopic analysis and the finding that some minerals have extraordinarily high Fe/Ni ratios. The initial such discovery was by Tachibana and Huss (2003), who found good correlations of excess ^{60}Ni with Fe/Ni ratios in sulfide minerals of the (LL3.1) unequilibrated ordinary chondrites Bishunpur and Krymka, which imply $^{60}Fe/^{56}Fe$ ratios of between 1.0×10^{-7} and 1.8×10^{-7}. Mostefaoui et al. (2005) reported similarly good correlations in troilite from Semarkona (LL3.0) with a slope corresponding to $^{60}Fe/^{56}Fe=(9.2\pm2.4)\times10^{-7}$; a weighted regression through their data excluding data points they rejected as outliers gives $^{60}Fe/^{56}Fe=(9.5\pm1.3)\times10^{-7}$. They also measured nickel isotopes in magnetite and found a correlation implying $^{60}Fe/^{56}Fe=(1.1\pm0.4)\times10^{-7}$. If the two correlations found by Mostefaoui et al. (2005) are isochrons, magnetite is $\sim$5 Ma younger than troilite. With plausible assumptions, Tachibana and Huss (2003) estimated $(^{60}Fe/^{56}Fe)_0$ for solar system formation of between 1×10^{-7} and 6×10^{-7} with a probable value (depending on the age of the sulfides relative to CAIs) of $(\sim3–4)\times10^{-7}$. Mostefaoui et al. (2005) preferred to simply consider their measured $^{60}Fe/^{56}Fe$ value of 9.2×10^{-7} as a lower limit to the solar system initial value. Further progress came with the measurement by Tachibana et al. (2006) of nickel isotopes in ferromagnesian silicates in chondrules in Semarkona and Bishunpur. They found correlations of excess ^{60}Ni with Fe/Ni ratio consistent with $^{60}Fe/^{56}Fe=(2–3.7)\times10^{-7}$. Since ^{26}Al–^{26}Mg chronometry indicates that these chondrules are 1.5–2 Ma older than CAIs, they estimated an initial solar system $^{60}Fe/^{56}Fe$ ratio of $(5–10)\times10^{-7}$. These data are consistent with an upper limit of $(^{60}Fe/^{56}Fe)_0\sim3.5\times10^{-7}$ derived from analyses of nickel isotopes in FeO-rich olivine from a (LL3.0) Semarkona chondrule that exhibited $(^{26}Al/^{27}Al)_0=0.9\times10^{-5}$ (Kita et al., 2000).

A recently recognized technical issue has called into question much of the SIMS measurements of the ^{60}Fe–^{60}Ni system and most of the conclusions reached in the previous paragraph. One of the difficulties of the SIMS measurements of high-Fe/Ni phases is that nickel count rates are extremely low, so low that normal Poisson statistics cannot be used to estimate uncertainties. Ogliore et al. (2011) and Coath et al. (2013) have derived statistical methods for treating such data. The end result is that many of the SIMS-derived excess $^{60}Ni/^{58}Ni$ values turned out to be artifacts of inadequate consideration of this effect (Telus et al., 2012). All but one of the analyses reported by Tachibana and Huss (2003) and Tachibana et al. (2006) have $^{60}Fe/^{56}Fe$ ratios unresolved from zero and the remaining sample, Semarkona chondrule SMK1–4, gives a barely detected ratio of $(1.2\pm0.9)\times10^{-7}$ (2σ).

Multicollector ICPMS techniques have enabled high-precision nickel isotopic analyses and allowed considerable progress in developing the ^{60}Fe–^{60}Ni system over the past few years. Quitté et al. (2006) analyzed metal in 33 iron meteorites and 10 coexisting sulfides. They found no excesses in ^{60}Ni but did find excesses in ^{61}Ni correlated with deficits in ^{60}Ni in some sulfides that could not be explained by known analytical artifacts. They suggested admixture of an *s*-process component, but it was unclear why it was restricted to sulfides and not coexisting metal. No useful upper limit on $^{60}Fe/^{56}Fe$ could be derived.

Quitté et al. (2007) measured nickel isotopic compositions in CAIs and found correlated anomalies in ^{60}Ni and ^{62}Ni. The presence of nucleosynthetic anomalies prevented a firm conclusion from being reached on the early solar system $^{60}Fe/^{56}Fe$ ratio.

Bizzarro et al. (2007) found consistent ^{60}Ni deficits of -0.24 ε-units in iron meteorites, pallasites, ureilites, and the Sahara 99 555 angrite, as well as deficits and excesses in ^{62}Ni covering a range of ~1 ε-unit among bulk meteorites of many types. They concluded that planetesimals formed in the first million years of solar system history had no ^{60}Fe because ^{60}Fe was introduced 1 Ma after solar system formation. However, Dauphas et al. (2008) measured iron meteorites with higher precision and showed that there were no significant ^{60}Ni or ^{62}Ni anomalies. They also measured iron isotopes and found no isotopic anomalies. Since significant ^{58}Fe anomalies are required by nucleosynthesis modeling to accompany ^{60}Fe, they ruled out the Bizzarro et al. (2007) idea of late injection of ^{60}Fe. They determined an upper limit for early solar system $^{60}Fe/^{56}Fe$ of $<6\times10^{-7}$, which was consistent with the value inferred from in situ measurements, $(5–10)\times10^{-7}$ (Tachibana et al., 2006). Chen et al. (2009) also found no nickel isotopic anomalies in iron meteorites and chondrites, but Regelous et al. (2008) reported small anomalies in ^{60}Ni and ^{62}Ni in bulk iron and chondritic meteorites. From bulk carbonaceous chondrites, they found an upper limit of early solar system $^{60}Fe/^{56}Fe$ of $<3\times10^{-7}$, which is lower than the value from in situ measurement.

Quitté et al. (2010) reported nickel isotopes in angrites, ureilites, and CB chondrites. They obtained internal isochrons on the D'Orbigny, Sahara 99555 , and NWA 2999 angrites corresponding to $^{60}Fe/^{56}Fe$ ratios of $(4.1\pm2.6)\times10^{-9}$, $(1.8\pm0.5)\times10^{-9}$, and $<0.5\times10^{-9}$, respectively, as well as a bulk isochron from these three angrites, corresponding to a $^{60}Fe/^{56}Fe$ ratio of $(3.12\pm0.78)\times10^{-9}$. The latter isochron was interpreted as recording differentiation of the angrite parent bodies with the internal isochrons recording crystallization ages. Using the ^{53}Mn–^{53}Cr system, they back-calculated an early solar system ^{60}Fe/^{56}Fe ratio of $(1.8–2.9)\times10^{-8}$, a value more than an order of magnitude lower than that inferred from in situ measurements. Ureilites and the CB chondrite Gujba did not provide meaningful internal isochrons. Quitté et al. (2011) reported that the eucrites Bouvante and Juvinas showed clear evidence for in situ decay of ^{60}Fe, but the ^{60}Fe–^{60}Ni system was disturbed, making chronological interpretation difficult.

Nickel and iron isotopes have been measured in eucrites, ureilites, and aubrites as well as in chondrules from the unequilibrated ordinary chondrites Semarkona, Chainpur, and NWA 5717 and the CB chondrite Gujba (Tang and Dauphas, 2011, 2012). Internal isochrons from the D'Orbigny angrite and Semarkona and NWA 5717 chondrules and whole-rock isochrons from groups of meteorites were back-calculated using the ^{53}Mn-^{53}Cr chronometer and the early solar system ^{53}Mn/^{55}Mn ratio given in **Table 1** to obtain an overall early solar system ^{60}Fe/^{56}Fe ratios of $(7.1\pm2.3)\times10^{-9}$, much lower than the value inferred from in situ measurements and in a range consistent with inheritance of ^{60}Fe from the galactic background rather than a supernova contribution shortly before solar system formation (Tang and Dauphas, 2012). Compatible but slightly less stringent limits have been obtained by Spivak-Birndorf et al. (2011, 2012) from nickel isotopic analyses of angrites, ureilites, and ordinary chondrite chondrules. Tang and Dauphas (2012) also reported a bulk rock isochron for eucrites and inferred that core formation and global differentiation of Vesta occurred $3.7^{+2.5}_{-1.7}$ Ma after solar system formation, a time difference that is consistent with that inferred from the ^{53}Mn–^{53}Cr system.

The early solar system ^{60}Fe/^{56}Fe ratio of $(7.1\pm2.3)\times10^{-9}$ (Tang and Dauphas, 2012) is adopted here, as it is the highest precision data available and it is consistent with other high-precision data and all but one of the extant in situ measurements (Telus et al., 2012).

1.11.4.8 Manganese-53

Manganese-53 decays by electron capture to ^{53}Cr with a half-life of 3.7 Ma. This relatively long half-life and the fact that manganese and chromium are reasonably abundant elements that undergo relative fractionation in evaporation/condensation processes and magmatic processes make the ^{53}Mn–^{53}Cr system particularly interesting for bridging the time period from nebular events to accretion and differentiation of early-formed planetesimals. Accordingly, this system has been intensively investigated, and evidence of live ^{53}Mn has now been found in nebular components, such as: (1) CAIs (Birck and Allègre, 1985, 1988; Papanastassiou et al., 2002); (2) chondrules (Nyquist et al., 2001; Yamashita et al., 2010; Yin et al., 2007); (3) bulk ordinary chondrites (Lugmair and Shukolyukov, 1998; Nyquist et al., 2001); (4) bulk carbonaceous chondrites (Birck et al., 1999; Moynier et al., 2007; Petitat et al., 2011b; Qin et al., 2010a); (5) CI carbonates (Endress et al., 1996; Fujiya et al., 2012; Hoppe et al., 2007; Hutcheon and Phinney, 1996; Hutcheon et al., 1999a,b; Petitat et al., 2011b); (6) fayalite in CV chondrites (Jogo et al., 2009); (7) enstatite chondrite sulfides (Wadhwa et al., 1997); and (8) various achondrites including angrites, eucrites, diogenites, pallasites, ureilite, and SNC meteorites (Lugmair and Shukolyukov, 1998; Nyquist et al., 2003; Qin et al., 2010a,b; Yamakawa et al., 2010). Due to the wealth of high-quality data, an impressively detailed high-resolution relative chronometry can be developed (e.g., Lugmair and Shukolyukov, 2001), however interpretation of the ^{53}Mn–^{53}Cr system with respect to other chronometers is complex, particularly with respect to nebular events. The primary reasons for these complexities are difficulty in evaluating the initial ^{53}Mn/^{55}Mn of the solar system and in establishing its homogeneity in the nebula (see discussions in Birck et al., 1999; Lugmair and Shukolyukov, 2001; Nyquist et al., 2001; Trinquier et al., 2007, 2008).

As with ^{26}Al, ^{41}Ca, and ^{10}Be, the obvious samples in which to try to establish the solar system initial value for ^{53}Mn/^{55}Mn are CAIs. However, in this case there are three factors which work against this goal: (1) volatility-controlled fractionation is not favorable when the parent, ^{53}Mn, is more volatile than the daughter, ^{53}Cr; (2) both manganese and chromium are moderately volatile elements and significantly depleted in CAIs; and (3) the daughter element is known to exhibit nucleogenetic anomalies in most CAIs (e.g., Papanastassiou, 1986). Together, these properties mean that there are no mineral phases with large Mn/Cr in CAIs, and it is not feasible to find large ^{53}Cr excesses that are uniquely and fully attributable to ^{53}Mn decay. Birck and Allègre (1988) first demonstrated the in situ decay of ^{53}Mn by correlating ^{53}Cr excesses with Mn/Cr in mineral separates of an Allende inclusion, deriving an initial ^{53}Mn/^{55}Mn$\,=(3.7\pm1.2)\times10^{-5}$. Comparison to other Allende CAIs led these authors to estimate $\sim4.4\times10^{-5}$ as the best initial ^{53}Mn/^{55}Mn for CAIs; however, Nyquist et al. (2001) prefer a somewhat lower value $(2.8\pm0.3)\times10^{-5}$ based on the same mineral separate analyses plus consideration of non-radiogenic chromium in a spinel separate from an Efremovka CAI. Birck et al. (1999) emphasized that refractory inclusions are inconsistent with solar system evolution of the ^{53}Mn–^{53}Cr system, noting that the inferred chronology is necessarily model-dependent. Lugmair and Shukolyukov (1998) reach a similar assessment, describing the 'chronological meaning of ^{53}Mn/^{55}Mn ratios in CAIs' as 'tentative.' Papanastassiou et al. (2002) also studied ^{53}Mn–^{53}Cr systematics of CAIs and concluded that although spinel preserved the initial ^{53}Cr/^{52}Cr ratio, manganese with live ^{53}Mn was introduced during secondary alteration, so it was not clear what event was being dated in CAIs. As shown in the succeeding text, the early solar system ^{53}Mn/^{55}Mn can be reliably derived from differentiated meteorites.

Chromium has four stable isotopes, ^{50}Cr, ^{52}Cr, ^{53}Cr, and ^{54}Cr. Mass fractionation in isotopic measurements can alter ^{53}Cr/^{52}Cr ratios, but these are corrected for by normalizing measured data for all isotopes to the terrestrial ^{50}Cr/^{52}Cr ratio. Under the assumption that there are no nucleosynthetic anomalies in ^{54}Cr, Lugmair and colleagues routinely used the small deviations in the mass-fractionation corrected ^{54}Cr/^{52}Cr ratio to make a 'second-order' correction on ^{53}Cr/^{52}Cr (e.g., Lugmair and Shukolyukov, 1998). It has been known for some time that CI and CM chondrites have nucleosynthetic ^{54}Cr anomalies (Podosek et al., 1997; Rotaru et al., 1992). This was recognized for carbonaceous chondrites and ^{54}Cr anomalies were even recognized at the Cretaceous–Tertiary boundary and used to identify the impactor (Shukolyukov and Lugmair, 1998). Trinquier et al. (2007, 2008) have recently analyzed a number of meteorites, correcting chromium isotopic data only for mass fractionation using $^{50}Cr/^{52}Cr$ and found that eucrites, diogenites, mesosiderites, and pallasites have a uniform deficit in ^{54}Cr of 0.73 ± 0.02 ε-units (parts in 10^4) and that carbonaceous chondrites are enriched in ^{54}Cr by 0.6–1.5 ε. Trinquier et al. (2008) reported a new ^{53}Mn–^{53}Cr isochron for basaltic achondrites without making a second-order correction. Their slope corresponded to $^{53}Mn/^{55}Mn = (4.21 \pm 0.42) \times 10^{-6}$, in excellent agreement with Lugmair and Shukolyukov (1998), but the intercept was $\varepsilon^{53}Cr = -0.12 \pm 0.05$, rather than +0.25, a shift of 0.4 ε (**Figure 7**). Lugmair and Shukolyukov (1998) had asserted that a range in intercepts among bulk meteorites of different types implied a radial gradient in $^{53}Mn/^{55}Mn$ in the early solar system, but the new data of Trinquier et al. (2007, 2008) are consistent with $^{53}Mn/^{55}Mn$ being homogeneous in the early solar system and other workers have concurred with this assessment.

The initial $^{53}Mn/^{55}Mn$ ratio of the solar system must be inferred from well-defined isochrons on younger objects of known age. With the discovery of variations in $^{235}U/^{238}U$ ratios, there are relatively few anchors with reliable ages. The obvious choice is the D'Orbigny angrite, but a well-defined internal isochron measured by Glavin et al. (2004) was done before it was recognized that second-order corrections to ^{54}Cr can be problematic. However, the second-order correction affects the intercept more than the slope of an isochron (e.g., **Figure 7**). The Glavin et al. (2004) isochron is used, corresponding to a $^{53}Mn/^{55}Mn$ ratio of $(3.24 \pm 0.04) \times 10^{-6}$, with the uranium isotope-corrected Pb–Pb ages of D'Orbigny, 4563.37 ± 0.25 Ma (Brennecka and Wadhwa, 2012), and the weighted average of Allende CAI SJ101 and three Efremovka CAIs, 4567.30 ± 0.16 Ma (Amelin et al., 2010; Connelly et al., 2012), to infer an early solar system $^{53}Mn/^{55}Mn$ ratio of $(6.71 \pm 0.56) \times 10^{-6}$. This value agrees with the value

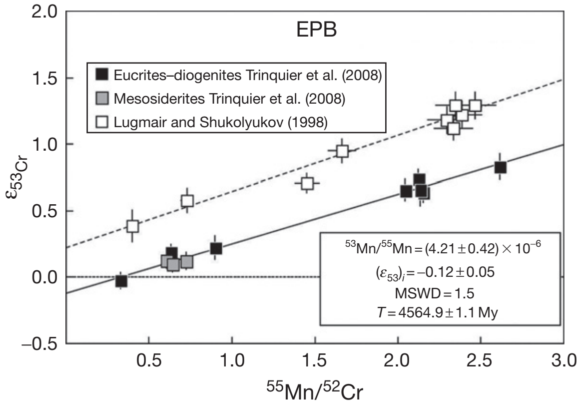

Figure 7 ^{53}Mn–^{53}Cr isochrons for meteorites that formed on the HED (howardite–eucrite–diogenite) parent body, likely Vesta. The isochrons of Lugmair and Shukolyukov (1998) and Trinquier et al. (2008) are nearly the same, but the newer data show a significantly different intercept because the older technique of making a second-order correction based on ^{54}Cr was not used (see text). Figure slightly modified from Trinquier A, Birck J-L, Allègre CJ, Göpel C, and Ulfbeck D (2008) ^{53}Mn–^{53}Cr systematics of the early solar system revisited. *Geochimica et Cosmochimica Acta* 72: 5146–5163.

calculated by Trinquier et al. (2008), $(6.28 \pm 0.66) \times 10^{-6}$, based on a well-defined ^{53}Mn–^{53}Cr isochron for the St. Marguerite chondrite, for which no ^{54}Cr second-order correction was done, and the Pb–Pb ages of phosphates in the St. Marguerite and CAIs from CV chondrites, for which the uranium isotope ratios were not measured. Now that it is known that ^{54}Cr second-order corrections should not be done and uranium isotope measurements are required for accurate Pb–Pb ages, neither of the aforementioned approaches is ideal, but are the best available at this writing.

Whole chondrule ^{53}Mn–^{53}Cr isochrons have been reported for the ordinary chondrites Chainpur (LL3.4) and Bishunpur (LL3.1) by Nyquist et al. (2001). The chondrules from both meteorites are consistent with a single isochron with $(^{53}Mn/^{55}Mn)_0 = (8.8 \pm 1.9) \times 10^{-6}$ and an intercept $\varepsilon(^{53}Cr) = -0.03 \pm 0.06$. If the chondrule data are considered with ^{53}Mn–^{53}Cr data for whole chondrites (Nyquist et al., 2001), then the slope increases slightly to $(^{53}Mn/^{55}Mn)_0 = (9.5 \pm 0.7) \times 10^{-6}$ which Nyquist and colleagues interpret as reflecting the time of Mn/Cr fractionation during the condensation of chondrule precursors. However, the ratio inferred by Nyquist et al. (2001) is higher than the early solar system ratio inferred by Trinquier et al. (2008) and this work, which seems unlikely. Yin et al. (2007) studied the ^{53}Mn–^{53}Cr system in a suite of chondrules from the Chaipur chondrite and obtained a lower $^{53}Mn/^{55}Mn$ ratio of $(5.1 \pm 1.6) \times 10^{-6}$ which corresponds to formation 1.4 Ma after CAIs.

As alluded to earlier in the discussion of absolute ages of differentiated objects, the eucrites have suffered a more prolonged and complex thermal and shock history, which is reflected in their internal ^{53}Mn–^{53}Cr systematics. Despite this, excesses of ^{53}Cr in *bulk* samples of eucrites are well correlated with Mn/Cr, indicating large-scale differentiation on the eucrite parent body prior to the decay of ^{53}Mn (Lugmair and Shukolyukov, 1998). The slope of the correlation line yields $^{53}Mn/^{55}Mn = (4.7 \pm 0.5) \times 10^{-6}$. As mentioned earlier, issues with second-order corrections based on ^{54}Cr have little effect on slopes of isochrons: Trinquier et al. (2008) obtained a $^{53}Mn/^{55}Mn$ ratio of $(4.21 \pm 0.42) \times 10^{-6}$ for eucrites and diogenites (**Figure 7**). Thus, these data indicate that the parent asteroid of the eucrites (Vesta) was totally molten a little more than 2 Ma after CAI formation. It should be clear that this time does not necessarily represent the crystallization age of individual eucrite meteorites, but the last time of global chromium isotope equilibration and Mn/Cr fractionation. In fact, internal ^{53}Mn–^{53}Cr isochrons for individual cumulate and noncumulate eucrites show a range of apparent $^{53}Mn/^{55}Mn$ values, from close to the global fractionation event (e.g., 3.7×10^{-6} for Chervony Kut) to essentially 'dead' ^{53}Mn (e.g., for the Caldera eucrite, Wadhwa and Lugmair, 1996). It is not certain whether these ages, especially the young ones, reflect prolonged igneous activity over a period of tens of millions of years, or cooling ages, or disturbance of the ^{53}Mn–^{53}Cr system by impacts, or some combination of the aforementioned (Lugmair and Shukolyukov, 1998).

The ^{53}Mn–^{53}Cr system has also proved useful in constraining the timescales of nebular fractionation. Shukolyukov and Lugmair (2006) measured several bulk carbonaceous chondrites and found that they lie along an isochron corresponding to $^{53}Mn/^{55}Mn = (8.5 \pm 1.5) \times 10^{-6}$. They noted the similarity of this value to the inferred CAI value and suggested that nebular fractionation of Mn/Cr occurred essentially at the same time as CAI formation. Moynier et al. (2007) repeated this experiment with another suite of bulk carbonaceous chondrites and found $^{53}Mn/^{55}Mn=(8.1\pm1.2)\times10^{-6}$. However, both of these $^{53}Mn/^{55}Mn$ ratios are slightly higher than current estimates of the early solar system ratio. Trinquier et al. (2008) found that bulk ordinary, enstatite, and carbonaceous chondrites lie on an isochron corresponding to $^{53}Mn/^{55}Mn=(6.5\pm1.9)\times10^{-6}$, a slope indistinguishable from the early solar system value, indicating nebular Mn/Cr fractionation at around the same time as CAI formation (with an uncertainty of 1.7 Ma). They also used internal ^{53}Mn–^{53}Cr isochrons to conclude that metamorphism occurred on carbonaceous chondrites 1–6 Ma after CAI formation. Scott and Sanders (2009) further examined the implications of the bulk chondrite isochron and proposed that planetesimals formed very early, but were broken up and reaccreted to form the carbonaceous chondrite parent bodies 1–5 Ma after CAIs. Qin et al. (2010a) analyzed a number of bulk carbonaceous chondrites and found that although they have different anomalies in ^{54}Cr, they all have about the same ^{53}Cr excess and thus do not give a well-defined isochron. They did a number of tests of their procedures and suggested that earlier workers may not have completely dissolved their samples. By combining data for bulk carbonaceous and ordinary chondrites, they obtained an isochron corresponding to $^{53}Mn/^{55}Mn=(5.4\pm2.4)\times10^{-6}$, which is in agreement with current estimates of the early solar system $^{53}Mn/^{55}Mn$ ratio, but is not well constrained, as the uncertainty translates to a range of 2.6 Ma.

Secondary alteration on the parent bodies of some carbonaceous chondrites can be dated because of the high Mn/Cr ratios in some aqueously precipitated minerals. Carbonates from CI and CM chondrites show large ^{53}Cr excesses correlated with Mn/Cr; inferred initial $^{53}Mn/^{55}Mn$ ratios range from $(5.2\pm1.1)\times10^{-6}$ to $(1.42\pm0.32)\times10^{-6}$ (Endress et al., 1996; Fujiya et al., 2012; Hoppe et al., 2007; Petitat et al., 2011b), corresponding to formation 1.4 ± 1.2 to 8.4 ± 1.2 Ma after CAI formation. Fayalite (FeO-rich olivine) from the oxidized and aqueously altered CV3 chondrites Mokoia, Kaba, and Vigarano formed with very high $^{55}Mn/^{52}Cr$ ratios ($>10^4$) and all show the same $^{53}Mn/^{55}Mn$ ratio of $\sim2.3\times10^{-6}$ (Hua et al., 2005; Hutcheon et al., 1998; Jogo et al., 2009), indicating formation 5.8 Ma after CAIs.

1.11.4.9 Palladium-107

Palladium-107 β^--decays to ^{107}Ag with a half-life of 6.5 Ma. Evidence for this now-extinct nuclide is found in metallic phases of iron meteorites since large Pd/Ag fractionations occur during magmatic partitioning of metal (Kelly and Wasserburg, 1978; see also review by Wasserburg, 1985). Kaiser and Wasserburg (1983) demonstrated that a linear correlation exists between excess $^{107}Ag/^{109}Ag$ and Pd/Ag in different fractions of metal and sulfide from the Grant group IIIB iron meteorite and from the isochron inferred an initial $^{107}Pd/^{108}Pd=\sim1.7\times10^{-5}$ at the time of crystallization of this meteorite. Extrapolation back to the time of CAI formation would yield an initial $^{107}Pd/^{108}Pd$ of approximately twice this value for the solar system, though with considerable uncertainty. Further isochrons were determined in many other iron and stony-iron meteorites, showing that there is a wide range of initial $^{107}Pd/^{108}Pd$ ratios, but that many samples have ratios in the range $(1.5–2.5)\times10^{-5}$ (Chen and Wasserburg, 1996; Chen et al., 2002). There are a few iron meteorites and pallasites for which ^{107}Pd–^{107}Ag systematics have been studied and the ^{53}Mn–^{53}Cr systematics have been determined in phosphate inclusions (Chen and Wasserburg, 1996). Some are clearly disturbed, but extrapolation of the line through four iron meteorites to the early solar system $^{53}Mn/^{55}Mn$ ratio of $\sim6.7\times10^{-6}$ implies an early solar system $^{107}Pd/^{108}Pd$ ratio of $\sim5\times10^{-6}$. Carlson and Hauri (2001) developed ICPMS methods for determining silver isotope ratios with high precision, thus permitting the investigation of phases with more moderate Pd/Ag fractionation. They found good isochrons for the Brenham pallasite and the Grant IIIB iron meteorite, both with inferred initial $^{107}Pd/^{108}Pd=1.6\times10^{-5}$. A two-point correlation between metal and sulfide was also determined for Canyon Diablo group IA iron meteorite, yielding an apparent initial $^{107}Pd/^{108}Pd$ essentially identical to the highest $^{107}Pd/^{108}Pd$ ratio previously found for the Gibeon group IVB iron meteorite (Chen and Wasserburg, 1990). Interpreted chronologically, the data imply that Brenham and Grant formed about 3.5 Ma after Canyon Diablo.

Theis et al. (2013) studied the palladium-silver systematics of group IAB iron meteorites and found ages of 15–19 Ma after solar system formation. Group IAB irons appear to have formed by partial melting of metal and sulfide, which then infiltrated silicate. Hafnium-tungsten dating indicates that core formation on the IAB parent body occurred ∼5 Ma after solar system formation (see **Section 1.11.4.10**). A catastrophic impact then broke up and reassembled the parent body. The Theis et al. results indicate that there was sufficient heating on the IAB parent body for partial melting of metal and sulfide 15 Ma after solar system formation. Slow cooling followed, as indicated by the late date from the lead-thallium system (see **Section 1.11.4.13**).

Schönbächler et al. (2008) found small variations in $^{107}Ag/^{109}Ag$ that correlated with Pd/Ag ratios among bulk carbonaceous chondrites. Assuming that this represents an isochron and based on the ^{53}Mn–^{53}Cr evidence that volatility fractionation preserved in bulk carbonaceous chondrites occurred at essentially the same time as CAI formation, they recommended an early solar system $^{107}Pd/^{108}Pd$ ratio of $(5.9\pm2.2)\times10^{-5}$ which is in agreement with, but perhaps more robust than, the value inferred from iron meteorites.

1.11.4.10 Hafnium-182

Hafnium-182 β^--decays to ^{182}W with a half-life of 8.90 Ma. The importance of the ^{182}Hf–^{182}W system arises from its unique sensitivity to metal–silicate fractionation and the rather long half-life of ^{182}Hf, which makes this system a useful probe for both nebular and planetary processes. Specifically, tungsten is highly siderophile, whereas hafnium is retained in silicates during melting and metal segregation. Thus, tungsten isotopic compositions could be very different in silicates and metal from distinct planetary objects depending on whether or not metal/silicate fractionation in those objects predated significant decay of ^{182}Hf. The ^{182}Hf–^{182}W system can be used in two ways: (1) the slopes of isochrons give $^{182}Hf/^{180}Hf$ ratios at the time of crystallization or Hf/W fractionation, which can be converted to time differences, and (2) the intercepts of isochrons, or the tungsten isotopic compositions of iron meteorites that have no hafnium, can be used to date core formation of asteroids and planets. Tungsten has five stable isotopes, ^{180}W (0.12%), ^{182}W (26.50%), ^{183}W (14.31%), ^{184}W (30.64%), and ^{186}W (28.43%). Data are normalized to ^{183}W or ^{184}W (both have been used) and instrumental mass fractionation is corrected for by normalizing to the terrestrial $^{186}W/^{183}W$ or $^{186}W/^{184}W$ ratio. Since tungsten isotopic variations are small, they are usually expressed as $\varepsilon^{182}W$ values, in parts per 10 000. Inferred amounts of ^{182}Hf are normalized to stable ^{180}Hf, an abundant (35.08%) isotope of hafnium.

Since the discovery that ^{182}Hf was present in the early solar system (Harper and Jacobsen, 1996; Harper et al., 1991; Lee and Halliday, 1995), there have been a number of significant changes in the understanding of the ^{182}Hf–^{182}W system. The initial estimate of the early solar system was $^{182}Hf/^{180}Hf \geq (2.63 \pm 0.13) \times 10^{-4}$, based on the difference in tungsten isotopic composition between chondrites ($\varepsilon^{182}W \sim 0$) and hafnium-free iron meteorites ($\varepsilon^{182}W \sim -4$) (Lee and Halliday, 1995). A number of ^{182}Hf–^{182}W studies of chondrites, achondrites, and the Moon were done in the next few years (Halliday, 2000; Halliday and Lee, 1999; Lee and Halliday, 1996, 2000a, b; Quitté et al., 2000), leading to the important conclusions that the moon-forming giant impact occurred at least 50 Ma after formation of the Earth and that core formation on Vesta occurred more than 10 Ma after CAI formation.

There was a seismic shift in the world of ^{182}Hf–^{182}W chronometry with the realization that the early measurements of chondrites were in error and chondrites actually have $\varepsilon^{182}W$ values of ~ -2 rather than 0 (Kleine et al., 2002; Schoenberg et al., 2002; Yin et al., 2002). This shift is highly significant affecting all of the prior conclusions. Now, the early solar system value was $^{182}Hf/^{180}Hf = \sim 1 \times 10^{-4}$, the moon-forming impact occurred ~ 30 Ma after CAIs, and core formation on Vesta occurred ~ 3 Ma after CAIs. There has never been a satisfactory explanation published of why the early $\varepsilon^{182}W$ values for chondrites were incorrect, but all laboratories working on the ^{182}Hf–^{182}W system for the last 10 years or so agree on the chondritic value. The best estimate of the present-day chondritic $\varepsilon^{182}W$ value comes from carbonaceous chondrites, which have solar Hf/W ratios. The data for chondrites were summarized by Kleine et al. (2009) and carbonaceous chondrites have an average $\varepsilon^{182}W$ value of -1.9 ± 0.1.

Internal isochrons, demonstrating good correlations of $^{182}W/^{180}W$ with Hf/W, are found for several separates of ordinary chondrites (Kleine et al., 2002; Yin et al., 2002); samples of whole-rock carbonaceous chondrites and a CAI from Allende also fall within error of these isochrons (Yin et al., 2002). The Pb–Pb ages of phosphates in the ordinary chondrites (Kleine et al., 2002) and the coincidence of the CAI data (Yin et al., 2002) allow an estimate of the initial $^{182}Hf/^{180}Hf$ of the solar system of 1.0–1.1×10^{-4} with an initial $^{182}W/^{180}W$ significantly ($\sim -3\varepsilon$) lower than terrestrial mantle samples. A regression through data for two bulk CAIs, several fragments of a single CAI and bulk carbonaceous chondrites yielded a more precise early solar system $^{182}Hf/^{180}Hf$ value, $(1.07 \pm 0.10) \times 10^{-4}$, and $\varepsilon^{182}W$ value, -3.47 (Kleine et al., 2005a). Burkhardt et al. (2008) obtained internal isochrons on four CAIs from the Allende CV chondrite, all of which are consistent with the same $^{182}Hf/^{180}Hf$ ratio, as are the bulk CAI data. A combined isochron (**Figure 8**) with all the mineral separate data gives a slope corresponding to $^{182}Hf/^{180}Hf = (9.72 \pm 0.44) \times 10^{-5}$. The intercept of the Burkhardt et al. (2008) isochron was $\varepsilon^{182}W_0 = -3.28 \pm 0.12$. Burkhardt et al. (2012) measured tungsten isotopic compositions of leachates from the Murchison CM chondrite. The covariation of isotope ratios in leachates provided a way to correct measured ^{182}W anomalies using $^{183}W/^{184}W$ ratios. The correction shifted the initial solar system $\varepsilon^{182}W$ value to -3.51 ± 0.10 and led to a very slight shift in the $^{182}Hf/^{180}Hf$ ratio to $(9.81 \pm 0.41) \times 10^{-5}$, the values adopted here, which affect Hf/W model ages and the evolution of $\varepsilon^{182}W$ with time.

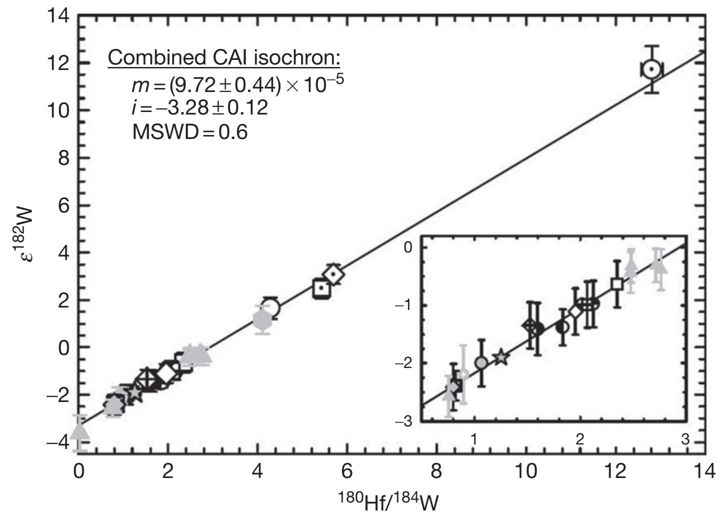

Figure 8 Combined ^{182}Hf–^{182}W isochron for five CAIs. Gray symbols are for a single CAI measured by Kleine et al. (2005a), and the remaining symbols are for four CAIs measured by Burkhardt et al. (2008). Reproduced from Burkhardt C, Kleine T, Bourdon B, et al. (2008) Hf–W mineral isochron for Ca, Al-rich inclusions: Age of the solar system and the timing of core formation in planetesimals. *Geochimica et Cosmochimica Acta* 72: 6177–6197.

Hafnium-182 decay leads to small variations in tungsten isotopic composition. The difference in $\varepsilon^{182}W$ between the early solar system value of -3.51 and the present-day bulk solar system value of -1.9 (the value found in bulk carbonaceous chondrites, Kleine et al., 2009) can be used as a chronometer if separation of a hafnium-free core occurred from a chondritic Hf/W reservoir in the first few million years of solar system history while ^{182}Hf was live. However, neutron capture effects due to cosmic ray exposure can also affect tungsten isotopic composition. Due to their long exposure ages, this problem was first recognized in iron meteorites, some of which have uncorrected $\varepsilon^{182}W$ values similar or below the early solar system estimated value of $\varepsilon^{182}W = -3.51$ (Kleine et al., 2005a; Markowski et al., 2006a,b; Qin et al., 2008b; Scherstén et al., 2006). The values below the early solar system value apparently result from cosmic ray exposure effects, but it does appear that a number of iron meteorites have the same tungsten isotopic composition as the early solar system. Qin et al. (2008a) showed that group IVB iron meteorites also have nucleosynthetic anomalies in ^{184}W, which makes a correction necessary to $\varepsilon^{182}W$ values, but only shifts ages by ~ 0.5 Ma. Even after correction for cosmic ray exposure and nucleosynthetic effects, some iron meteorites have lower $\varepsilon^{182}W$ values than the Burkhardt et al. (2008) CAI isochron intercept, -3.28. This problem was solved with the revised early solar system $\varepsilon^{182}W$ value of Burkhardt et al. (2012), which implies that cores formed on the parent bodies of magmatic iron meteorites within the first 2 Ma after CAI formation. The early formation of asteroidal cores was one of the major discoveries made possible by development of the ^{182}Hf–^{182}W system. Asteroidal core formation was extended to the stony-iron pallasites and mesosiderites by Quitté et al. (2005), who showed that the stony irons have a range of $\varepsilon^{182}W$ values from -4.2 to -1.9, indicating early core formation with later reequilibration of metal with silicate.

Snyder et al. (2001), Markowski et al. (2006a,b), Qin et al. (2008b), and Schulz et al. (2009, 2010) studied the ^{182}Hf–^{182}W system in nonmagmatic iron meteorites. Schulz et al. (2012) measured samarium isotopes in silicate-bearing nonmagmatic iron meteorites to correct for cosmic ray exposure effects on tungsten isotopes. Their data indicate that core formation on the IAB parent body occurred ~ 5 Ma after CAI formation. Group IIE irons are more complicated: Qin et al. (2008b) found a range of $\varepsilon^{182}W$ values and, based on a larger sample of IIE irons, Schulz et al. (2012) suggest that three melt pool formation events occurred on the IIE parent asteroid, at 3, 13, and 28 Ma after CAIs. Touboul et al. (2009b) studied the ^{182}Hf–^{182}W system in the primitive acapulcoite and lodranite achondrites. They inferred that the parent body of these meteorites accreted 1.5–2 Ma after CAI formation and reached a thermal maximum ~ 3 Ma after CAI formation. It also appears that ureilites differentiated early, also within the first 1–2 Ma of solar system history, as they have very low $\varepsilon^{182}W$ values (Lee et al., 2009).

Tungsten isotopes in eucrites are complicated and have been affected by core formation, planetary differentiation, and metamorphic redistribution of tungsten. Kleine et al. (2009) reviewed the ^{182}Hf–^{182}W record of eucrites. Model ages for core formation on the eucrite parent body are 1–4 Ma after CAI formation (Touboul et al., 2008). Srinivasan et al. (2007) were able to measure tungsten isotopes in eucrite zircons by ion microprobe, which showed that zircon crystallized <6.8 Ma after eucrite parent-body core formation and that metamorphism occurred at least 8.9 Ma after core formation. The angrites, particular those with quenched textures, D'Orbigny and Sahara 99555, have well-defined ^{182}Hf–^{182}W internal isochrons (Kleine et al., 2012; Markowski et al., 2007). Timescales implied by the ^{182}Hf–^{182}W, ^{53}Mn–^{53}Cr and Pb–Pb systems are internally consistent. A tungsten isotopic evolution diagram suggests that angrites sampled two mantle reservoirs with enhanced and different Hf/W ratios compared to chondritic. These mantle sources are the result of separate core formation events within 2 Ma of CAIs. Angrites crystallized 3.9–11.3 Ma after CAI formation (Kleine et al., 2012).

Application of the ^{182}Hf–^{182}W system to the timescales of accretion and core formation of the Earth is discussed with other isotopic and chemical evidence in **Chapter 2.8**. It is difficult to obtain firm constraints from the ^{182}Hf–^{182}W system because of early removal of tungsten into the core and overprinting from late accretion. The U–Pb and ^{182}Hf–^{182}W systems taken with chemical evidence suggest protracted accretion of the Earth and disequilibrium core formation. Touboul et al. (2012) reported small but well-resolved ^{182}W excesses in komatiites from Kostomuksha, but none in those from Komati, indicating that mantle heterogeneities from the first 30 Ma of solar system history are preserved. Willbold et al. (2011) found that 3.8-Ga-old rocks from Isua, Greenland, have slightly higher $\varepsilon^{182}W$ than other terrestrial rocks, which they suggested was related to late meteorite bombardment.

Tungsten isotopic studies of the Moon have proven difficult because of a significant contribution to ^{182}W anomalies from neutron capture on ^{181}Ta during cosmic ray exposure. Initial studies of the Moon did not take this effect into account and led to the conclusion that the Moon formed early and that the mantle remains poorly mixed (Lee et al., 1997). Leya et al. (2000) corrected previous data for cosmic ray effects and concluded that some of the ^{182}W excesses are radiogenic and that the Moon formed within the first 50 Ma of solar system history. Lee et al. (2002) confirmed the cosmic ray effect and analyzed samples with low cosmic ray exposure, which seem to be consistent with early formation of the Moon. Kleine et al. (2005b) attempted to avoid cosmic ray effects from ^{181}Ta by measuring tungsten isotopes in lunar metal grains. Some heterogeneities remained and they concluded that the lunar magma ocean crystallized ~ 50 Ma after solar system formation. Touboul et al. (2007) separated metal with greater care than previous workers and found no tungsten isotope variations, which implies that the Moon formed at least 60 Ma after solar system formation. The tungsten isotopic composition of the Moon is identical to that of the Earth, as are oxygen isotopes (Wiechert et al., 2001) and titanium isotopes (Zhang et al., 2012), which has implications for the origin of the Moon. Careful selection of lunar ferroan anorthosites reinforced the conclusion that the Moon has a homogeneous terrestrial tungsten isotopic composition (Touboul et al., 2009a).

Tungsten isotope constraints on processes on Mars are discussed in **Chapter 2.10**. A number of ^{182}Hf–^{182}W studies of Mars have been done, but were unable to tightly constrain the time of formation of Mars, because of uncertainty in the Hf/W ratio of the Martian mantle. Nimmo and Kleine (2007) were able to constrain this ratio to a precision of 25% using literature trace element data and concluded that Mars formed 0–10 Ma after solar system formation. Dauphas and Pourmand (2011) showed that there is an excellent correlation between Th/Hf and $^{176}Hf/^{177}Hf$ ratios in Martian meteorite samples, which they were able to use to tightly constrain the Hf/W ratio of the Martian mantle. This led to the remarkable conclusion that Mars accreted very rapidly and reached half its present size in only $1.8^{+0.9}_{-1.0}$ Ma after solar system formation. They suggest that Mars is a stranded planetary embryo (for more on embryos and planet formation, see **Chapter 2.4**).

1.11.4.11 Curium-247

Curium-247 decays by a series of α- and β⁻-decays to ^{235}U and can manifest itself as variations in the $^{235}U/^{238}U$ ratio. There are no stable isotopes of curium, so $^{235}U/^{238}U$ ratio variations must be related to two other elements that have been suggested as proxies for curium, namely, thorium and neodymium. This leads to two estimates for the early solar system $^{247}Cm/^{235}U$ ratio, $(2.4\pm0.6)\times10^{-4}$ based on Th/U and $(1.1\pm0.2)\times10^{-4}$ based on Nd/U (Brennecka et al., 2010). The implications for the U–Pb chronometer are discussed in detail in **Section 1.11.3.1.** The identification of ^{247}Cm as an early solar system short-lived radionuclide remains tentative, because other physical processes like evaporation or condensation might have led to small variations in $^{235}U/^{238}U$ ratios.

1.11.4.12 Iodine-129

Iodine-129 β^--decays to ^{129}Xe with a half-life of 15.7 Ma. As mentioned in the historical introduction (**Section 1.11.1.3**), ^{129}I was the first extinct isotope whose presence in the early solar system was inferred, from excesses of its daughter ^{129}Xe in meteorites (Jeffery and Reynolds, 1961). ^{129}I–^{129}Xe dating typically uses a method analogous to the ^{40}Ar–^{39}Ar method of potassium-argon dating, in which neutron irradiation is used to convert some stable ^{127}I into ^{128}Xe by neutron capture and β^- decay. In current practice, a standard and sample are irradiated together, and the I–Xe age of the sample is measured relative to that of the standard. The standard most widely used since the 1980s is enstatite from the Shallowater enstatite chondrite. The absolute Pb–Pb age of Shallowater enstatite, 4562.3±0.4 Ma, was established by Gilmour et al. (2006) and slightly revised by Gilmour et al. (2009). Both parent and daughter are mobile elements, and coupled with the relatively long half-life, this means that closure effects on the ^{129}I–^{129}Xe system likely limit its utility to parent-body processes (e.g., Swindle et al., 1996), although arguments have been advanced that ^{129}I–^{129}Xe can date nebular events in favorable circumstances (Whitby et al., 2001). New analytical techniques that enable the investigation of single mineral phases (Crowther et al., 2008; Gilmour and Saxton, 2001) have helped in the understanding of apparent I–Xe isochrons (as differentiated from mixing lines of multiple phases) and enabled more confident chronological interpretations, particularly of secondary mineral phases formed on asteroidal parent bodies. Brazzle et al. (1999) demonstrated concordancy between I–Xe and Pb–Pb chronometers for chondrite phosphates over a timescale of tens of millions of years. At another extreme, Whitby et al. (2000) found an initial ratio of $^{129}I/^{127}I=(1.35\pm0.05)\times10^{-4}$ in halite from a relatively unequilibrated ordinary chondrite. This result is close to the estimated initial value for the solar system ($\sim10^{-4}$), implying that the aqueous activity responsible for precipitating the halite occurred immediately upon accretion, probably within a few million years of CAI formation (Whitby et al., 2000). ^{129}I–^{129}Xe dating has recently been reviewed by Gilmour et al. (2006) and Hohenberg and Pravdivtseva (2008).

1.11.4.13 Lead-205

Lead-205 decays by electron capture to ^{205}Tl with a half-life of 17.3 Ma. It is unique among the short-lived radionuclides present in the early solar system in being produced only by *s*-process nucleosynthesis (see **Chapter 2.1**). Nielsen et al. (2006) reported a correlation between $^{205}Tl/^{203}Tl$ and $^{204}Pb/^{203}Tl$ ratios among metal and troilite from the IAB iron meteorites Toluca and Canyon Diablo that was consistent with $^{205}Pb/^{204}Pb=(7.4\pm1.0)\times10^{-5}$. The range in $^{205}Tl/^{203}Tl$ is ~5‰ and Nielsen et al. (2006) concluded that mixing of mass-fractionated components is unlikely to be the cause of this variation. Nielsen et al. (2006) used the ^{129}I–^{129}Xe age of silicate inclusions in group IAB iron meteorites to calculate an early solar system $^{205}Pb/^{204}Pb$ value of $(1.0–2.1)\times10^{-4}$. Baker et al. (2010) investigated the ^{205}Pb–^{205}Tl system in bulk carbonaceous chondrites. They found a good correlation between $^{205}Tl/^{203}Tl$ and $^{204}Pb/^{203}Tl$ ratios (**Figure 9**), consistent with an initial solar system $^{205}Pb/^{204}Pb$ value of $(1.0\pm0.4)\times10^{-3}$, significantly higher than the previous value of Nielsen et al. (2006). This value implies formation of group IAB silicate inclusions 57^{+14}_{-10} Ma after solar system formation, which is in conflict with the shorter, but rather uncertain, intervals of ~20 Ma inferred from ^{109}Pd–^{109}Ag and ^{129}I–^{129}Xe ages (Baker et al., 2010), but may indicate a

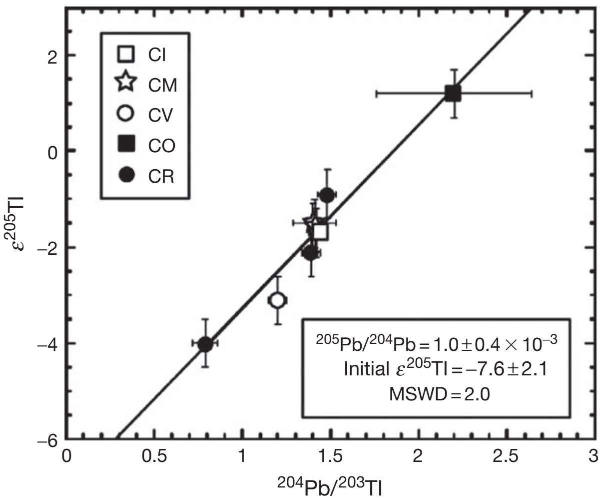

Figure 9 ^{205}Pb–^{205}Tl isochron for bulk carbonaceous chondrites. Reproduced from Baker RGA, Schönbächler M, Rehkämper J, Williams H, and Halliday AN (2010) The thallium isotope composition of carbonaceous chondrites – New evidence for live ^{205}Pb in the early solar system. *Earth and Planetary Science Letters* 291: 39–47.

complex thermal history (Section 1.11.4.9). The utility of the $^{205}Pb-^{205}Tl$ system as a chronometer remains limited, because thallium has only two stable isotopes, $^{205}Tl/^{203}Tl$ variations are small, and natural mass fractionation may have occurred.

1.11.4.14 Niobium-92

Niobium-92 decays by electron capture to ^{92}Zr with a half-life of 36 Ma. ^{92}Nb is a *p*-process nuclide (see Chapter 2.1). The first hint that this isotope was present in the early solar system was based on an $8.8 \pm 1.7\varepsilon$ excess in ^{92}Zr in a niobium-rich rutile grain from the Toluca IAB iron meteorite (Harper, 1996). This corresponded to an initial $^{92}Nb/^{93}Nb$ ratio of $(1.6 \pm 0.3) \times 10^{-5}$, but the time of formation of Toluca rutile is not known. Three subsequent studies that used MC-ICPMS to measure zirconium isotopic composition reported that the initial solar system $^{92}Nb/^{93}Nb$ was $\sim 10^{-3}$, higher by two orders of magnitude (Münker et al., 2000; Sanloup et al., 2000; Yin et al., 2000). This initial $^{92}Nb/^{93}Nb$ is nearly one quarter of the *p*-process production ratio (Harper, 1996) and was difficult to understand, as most ^{93}Nb is made by the *s*-process. The situation has been resolved with the work of Schönbachler et al. (2002), who reported internal $^{92}Nb-^{92}Zr$ isochrons for the Estacado H6 chondrite and for a clast from the Vaca Muerta mesosiderite, both of which give an initial solar system $^{92}Nb/^{93}Nb$ of $\sim 10^{-5}$, a much more plausible value in terms of nucleosynthetic considerations. This lower initial ratio limits the utility of the $^{92}Nb-^{92}Zr$ for chronometry.

1.11.4.15 Samarium-146

Samarium-146 decays by α-decay to ^{142}Nd with a half-life of 68 ± 7 Ma (Kinoshita et al., 2012). An important property of the Sm–Nd system is that the short-lived $^{146}Sm-^{142}Nd$ chronometer can be used along with the long-lived $^{147}Sm-^{143}Nd$ chronometer ($T_{1/2} = 117$ Ga) to study mantle–crust evolution on differentiated planets. The presence in the early solar system of ^{146}Sm was first demonstrated by Lugmair et al. (1983). There was significant interest in this system in meteorites in the 1980s and early 1990s (e.g., Prinzhofer et al., 1989; Stewart et al., 1994). There has been renewed interest in the $^{146}Sm-^{142}Nd$ system in the past 10 years since the development of robust measurements of small variations in the neodymium isotopic composition of Archean rocks (Caro et al., 2003), implying differentiation of the Earth's mantle within the first 200 Ma of solar system history. This work was preceded by a 10-year search for effects of ^{146}Sm decay in Archean rocks in which small effects were claimed but disputed by others. Application of the coupled $^{146}Sm-^{142}Nd$ and $^{147}Sm-^{143}Nd$ systems to planetary differentiation is discussed in more detail in Chapter 1.12. For a more detailed discussion of the application of the $^{146}Sm-^{142}Nd$ system to early Earth history, see Caro (2011).

The recent remeasurement of the half-life of ^{146}Sm led to a decrease from 103 to 68 Ma (Kinoshita et al., 2012). This has led to a revision of the early solar system $^{146}Sm/^{144}Sm$ ratio to 0.0094 ± 0.0005 compared to the previous value of 0.0085 ± 0.0007 (Boyet et al., 2010). Kinoshita et al. (2012) briefly discussed the implications of the new half-life for lunar and Martian chronology, but the chronological implications of many previous $^{146}Sm-^{142}Nd$ studies will need to be reevaluated.

1.11.4.16 Plutonium-244

Plutonium-244 is the longest lived of the short-lived isotopes considered to be extinct on Earth today (Lachner et al., 2012). ^{244}Pu mostly decays by α-decay to ^{240}U, which decays further to join the ^{232}Th decay chain, ending at ^{208}Pb. As ^{208}Pb excesses could arise from ^{244}Pu or much more abundant ^{232}Th, the presence of ^{244}Pu can be recognized from the unique pattern of xenon isotopes that arise from the minor fraction of ^{244}Pu that decays by spontaneous fission (Alexander et al., 1971). The early solar system $^{244}Pu/^{238}U$ ratio of 7×10^{-3} is based on xenon isotopic analysis of the St. Severin chondrite (Hudson et al., 1988). However, ^{244}Pu has not been developed for chronological applications for a very practical reason: there are no long-lived isotopes of plutonium against which to normalize its abundance. The primary application of ^{244}Pu in meteorite studies is for obtaining cooling rates from the annealing of fission tracks in appropriate minerals (e.g., Pellas and Storzer, 1981; Pellas et al., 1997).

1.11.5 Origins of the Short-Lived Nuclides

The ability of short-lived radioisotopes to function as chronometers for the early solar system is critically dependent on there having been an initially uniform distribution of the radioactivity throughout the nebula or at least in those regions from which meteoritic components are derived. Only in this circumstance can differences in initial abundances of a radionuclide compared to a stable counterpart, as inferred by the excesses of the respective daughter isotope, be interpreted as due to radioactive decay from the initial inventory. The homogeneity of the distribution of radionuclides in the solar nebula depends, in turn, on the processes that created those isotopes some time before the formation of early solar system materials. For the longer-lived and some low-abundance isotopes listed in Table 1, ^{60}Fe, ^{182}Hf, ^{247}Cm, ^{129}I, ^{205}Pb, ^{92}Nb, ^{146}Sm, and ^{244}Pu, continuous nucleosynthesis may have been sufficient to produce a quasiequilibrium abundance of these species that was inherited by the solar nebula. However, the shorter half-life isotopes require a more immediate source (e.g., Meyer and Clayton, 2000; Wasserburg et al., 1996, 2006) and homogeneity must be assessed by testing consistency of derived chronologies.

1.11.5.1 Sources of Short-Lived Nuclides

The primary sources of most short-lived nuclides are almost certainly dying stars (^{7}Be, ^{36}Cl, and ^{10}Be being the exceptions). Massive stars (15–40 $M_{\odot}$) that end their lives as Type II supernovae can produce ^{41}Ca, ^{26}Al, ^{135}Cs, ^{60}Fe, ^{53}Mn, ^{107}Pd, ^{182}Hf, ^{247}Cm, ^{129}I, ^{92}Nb, ^{146}Sm, and ^{244}Pu prior to explosion and/or during explosive nucleosynthesis (including *p*-process and *r*-process nucleosynthesis). Aluminum-26 can also be produced in the more massive of these stars (Wolf–Rayet stars) and ejected from the star in stellar winds prior to the ultimate explosion. The AGB stage of stellar evolution of low-mass

(1.5–$3\,M_{\odot}$) stars is where most *s*-process nucleosynthesis takes place. AGB stars can produce ^{41}Ca, ^{26}Al, ^{135}Cs, ^{60}Fe, ^{107}Pd, ^{129}I, and ^{205}Pb (Wasserburg et al., 1994, 2006). Steady-state long-term galactic nucleosynthesis can explain the observed initial solar system abundances of ^{53}Mn, ^{182}Hf, ^{247}Cm, ^{146}Sm, and ^{244}Pu, as well as ^{235}U, ^{238}U, and ^{232}Th. As mentioned earlier, the early solar system level of ^{60}Fe remains uncertain. The low ^{60}Fe/^{56}Fe value inferred from chondrites and achondrites (e.g., Tang and Dauphas, 2012) is consistent with long-term galactic production. If the higher value inferred by in situ (SIMS) measurements (e.g., Telus et al., 2012) can be confirmed, it would imply a Type II supernova shortly before solar system formation and require an explanation for the lack of radiogenic ^{60}Ni in early protoplanetary melts. ^{129}I is anomalous, in that the early solar system contains 20–50 times less ^{129}I than is expected from uniform galactic production (Wasserburg et al., 2006). The remaining short-lived nuclides, ^{7}Be, ^{41}Ca, ^{36}Cl, ^{26}Al, ^{10}Be, ^{135}Cs, ^{107}Pd, and ^{205}Pb seem to require a late addition to solar system materials (Wasserburg et al., 2006), but multiple sources are needed.

Some short-lived nuclides are likely to have formed by spallation reactions with nuclear particles (protons, α-particles) accelerated by interaction with an active young Sun (e.g., Duprat and Tatischeff, 2007; Gounelle et al., 2001; Lee et al., 1998; Leya et al., 2003; Sahijpal and Soni, 2007). Beryllium-7 certainly requires local production by irradiation in the solar system because of its short half-life, but evidence for its presence in CAIs remains tentative (Chaussidon et al., 2006a,b). Beryllium-10 requires irradiation for production, as it cannot be made in stars, but the irradiation could either be local or by cosmic rays in the interstellar medium (Desch et al., 2004). However, the spread in initial ^{10}Be/^{9}Be among refractory objects of similar age is best explained as due to local irradiation with trapped cosmic rays likely to be only a minor component of the ^{10}Be inventory (Liu et al., 2009). Wielandt et al. (2012) suggested that FUN CAIs, which have low, but detectable ^{10}Be/^{9}Be ratios, represent the baseline level in presolar materials, and that normal CAIs, with higher, but variable ^{10}Be/^{9}Be ratios, require an additional spallation component that forms in the solar system. Chlorine-36 is only found in minerals that form by secondary alteration in CAIs. Correction to an early solar system value using ^{26}Al in the same minerals leads to ^{36}Cl/^{35}Cl ratios so high that they cannot be produced in supernovae or AGB stars (Hsu et al., 2006; Jacobsen et al., 2011), so a late stage solar system irradiation seems to be required. There are ways to make ^{26}Al and ^{53}Mn by solar system irradiation, but the irradiation needed to explain ^{10}Be underproduces ^{26}Al and ^{53}Mn by a factor of 10 (Duprat and Tatischeff, 2007).

This leaves a number of short-lived nuclides that require a late stellar source: ^{26}Al, ^{135}Cs, ^{107}Pd, and ^{205}Pb. All of these isotopes can be made in AGB stars, and all but ^{205}Pb can be made in Type II supernovae, but production of observed levels in supernovae gives a higher level of ^{53}Mn than is observed (Wasserburg et al., 2006). The major difficulty with AGB stars is that this brief stage occurs after more than a billion years of stellar evolution and thus would require the coincidence that an AGB star was in the vicinity of the Sun's stellar nursery. Also, shock waves from planetary nebulae around AGB stars seem to be too thick to inject the required amounts of short-lived nuclides (Boss and Keiser, 2010). On the other hand, massive stars evolve rapidly before star-forming regions can disperse, so that they can trigger star formation (Boss and Keiser, 2012; Cameron, 2001a,b; Cameron and Truran, 1977; Cameron et al., 1995; Hester et al., 2004). The injection of radioactive stellar debris in a 'triggered' collapse scenario for solar system formation was recently reviewed by Boss (2012).

1.11.6 Short-Lived Nuclides as Chronometers

There are two key properties of short-lived nuclide systems that are required for use as chronometers: (1) the level of the nuclide must be high enough to provide significant variation in the isotopic composition of the daughter isotopes, and (2) the short-lived nuclide must be uniformly distributed in the solar system. There are a few isotopes that meet the first requirement and assessment of the second requirement is difficult. Although ^{10}Be and ^{60}Fe are important for delimiting possible origins of short-lived radioactivity, it is ^{26}Al, ^{53}Mn, and ^{182}Hf that have proven most useful for chronology. The early solar system level of ^{60}Fe remains uncertain at this writing, but it seems more likely that the level was low; it is now clear that ^{10}Be is not correlated with ^{26}Al and a poor chronometer because it was synthesized by irradiation over an extended period of time or produced inhomogeneously within the solar nebula.

A number of approaches have been used to assess the question of uniformity of distribution of short-lived nuclides. Villeneuve et al. (2009) used the relationship between evolution of magnesium isotopic composition in chondrules and their ^{26}Al–^{26}Mg ages relative to CAIs to argue that ^{26}Al/^{27}Al was uniformly distributed in the early solar system to a precision of 10%. Schiller et al. (2010) measured magnesium isotopic composition of bulk chondrites and concluded that no more than 30% heterogeneity in ^{26}Al/^{27}Al was possible. However, Larsen et al. (2011) found a correlation between excess ^{26}Mg and nucleosynthetic anomalies in ^{54}Cr in bulk meteorites and argued that either ^{26}Al/^{27}Al was heterogeneously distributed or that magnesium isotopic composition was heterogeneous to a small extent. Dauphas et al. (2008) used the uniformity of ^{60}Ni anomalies in bulk meteorites and the uniformity of ^{58}Fe anomalies (^{58}Fe and ^{60}Fe are coproduced in all potential stellar sources of ^{60}Fe) to show that ^{60}Fe was homogeneously distributed in the early solar system to a precision of 10%.

The other significant test of chronometers based on short-lived nuclides is the degree to which they agree with one another and with the only long-lived chronometer with the precision necessary to test concordance. There is now a significant body of data to allow the ^{26}Al–^{26}Mg, ^{53}Mn–^{53}Cr, ^{182}Hf–^{182}W, and Pb–Pb chronometers to be compared. In principle, the record of each of the now-extinct isotopes can be interpreted to infer a chronology for various events that caused chemical fractionations in early solar system materials. Here, the consistency of these records is evaluated, both internally and with each other, as well as with the Pb–Pb chronometer, to determine what quantitative constraints can be confidently inferred for the sequence and duration of processes in the solar nebula and on earliest planetesimals (planetary-scale differentiation, e.g., relative to the Earth, is considered in

Chapter 2.8). To obtain reference points for cross-calibrating relative and absolute chronologies, it is necessary to use samples that achieved rapid isotopic closure following a well-defined fractionation event and for which a robust and high-precision data set exists. By these criteria, only two anchor points are possible for the cross-calibration: (1) the Pb–Pb, ^{26}Al–^{26}Mg, and ^{182}Hf–^{182}W records in CAIs and (2) the Pb–Pb, ^{26}Al–^{26}Mg, ^{53}Mn–^{53}Cr, and ^{182}Hf–^{182}W records in angrites. At this writing, only a limited range of tests is possible because of the necessity of having Pb–Pb data on materials for which the uranium isotopic composition has also been measured.

The D'Orbigny angrite quenched rapidly and experienced no later disturbances of any of the chronometric systems, so it has become a very useful anchor point for planetary differentiation processes. Four CAIs (Amelin et al., 2010; Connelly et al., 2012) have a published precise common Pb–Pb age and measured uranium isotopic compositions, and this absolute age can be brought into concordance with the record of short-lived radioisotopes in D'Orbigny. The uranium-corrected Pb–Pb age of the D'Orbigny angrite, 4563.37 ± 0.25 Ma (Brennecka and Wadhwa, 2012) in conjunction with the initial ^{182}Hf/^{180}Hf determined for D'Orbigny, $(7.10 \pm 0.17) \times 10^{-5}$ (Kleine et al., 2012), yields an age of the solar system of 4567.31 ± 0.66 Ma, which is in excellent agreement with the uranium-corrected Pb–Pb age of the CAI SJ-101 and the three Efremovka CAIs, 4567.30 ± 0.16 Ma (Amelin et al., 2010; Connelly et al., 2012).

Brennecka and Wadhwa (2012) measured uranium isotopic compositions in several angrites and the unique achondrite NWA2976, showed that they all have the same uranium isotopic composition and corrected some literature Pb–Pb ages. These corrected ages, along with ages for LEW86010 (Amelin, 2008a) and Sahara 99 555 (Amelin, 2008b) corrected using the same offset, were used with the uranium-corrected average Pb–Pb age of the four CAIs (Amelin et al., 2010; Connelly et al., 2012) to compare Pb–Pb ages with relative times from the ^{26}Al–^{26}Mg, ^{53}Mn–^{53}Cr, and ^{182}Hf–^{182}W systems (**Figure 10**). The three systems show remarkably good concordance with the Pb–Pb chronometer, strongly suggesting uniform distribution within the solar system for ^{26}Al/^{27}Al, ^{53}Mn/^{55}Mn, and ^{182}Hf/^{180}Hf. However, there is a problem: using the Pb–Pb and ^{182}Hf–^{182}W systems, CAIs are 3.93 ± 0.31 and 3.94 ± 0.66 Ma, respectively, older than D'Orbigny, but using the ^{26}Al–^{26}Mg system, CAIs are 5.07 ± 0.08 Ma older than D'Orbigny. There are several possible explanations for this discrepancy: ^{26}Al/^{27}Al might have been higher in the CAI-forming region than elsewhere in the solar nebula (Larsen et al., 2011), or the Pb–Pb, ^{182}Hf–^{182}W, and ^{26}Al–^{26}Mg systems may not date the same events in CAI formation history. Such a direct comparison is currently available for only four CAIs and several of angrites, but they span approximately the first 10 Ma of solar system history.

1.11.6.1 Formation Timescales of Nebular Materials

A consistent timescale for fractionation events that occurred during high-temperature processing of nebular materials is obtained by fixing the canonical ^{26}Al/^{27}Al value (5.23×10^{-5}) measured in CAIs to the absolute timescale provided by the recent high-precision Pb–Pb isochron age of 4567.30 ± 0.16 Ma, (Amelin et al., 2010; Connelly et al., 2012). There is an uncertainty in tying these timescales together here, in that a uranium-corrected Pb–Pb age is available for only four CAIs for which the ^{26}Al–^{26}Mg system has not been studied and it is not clear whether the Pb–Pb age of CAIs is the crystallization age. Nevertheless, using the CAI absolute timescale, the initial ^{26}Al/^{27}Al values inferred for chondrules from the most unequilibrated chondrites (**Figure 5**) indicate that chondrule formation began by ~4566 Ma and continued probably for another ~2 Ma.

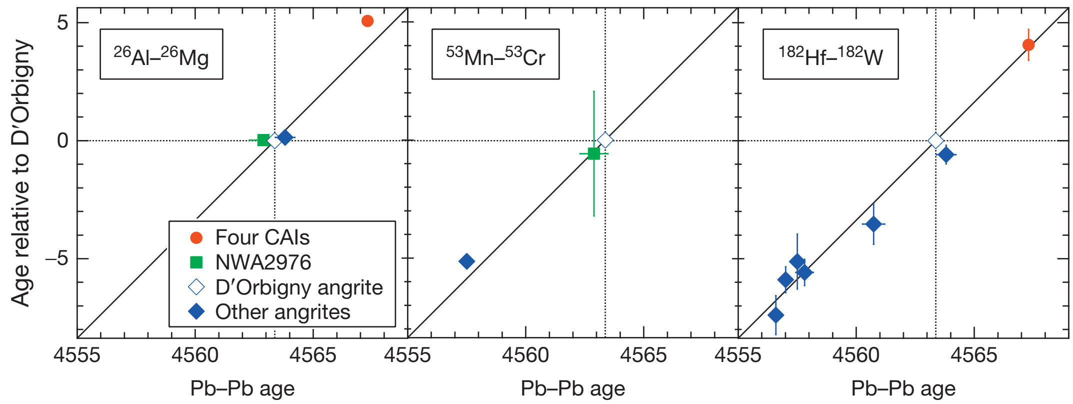

Figure 10 A comparison of relative ages calculated from the ^{26}Al–^{26}Mg, ^{53}Mn–^{53}Cr, and ^{182}Hf–^{182}W systems with absolute ages from the uranium-isotope-corrected Pb–Pb system. All ages based on short-lived radionuclides are relative to the age of the D'Orbigny angrite. Overall, short-lived and absolute chronometers are highly concordant. The major discrepancy is that the ^{26}Al–^{26}Mg and Pb–Pb ages for CAIs disagree by 1.14 ± 0.32 Ma. Pb–Pb data for most angrites and the unique achondrite NWA2976 are from Brennecka and Wadhwa (2012). Pb–Pb ages for LEW86010 (Amelin, 2008a) and SAH99444 (Amelin, 2008b) were corrected using the average uranium isotope ratio for angrites of Brennecka and Wadhwa (2012). The CAIs for which uranium-isotope-corrected Pb–Pb ages are available are Allende SJ101 and three Efremovka CAIs (Amelin et al., 2010; Connelly et al., 2012), all of which have the same age and are assumed to be representative of the CAIs used to infer initial solar system ^{26}Al/^{27}Al (Jacobsen et al., 2008) and ^{182}Hf/^{180}Hf (Burkhardt et al., 2008, 2012) from bulk CAI isochrons. ^{26}Al–^{26}Mg data for angrites are from Schiller et al. (2010) and for NWA2976 are from Bouvier et al. (2011). ^{53}Mn–^{53}Cr data for D'Orbigny are from Glavin et al. (2004) and for the LEW86010 angrite are from Lugmair and Shukolyukov (1998). ^{182}Hf–^{182}W data for angrites and NWA2976 are from Kleine et al. (2012).

The $^{53}Mn–^{53}Cr$ system can only be tied to CAI formation indirectly, as CAIs are depleted in manganese. The most reliable anchor point for chronology is the D'Orbigny angrite, which formed 3.8 Ma after CAIs, according to the Pb–Pb chronometer. Nonetheless, the $^{53}Mn–^{53}Cr$ system indicates that a suite of chondrules from the Chainpur chondrite formed 1.4 Ma after chondrites (Yin et al., 2007), in good agreement with the time range inferred from the $^{26}Al–^{26}Mg$ system.

One clear difficulty with using the $^{26}Al–^{26}Mg$ system as a chronometer is isotopically anomalous CAIs that apparently formed lacking any significant live ^{26}Al. These refractory inclusions, which include the FUN CAIs and the hibonite PLACs, typically exhibit very large anomalies in 'stable' isotopes (e.g., calcium or titanium) that are most readily interpreted as indicating a lack of mixing with average solar nebula materials. Because isotopic homogenization is expected to be an ongoing process during nebular evolution, the preservation of these anomalies argues strongly for a very 'primitive' nature of these materials, that is, they probably formed early (not late) and also they escaped any significant isotopic reequilibration from later heating (MacPherson et al., 1995; Sahijpal and Goswami, 1998). Sahijpal and Goswami (1998) suggested that the highly anomalous CM hibonite grains might have formed in a triggered collapse scenario just prior to injection of the radionuclides (^{41}Ca and ^{26}Al), which could theoretically trail the shock front (Foster and Boss, 1997). One of the highest priorities in early solar system chronology is measurement of absolute Pb–Pb ages on FUN CAIs and PLACs to establish whether they are older or younger than typical CAIs.

The good concordance of the $^{26}Al–^{26}Mg$ and Pb–Pb systems indicates that $^{26}Al/^{27}Al$ records do have chronological significance for most CAIs and chondrules. Chondrule formation ages relative to normal CAIs imply a duration of at least ~2–3 Ma for the solar nebula. Such a duration is plausible from an astrophysical viewpoint (Cameron, 1995; Podosek and Cassen, 1994), and it has interesting implications for timescales of accretion and radioactive heating of early-formed planetary bodies.

A relatively long interval (>4 Ma) between CAIs and chondrules can be inferred on the basis of I–Xe dating (see Swindle et al., 1996 for a review). At face value, this might be seen as support for an extended period of chondrule formation; however, in detail, it does not work. The siting of ^{129}I is uncertain in both CAIs and chondrules, and I–Xe apparent ages of chondrules span an interval of up to several tens of millions of years, implicating asteroidal rather than nebular processes (e.g., Swindle et al., 1991).

1.11.6.2 Timescales of Planetesimal Accretion and Early Chemical Differentiation

The developments of the $^{26}Al–^{26}Mg$ and $^{182}Hf–^{182}W$ systems in the past 10 years have revolutionized the understanding of the timescales of processes on planetesimals. Whereas it used to be thought that most processing in the parent bodies of the differentiated meteorites occurred a few Ma after CAI formation, it is now clear that melting of asteroidal bodies occurred very early in solar system history. Studies of the $^{182}Hf–^{182}W$ system initially led to the uncomfortable conclusion that iron meteorite parent bodies might have experienced core formation prior to CAI formation, but with the development of correction techniques for cosmic ray exposure effects in iron meteorites (e.g., Markowski et al., 2006a; Qin et al., 2008b) and for nucleosynthetic effects on tungsten in CAIs (Burkhardt et al., 2012), it now seems clear that the core formation events that led to most iron meteorites occurred in the first 2 Ma after CAI formation (Burkhardt et al., 2012). This is consistent with early formation of olivine cumulate, $1.24^{+0.40}_{-0.28}$ Ma after CAIs, inferred for the parent bodies of pallasites (Baker et al., 2012) and early formation of diogenites as cumulates on Vesta from 0.5 to 3 Ma after CAIs (Schiller et al., 2011).

Although the interpretation of apparent initial $^{53}Mn/^{55}Mn$ values in terms of a chronology for nebular fractionation events is problematic, the $^{53}Mn–^{53}Cr$ system seems amenable to timing chemical fractionations associated with 'geologic' activity on early-formed planetary bodies. Using D'Orbigny as an anchor point for the Pb–Pb (Brennecka and Wadhwa, 2012) and $^{53}Mn–^{53}Cr$ (Glavin et al., 2004) systems, the bulk eucrite–diogenite $^{53}Mn–^{53}Cr$ isochron of Trinquier et al. (2008) implies 'global' differentiation of Vesta at 4564.78 ± 0.54 Ma, only 2.5 Ma after the Pb–Pb date for CAI formation. As mentioned previously, individual eucrites show internal Mn–Cr isochrons that indicate attainment of isotopic closure from just slightly after this time to significantly later, implying an extended ($>10^7$ years) history of thermal activity on the HED asteroid.

The $^{53}Mn–^{53}Cr$ isochron for the HED parent body is generally consistent with the timing of other indicators of early planetary processes. The Pb–Pb age for the oldest phosphates, from the least metamorphosed (H4) chondrites studied, postdates HED differentiation by ~2 Ma. This is approximately equivalent to the Mn–Cr closure age for Chervony Kut, the noncumulate eucrite with the highest individual $^{53}Mn/^{55}Mn$ initial ratio. Other achondrites, including a pallasite and the unusual basaltic achondrite Acapulco, have $^{53}Mn–^{53}Cr$ ages ~8–10 Ma after the HED differentiation event. These timescales are consistent with the notion that a variety of differentiated meteorites sample various depths in asteroids of various sizes during this early epoch following accretion.

The $^{53}Mn–^{53}Cr$ system is well suited to date aqueously precipitated minerals on carbonaceous chondrite parent bodies. Carbonates show a wide range of $^{53}Mn–^{53}Cr$ ages, from 1.3 ± 1.1 to 8.3 ± 1.2 Ma after CAI formation; fayalite from CV3 chondrites appears to have formed 5.7 Ma after CAIs. This implies that aqueous activity on some chondrite parent bodies was contemporaneous with chondrule formation elsewhere.

1.11.7 Conclusions

Both chondrites and differentiated meteorites preserve records of short-lived radionuclides that are now extinct but which were present when the solar system formed (**Table 1**). These isotopic records yield information on the amount of radioactivity contained by ancient solar system minerals, from which the relative timing of chemical fractionations between parent and daughter elements can be inferred (assuming that the short-lived radionuclides were originally distributed homogenously). The fractionation events can often be related to thermal processes occurring in the solar nebula or on early accreted planetesimals, thus allowing a high-resolution relative chronology to be delineated.

The existence of ^{10}Be, ^{36}Cl, and ^{26}Al in various early solar system materials provides strong evidence for a multiplicity of sources for short-lived isotopes. The first two isotopes most likely result from local production by energetic particle irradiation, perhaps near the forming Sun, whereas the latter is evidence for seeding of the solar nebula by freshly synthesized stellar ejecta. In principle, the inventory of other radioisotopes may contain contributions from both these sources in addition to other nondiscrete ('background') sources such as galactic stellar nucleosynthesis or spallogenic nuclear reactions in the protosolar molecular cloud. However, correlations of radiogenic isotope signatures in CAIs and hibonite grains indicate that spallogenic contributions to the abundance of ^{26}Al are minor.

1.11.7.1 Implications for Solar Nebula Origin and Evolution

The short lifetime of ^{26}Al coupled with the evidence for an external origin has important implications for the origin of the solar system. Based on estimated production rates and isotope mixing during interstellar transit and injection into the solar system, a duration of at <2 Ma can be accommodated for the total time between nucleosynthetic production and incorporation of these isotopes into crystalline solids in the early solar system. Such a rapid timescale suggests a triggering mechanism for fragmentation and collapse of a portion of the presolar molecular cloud to the form the early Sun and its accretion disk. Although it is known that many AGB stars contributed dust to the early solar nebula (see **Chapter 1.4**) and that a wind from such a star could theoretically provide a sufficient shock to initiate collapse, astrophysical considerations of stellar lifetimes suggest a nearby core collapse supernova as a more likely trigger. However, the apparently low ^{60}Fe level in the early solar system and relatively high ^{26}Al level suggest that perhaps a stellar wind from a massive star was the source of ^{26}Al.

Supernovae could be the source of most of the short-lived radionuclides (except ^{10}Be); however, there are difficulties in reconciling relative abundances of all species with a single event (see review by Goswami and Vanhala, 2000). While this may be aesthetically desirable, it is not required, especially for the longer-lived isotopes of **Table 1**. Other evidence indicates that it is probably not correct and that the truth is more complex than a single supernova triggering and injection. The 'last' supernova is not the source of large stable isotope anomalies in oxygen, calcium, or titanium, demonstrating that isotopic memories of other presolar components survived to be incorporated into early solar system minerals. Additionally, the evidence for pervasive ^{10}Be signatures in CAIs, the hint for ^{7}Be, and the abundant astronomical evidence for copious x-ray activity of YSOs indicates that early-formed solar system materials were most likely strongly irradiated if they were not shielded. Progress has been made in quantitatively assessing the proportion of those radionuclides (besides ^{26}Al) that were produced locally by solar energetic particles, but a full understanding of the sources of short-lived nuclides remains elusive.

Cross-calibration of the ^{26}Al–^{26}Mg, ^{53}Mn–^{53}Cr, and ^{182}Hf–^{182}W systems with uranium-isotope-corrected Pb–Pb ages of CAIs and the D'Orbigny angrite results in a self-consistent high-resolution chronology for the high-temperature phases of solar nebula evolution. A plausible scenario and timeline can be constructed:

(1) At nearly 4568 Ma, a shock wave, perhaps initiated by a 'nearby' supernova or stellar wind from a nearby massive star, triggers fragmentation and gravitational collapse of a portion of a molecular cloud;
(2) Near the central, hot regions of the nebula the first refractory minerals form by evaporation and/or recondensation and melting of mixtures of presolar dust grains from various interstellar heritages; these hibonite grains and FUN inclusions incorporate ^{10}Be produced by irradiation of the dust grains by solar energetic particles, but they do not sample the radioactivity accompanying the triggering shock wave;
(3) Shortly afterward, at ~4567 Ma, the fresh radioactivity arrives in the inner nebula, and most CAIs form over a short interval, incorporating ^{26}Al and ^{182}Hf; if the high-precision ^{26}Al–^{26}Mg data on large CV chondrite CAIs is representative of most refractory inclusions, then this interval might be as short as 4000 years (Larsen et al., 2011);
(4) High-temperature processing of some CAIs continues for a few hundred thousand years, but the survivors are dominated by early-formed CAIs (Ciesla, 2010);
(5) At ~4566 Ma, chondrule formation begins and continues for ~1–2 Ma; CAIs are largely absent from the nebular regions where chondrule melting occurs; and
(6) At ~4565–4564, CAIs have joined chondrules and nebular dust in accreting to planetesimals in the asteroid belt. If the latter process is considered as the termination of the nebular phase of solar system evolution, then its lifetime is ~4 Ma as recorded by radionuclides in nebular materials.

The timescales for accretion and early evolution of these planetesimals are also constrained by short-lived radioactivity. This record is best elucidated with the ^{53}Mn–^{53}Cr and ^{182}Hf–^{182}W isotopic systems. The ^{182}Hf–^{182}W isotopic system indicates that core separation on differentiated meteorites occurred within the first 2 Ma after CAI formation. Accretion of some planetesimals started very early, perhaps even before the bulk of chondrule formation began. By ~4565–4564, large-scale melting and differentiation occurred on the HED parent body, most likely the asteroid 4 Vesta, and perhaps even Mars (Dauphas and Pourmand, 2011). Some eucrites crystallized soon after mantle differentiation, quickly cooling through isotopic closure for magnesium and chromium by ~4564–4563 Ma. Energy from ^{26}Al decay probably contributed substantially to the heat required for melting, but Vesta was large enough that igneous activity continued for several tens of million years. Some angrites appear to have erupted early, cooling and quenching at ~4563 Ma, but others did not crystallize until 4557 Ma. Other asteroidal bodies, from which chondrites are derived, either accreted somewhat later than Vesta or remained as relatively small bodies for several million years. Absolute Pb–Pb ages of phosphates indicate that metamorphic temperatures were reached on some ordinary chondrite asteroids by ~4563 Ma; this timescale is consistent with the ^{26}Al/^{27}Al records of chondrules. Metamorphism on chondrite parent bodies continued for up to tens of millions of years as indicated by Pb–Pb and I–Xe dating. Aqueous activity (formation of carbonate) happened very early, on the parent asteroids of some carbonaceous chondrites. Accretion and differentiation of planetary embryos continued from this early epoch for a period of several tens of millions of years (see Chapters 2.4 and 2.8).

1.11.7.2 Future Directions

The quantitative comparison of various short-lived radionuclide systems with each other and with Pb–Pb chronology has only been made possible by new data obtained during the last decade or, in many cases, the last few years. Over this same time period, evidence for the decay of several important new short-lived isotopes in the early solar system has been discovered. Calibration of ^{26}Al–^{26}Mg, ^{53}Mn–^{53}Cr, and ^{182}Hf–^{182}W systems with the Pb–Pb system now seems to be well understood and consistent for differentiated meteorites, but further work is needed to establish the absolute age of CAIs with uranium-isotope-corrected Pb–Pb ages. The record of now-extinct isotopes in early solar system materials is becoming sufficiently well defined to allow construction of a plausible timeline and scenario for solar system origin. However, even though broad areas of consistency have been revealed, there remain significant problems that will require further investigation. One of the most important is trying to understand the role of energetic particle irradiation in the early solar system. Energetic processes associated with magnetic flare activity of the young Sun almost certainly occurred (Feigelson et al., 2002a,b; Preibisch et al., 2005); the question is what effect these had on isotopic and mineralogical records of early-formed solar system rocks.

Acknowledgments

The authors have benefited from intensely fun discussions about this subject with many colleagues, and although it is impossible to mention everyone, they would especially like to thank M. Chaussidon, D. D. Clayton, N. Dauphas, J. N. Goswami, M. Gounelle, G. R. Huss, I. D. Hutcheon, T. R. Ireland, N. T. Kita, A. N. Krot, T. Lee, L. Leshin, G. W. Lugmair, G. J. MacPherson, S. S. Russell, S. Sahijpal, F. Shu, G. Srinivasan, M. Wadhwa, G. J. Wasserburg, Q.-Z. Yin, E. D. Young, and E. K. Zinner.

References

Adams FC (2010) The birth environment of the solar system. *Annual Review of Astronomy and Astrophysics* 48: 47–85.
Alexander CMO'D, Boss AP, and Carlson RW (2001) The early evolution of the inner solar system: A meteoritic perspective. *Science* 293: 64–68.
Alexander EC Jr., Lewis RS, Reynolds JH, and Michel MC (1971) Plutonium-244: Confirmation as an extinct radioactivity. *Science* 172: 837–840.
Allègre CJ, Manhès G, and Göpel C (1995) The age of the Earth. *Geochimica et Cosmochimica Acta* 59: 1445–1456.
Amelin Y (2006) The prospect of high-precision Pb isotopic dating of meteorites. *Meteoritics and Planetary Science* 41: 7–17.
Amelin Y (2008a) U–Pb ages of angrites. *Geochimica et Cosmochimica Acta* 72: 221–232.
Amelin Y (2008b) The U–Pb systematics of angrite Sahara 99555. *Geochimica et Cosmochimica Acta* 72: 4874–4885.
Amelin Y, Connelly J, Zartman RE, Chen JH, Göpel C, and Neymark LA (2009) Modern U–Pb chronometry of meteorites: Advancing to higher time resolution reveals new problems. *Geochimica et Cosmochimica Acta* 73: 5212–5223.
Amelin Y, Kaltenbach A, Iizuka T, et al. (2010) U–Pb chronology of the solar system's oldest solids with variable $^{238}U/^{235}U$. *Earth and Planetary Science Letters* 300: 343–350.
Amelin Y and Krot AN (2007) Pb isotopic age of the Allende chondrules. *Meteoritics and Planetary Science* 42: 1321–1335.
Amelin Y, Krot AN, Hutcheon ID, and Ulyanov AA (2002) Lead isotopic ages of chondrules and calcium–aluminum-rich inclusions. *Science* 297: 1678–1683.
Amelin Y, Wadhwa M, and Lugmair GW (2006) Pb-isotopic dating of meteorites using ^{202}Pb–^{205}Pb double spike: Comparison with other high resolution chronometers. *Lunar and Planetary Science* 37: #1970.
André P, Ward-Thompson W, and Barsony M (2000) From prestellar cores to protostars: The initial conditions of star formation. In: Mannings V, Boss AP, and Russell SS (eds.) *Protostars and Planets IV*, pp. 59–96. Tucson, AZ: University of Arizona Press.
Baker J, Bizzarro M, Wittig N, Connelly J, and Haack H (2005) Early planetesimal melting from an age of 4.5662 Gyr for differentiated meteorites. *Nature* 436: 1127–1130.
Baker JA, Schiller M, and Bizzarro M (2012) ^{26}Al–^{26}Mg deficit dating ultramafic meteorites and silicate planetesimals differentiation in the early solar system? *Geochimica et Cosmochimica Acta* 77: 415–431.
Baker RGA, Schönbächler M, Rehkämper M, Williams HM, and Halliday AN (2010) The thallium isotope composition of carbonaceous chondrites – New evidence for live ^{205}Pb in the early solar system. *Earth and Planetary Science Letters* 291: 39–47.
Begemann F (1980) Isotopic anomalies in meteorites. *Reports on Progress in Physics* 43: 1309–1356.
Binzel RP and Xu S (1993) Chips off of asteroid 4 Vesta: Evidence for the parent body of basaltic achondrite meteorites. *Science* 260: 186–191.
Birck JL and Allègre CJ (1985) Evidence for the presence of ^{53}Mn in the early solar-system. *Geophysical Research Letters* 12: 745–748.
Birck JL and Allègre CJ (1988) Manganese chromium isotope systematics and the development of the early solar-system. *Nature* 331: 579–584.
Birck JL, Rotaru M, and Allègre CJ (1999) ^{53}Mn–^{53}Cr evolution of the early solar system. *Geochimica et Cosmochimica Acta* 63: 4111–4117.
Bizzarro M, Baker JA, and Haack H (2004) Mg isotope evidence for contemporaneous formation of chondrules and refractory inclusions. *Nature* 431: 275–278.
Bizzarro M, Baker JA, and Haack H (2005a) Corrigendum to Bizzarro et al. (2004). *Nature* 435: 1280.
Bizzarro M, Baker JA, Haack H, and Lundgaard KL (2005b) Rapid timescales for accretion and melting of differentiated planetesimals inferred from ^{26}Al–^{26}Mg chronometry. *The Astrophysical Journal* 632: L41–L44.
Bizzarro M, Ulfbeck D, Trinquier A, Thrane K, Connelly JN, and Meyer BS (2007) Evidence for a late supernova injection of ^{60}Fe into the protoplanetary disk. *Science* 316: 1178–1181.
Boss AP (2012) Mixing and transport of isotopic heterogeneity in the early solar system. *Annual Review of Earth and Planetary Sciences* 40: 23–43.
Boss AP and Keiser SA (2010) Who pulled the trigger: A supernova or an asymptotic giant branch star? *The Astrophysical Journal* 717: L1–L5.
Boss AP and Keiser SA (2012) Supernova-triggered molecular cloud collapse and the Rayleigh–Taylor fingers that polluted the solar nebula. *The Astrophysical Journal* 756: L9.
Bouvier A, Spivak-Birndorf LJ, Brennecka GA, and Wadhwa M (2011) New constraints on early solar system chronology from Al–Mg and U–Pb isotope systematics in the unique basaltic achondrite Northwest Africa 2976. *Geochimica et Cosmochimica Acta* 75: 5310–5323.
Bouvier A and Wadhwa M (2010) The age of the solar system redefined by the oldest Pb–Pb age of a meteoritic inclusion. *Nature Geoscience* 3: 637–641.
Boyet M, Carlson RW, and Horan M (2010) Old Sm–Nd ages for cumulate eucrites and redetermination of the solar system initial $^{146}Sm/^{147}Sm$ ratio. *Earth and Planetary Science Letters* 291: 172–181.
Brazzle RH, Pravdivtseva OV, Meshik AP, and Hohenberg CM (1999) Verification and interpretation of the I–Xe chronometer. *Geochimica et Cosmochimica Acta* 63: 739–760.
Brennecka GA and Wadhwa M (2012) Uranium isotope compositions of the basaltic angrite meteorites and the chronological implications for the early solar system. *Proceedings of the National Academy of Sciences* 109: 9299–9303.
Brennecka GA, Weyer S, Wadhwa M, Janney PE, Zipfel J, and Anbar AD (2010) $^{238}U/^{235}U$ variations in meteorites: Extant ^{247}Cm and implications for Pb–Pb dating. *Science* 327: 449–451.

Burkhardt C, Kleine T, Bourdon B, et al. (2008) Hf–W mineral isochron for Ca, Al-rich inclusions: Age of the solar system and the timing of core formation in planetesimals. *Geochimica et Cosmochimica Acta* 72: 6177–6197.

Burkhardt C, Kleine T, Dauphas N, and Wieler R (2012) Nucleosynthetic tungsten isotope anomalies in acid leachates of the Murchison chondrite: Implications for hafnium–tungsten chronometry. *The Astrophysical Journal* 753: L6 (6 pp).

Burkhardt C, Kleine T, Oberli F, Pack A, Bourdon B, and Wieler R (2011) Molybdenum isotope anomalies in meteorites: Constraints on solar nebula evolution and origin of Earth. *Earth and Planetary Science Letters* 312: 390–400.

Cameron AGW (1995) The first ten million years in the solar nebula. *Meteoritics and Planetary Science* 30: 133–161.

Cameron AGW (2001a) Extinct radioactivities, core-collapse supernovas, jets, and the r-process. *Nuclear Physics A* 688: 289C–296C.

Cameron AGW (2001b) Some properties of *r*-process accretion disks and jets. *The Astrophysical Journal* 562: 456–469.

Cameron AGW, Höflich P, Myers PC, and Clayton DD (1995) Massive supernovae, Orion gamma rays, and the formation of the solar system. *The Astrophysical Journal* 447: L53–L57.

Cameron AGW and Truran JW (1977) The supernova trigger for formation of the solar system. *Icarus* 30: 447–461.

Carlson RW, Boyet M, and Horan M (2007) Chondrite barium, neodymium, and samarium isotopic heterogeneity and early Earth differentiation. *Science* 316: 1175–1178.

Carlson RW and Hauri E (2001) Extending the ^{107}Pd–^{107}Ag chronometer to low Pd/Ag meteorites with MC–ICP–MS. *Geochimica et Cosmochimica Acta* 65: 1839–1848.

Caro G (2011) Early silicate earth differentiation. *Annual Review of Earth and Planetary Sciences* 39: 31–58.

Caro G, Bourdon B, Birck J-L, and Moorbath S (2003) ^{146}Sm–^{142}Nd evidence from Isua metamorphosed sediments for early differentiation of the Earth's mantle. *Nature* 423: 428–432.

Chaussidon M, Robert F, and McKeegan KD (2006a) Li and B isotopic variations in an Allende CAI: Evidence for the in situ decay of short-lived ^{10}Be and for the possible presence of the short-lived nuclide ^{7}Be in the early solar system. *Geochimica et Cosmochimica Acta* 70: 224–245.

Chaussidon M, Robert F, and McKeegan KD (2006b) Reply to the comment by Desch and Ouellette on "Li and B isotopic variations in an Allende CAI: Evidence for the in situ decay of short-lived ^{10}Be and for the possible presence of the short-lived nuclide ^{7}Be in the early solar system" *Geochimica et Cosmochimica Acta* 70: 5433–5436.

Chen JH, Papanastassiou DA, and Wasserburg GJ (2002) Re–Os and Pd–Ag systematics in group IIIAB irons and in pallasites. *Geochimica et Cosmochimica Acta* 66: 3793–3810.

Chen JH, Papanastassiou DA, and Wasserburg GJ (2009) A search for nickel isotopic anomalies in iron meteorites and chondrites. *Geochimica et Cosmochimica Acta* 73: 1461–1471.

Chen JH and Wasserburg GJ (1980) A search for isotopic anomalies in uranium. *Geophysical Research Letters* 7(1980): 275–278.

Chen JH and Wasserburg GJ (1981) The isotopic composition of uranium and lead in Allende inclusions and meteorite phosphates. *Earth and Planetary Science Letters* 52: 1–15.

Chen JH and Wasserburg GJ (1990) The isotopic composition of Ag in meteorites and the presence of ^{107}Pd in protoplanets. *Geochimica et Cosmochimica Acta* 54: 1729–1743.

Chen JH and Wasserburg GJ (1996) Live ^{107}Pd in the early solar system and implications for planetary evolution. In: Basu A and Hart S (eds.) *Earth Processes: Reading the Isotopic Code. Geophysical Monograph,* Vol. 95, pp. 1–20. Washington, DC: American Geophysical Union.

Chmeleff J, von Blanckenburg F, Kossert K, and Jakob D (2010) Determination of the ^{10}Be half-life by multicollector ICP-MS and liquid scintillation counting. *Nuclear Instruments and Methods in Physics Research Section B* 268: 192–199.

Ciesla FJ (2010) The distributions and ages of refractory objects in the solar nebula. *Icarus* 208: 455–467.

Clayton DD (1982) Cosmic chemical memory – A new astronomy. *The Quarterly Journal of the Royal Astronomical Society* 23: 174–212.

Clayton DD (1986) Interstellar fossil ^{26}Mg and its possible relation to excess meteoritic ^{26}Mg. *The Astrophysical Journal* 310: 490–498.

Clayton DD, Dwek E, and Woosley SE (1977) Isotopic anomalies and proton irradiation in the early solar system. *The Astrophysical Journal* 214: 300–315.

Coath CD, Steele RCJ, and Lunnon WF (2013) Statistial bias in isotope ratios. *Journal of Analytical Atomic Spectroscopy* 28: 52–58.

Condon DJ, McLean N, Noble SR, and Bowring SA (2010) Isotopic composition (^{238}U/^{235}U) isotope ratios of natural uranium standards. *Geochimica et Cosmochimica Acta* 74: 7127–7143.

Connelly JN, Amelin Y, Krot AN, and Bizzarro M (2008a) Chronology of the solar system's oldest solids. *The Astrophysical Journal* 675: L121–L124.

Connelly JN and Bizzarro M (2009) Pb–Pb dating of chondrules from CV chondrites by progressive dissolution. *Chemical Geology* 259: 143–151.

Connelly JN, Bizzarro M, Ivanova M, and Krot AN (2011) *Towards a new absolute chronology for the early solar system. Formation of the First Solids in the Solar System*. LPI Contribution No. 1639, #9056, Houston, TX: The Lunar and Planetary Institute.

Connelly JN, Bizzarro M, Krot AN, Nordlund Å, Wielandt D, and Ivanova MA (2012) The absolute chronology and thermal processing of solids in the solar protoplanetary disk. *Science* 338: 651–655.

Connelly JN, Bizzarro M, Thrane K, and Baker JA (2008b) The Pb–Pb age of angrite SAH99555 revisited. *Geochimica et Cosmochimica Acta* 72: 4813–4824.

Crowther SA, Mohapatra RK, Turner G, Blagburn DJ, Kehm K, and Gilmour JD (2008) Characteristics and applications of RELAX, an ultrasensitive resonance ionization mass spectrometer for xenon. *Journal of Analytical Atomic Spectrometry* 23: 938–947.

Dauphas N and Chaussidon M (2011) A perspective from extinct radionuclides on a young stellar object: The Sun and its accretion disk. *Annual Review of Earth and Planetary Sciences* 39: 351–386.

Dauphas N, Cook DL, Sacarabany A, et al. (2008) Iron 60 evidence for early injection and efficient mixing of stellar debris in the protosolar nebula. *The Astrophysical Journal* 686: 560–569 [See Dauphas et al. (2009) Erratum. *Astrophys*. *J*. 691, 1943, presenting a slightly revised data table that did not affect their conclusions.].

Dauphas N, Marty B, and Reisberg L (2002) Molybdenum evidence for inherited planetary scale isotope heterogeneity of the protosolar nebula. *The Astrophysical Journal* 565: 640–644.

Dauphas N and Pourmand A (2011) Hf–W–Th evidence for rapid growth of Mars and its status as a planetary embryo. *Nature* 473: 489–493.

Davis AM, Richter FM, Mendybaev RA, Janney PE, Wadhwa M, and McKeegan KD (2005) Isotopic mass fractionation laws and the initial solar system ^{26}Al/^{27}Al ratio. *Lunar and Planetary Science* 36: #2334.

De Leuw S, Rubin AR, Schmitt AK, and Wasson JT (2009) ^{53}Mn–^{53}Cr systematics of carbonates in CM chondrites: Implications for the timing and duration of aqueous alteration. *Geochimica et Cosmochimica Acta* 73: 7433–7442.

Desch SJ, Connolly HC Jr., and Srinivasan G (2004) An interstellar origin for the beryllium 10 in calcium-rich, aluminum-rich inclusions. *The Astrophysical Journal* 602: 528–542.

Desch SJ and Ouellette N (2006) Comment on "Li and B isotopic variations in an Allende CAI: Evidence for the in situ decay of short-lived ^{10}Be and for the possible presence of the short-lived nuclide ^{7}Be in the early solar system" *Geochimica et Cosmochimica Acta* 70: 5426–5432.

Duprat J and Tatischeff V (2007) Energetic constraints on in situ production of short-lived radionuclei in the early solar system. *The Astrophysical Journal* 671: L69–L71.

Endress M, Zinner E, and Bischoff A (1996) Early aqueous activity on primitive meteorite parent bodies. *Nature* 379: 701–703.

Fahey AJ, Goswami JN, McKeegan KD, and Zinner E (1987) ^{26}Al, ^{244}Pu, ^{50}Ti, REE, and trace element abundances in hibonite grains from CM and CV meteorites. *Geochimica et Cosmochimica Acta* 51: 329–350.

Feigelson ED, Broos P, Gaffney JA, et al. (2002a) X-ray emitting young stars in the Orion Nebula. *The Astrophysical Journal* 574: 258–292.

Feigelson ED, Garmire GP, and Pravdo SH (2002b) Magnetic flaring in the pre main-sequence sun and implications for the early solar system. *The Astrophysical Journal* 572: 335–349.

Foster PN and Boss AP (1997) Injection of radioactive nuclides from the stellar source that triggered the collapse of the presolar nebula. *The Astrophysical Journal* 489: 346–357.

Fujiya W, Sugiura N, Hotta H, Ichimura K, and Sano Y (2012) Evidence for the late formation of hydrous asteroids from young meteoritic carbonates. *Nature Communications* 3: 627 (6 pp).

Galer SJG and Lugmair GW (1996) Lead isotope systematics of non-cumulate eucrites. *Meteoritics* 31: A47–A48.

Galy A, Hutcheon ID, and Grossman L (2004) (^{26}Al/^{27}Al$_0$) of the solar nebula inferred from Al–Mg systematics in bulk CAIs from CV3 chondrites. *Lunar and Planetary Science* 35: #2334.

Galy A, Young ED, Ash RD, and O'Nions RK (2000) The formation of chondrules at high gas pressures in the solar nebula. *Science* 290: 1751–1753.

Gilmour JD, Crowther SA, Busfield A, Holland G, and Whitby JA (2009) An early I–Xe age for CB chondrite chondrule formation, and a re-evaluation of the closure age of Shallowater enstatite. *Meteoritics and Planetary Science* 44: 573–579.

Gilmour JD, Pravdivtseva OV, Busfield A, and Hohenberg CM (2006) The I–Xe chronometer and the early solar system. *Meteoritics and Planetary Science* 41: 19–31.
Gilmour JD and Saxton JM (2001) A time-scale of formation of the first solids. *Philosophical Transactions of the Royal Society of London* A359: 2037–2048.
Glavin DP, Kubny A, Jagoutz E, and Lugmair GW (2004) Mn–Cr isotope systematics of the D'Orbigny angrite. *Meteoritics and Planetary Science* 39: 693–700.
Goodrich CA, Hutcheon ID, Kita NT, Huss GR, Cohen BA, and Keil K (2010) ^{53}Mn–^{53}Cr and ^{26}Al–^{26}Mg ages of a feldspathic lithology in polymict ureilites. *Earth and Planetary Science Letters* 295: 531–540.
Göpel C, Manhès G, and Allègre CJ (1994) U–Pb systematics of phosphates from equilibrated ordinary chondrites. *Earth and Planetary Science Letters* 121: 153–171.
Goswami JN and Vanhala HAT (2000) Extinct radionuclides and the origin of the solar system. In: Mannings V, Boss AP, and Russell SS (eds.) *Protostars and Planets IV*, pp. 963–994. Tucson, AZ: University of Arizona Press.
Gounelle M, Chaussidon M, Morbidelli A, et al. (2009) A unique basaltic micrometeorite expands the inventory of solar system planetary crusts. *Proceedings of the National Academy of Sciences* 106: 6904–6909.
Gounelle M, Shu FH, Shang H, Glassgold AE, Rehm KE, and Lee T (2001) Extinct radioactivities and protosolar cosmic rays: Self-shielding and light elements. *The Astrophysical Journal* 548: 1051–1070.
Gray CM and Compston W (1974) Excess ^{26}Mg in the Allende meteorite. *Nature* 251: 495–497.
Gray CM, Papanastassiou DA, and Wasserburg GJ (1973) The identification of early condensates from the solar nebula. *Icarus* 20: 213–239.
Grossman L, Ebel DS, Simon SB, Davis AM, Richter FM, and Parsad NM (2000) Major element chemical and isotopic compositions of refractory inclusions in C3 chondrites: The separate roles of condensation and evaporation. *Geochimica et Cosmochimica Acta* 64: 2879–2894.
Halliday AN (2000) Terrestrial accretion rates and the origin of the Moon. *Earth and Planetary Science Letters* 176: 17–30.
Halliday A and Lee D-C (1999) Tungsten isotopes and the early development of the Earth and Moon. *Geochimica et Cosmochimica Acta* 63: 4157–4179.
Harper CL Jr. (1996) Evidence for ^{92g}Nb in the early solar system and evaluation of a new *p*-process cosmochronometer from ^{92g}Nb/^{92}Mo. *The Astrophysical Journal* 466: 437–456.
Harper CL Jr. and Jacobsen SB (1996) Evidence for ^{182}Hf in the early solar system and constraints on the timescale of terrestrial core formation. *Geochimica et Cosmochimica Acta* 60: 1131–1153.
Harper CL Jr., Völkening J, Heumann KG, Shih C-Y, and Wiesmann H (1991) ^{182}Hf–^{182}W: New cosmochronometric constraints on terrestrial accretion, core formation, the astrophysical site of the r-process, and the origin of the solar system. *Lunar and Planetary Science* 22: 515–516.
Hester JJ, Desch SJ, Healy KR, and Leshin LA (2004) The cradle of the solar system. *Science* 304: 1116–1117.
Heymann D and Dziczkaniec M (1976) Early irradiation of matter in the solar system: Magnesium (proton, neutron) scheme. *Science* 191: 79–81.
Hidaka H, Ohta Y, and Yoneda S (2003) Nucleosynthetic components of the early solar system inferred from Ba isotopic compositions in carbonaceous chondrites. *Earth and Planetary Science Letters* 214: 455–466.
Hidaka H, Ohta Y, Yoneda S, and DeLaeter JR (2001) Isotopic search for live ^{135}Cs in the early solar system and possibility of ^{135}Cs–^{135}Ba chronometer. *Earth and Planetary Science Letters* 193: 459–466.
Hidaka H and Yoneda S (2011) Diverse nucleosynthetic components in barium isotopes of carbonaceous chondrites: Incomplete mixing of s- and r-process isotopes and extinct ^{135}Cs in the early solar system. *Geochimica et Cosmochimica Acta* 75: 3687–3697.
Hohenberg CM and Pravdivtseva OV (2008) I–Xe dating: From adolescence to maturity. *Chemie der Erde* 68: 339–351.
Hoppe P, MacDougall D, and Lugmair GW (2007) High spatial resolution ion microprobe measurements refine chronology of carbonate formation in Orgueil. *Meteoritics and Planetary Science* 42: 1309–1320.
Hsu W, Guan Y, Leshin LA, Ushikubo T, and Wasserburg GJ (2006) A late episode of irradiation in the early solar system: Evidence from extinct ^{36}Cl and ^{26}Al in meteorites. *The Astrophysical Journal* 640: 525–529.
Hsu W, Huss GR, and Wasserburg GJ (2003) Al–Mg systematics of CAIs, POI, and ferromagnesian chondrules from Ningqiang. *Meteoritics and Planetary Science* 38: 35–48.
Hua J, Huss GR, Tachibana S, and Sharp TG (2005) Oxygen, silicon, and Mn–Cr isotopes of fayalite in the Kaba oxidized CV3 chondrite: Constraints for its formation history. *Geochimica et Cosmochimica Acta* 69: 1333–1348.
Hudson GB, Kennedy BM, Podosek FA, and Hohenberg CM (1988) The early solar system abundance of ^{244}Pu as inferred from the St. Severin chondrite. In: *Proceedings of the 19th Lunar Planetary Science Conference*, pp. 547–557.
Hutcheon ID, Armstrong JT, and Wasserburg GJ (1984) Excess ^{41}K in Allende CAI: Confirmation of a hint. *Lunar and Planetary Science* 15: 387–388.
Hutcheon ID, Browning L, Keil K, et al. (1999b) Timescale of aqueous activity in the early solar system. In: Ninth Goldschmidt Conference Abstracts, #97, www.lpi.usra.gov/meetings/gold99.
Hutcheon ID, Huss GR, and Wasserburg GJ (1994) A search for ^{26}Al in chondrites: Chondrule formation times. *Lunar and Planetary Science* 25: 587–588.
Hutcheon ID and Hutchison R (1989) Evidence from the Semarkona ordinary chondrite for ^{26}Al heating of small planets. *Nature* 337: 238–241.
Hutcheon ID and Jones RH (1995) The ^{26}Al–^{26}Mg record of chondrules: Clues to nebular chronology. *Lunar and Planetary Science* 26: 647–648.
Hutcheon ID, Krot AN, Keil K, Phinney DL, and Scott ERD (1998) ^{53}Mn–^{53}Cr dating of fayalite formation in the CV3 chondrite Mokoia: Evidence for asteroidal alteration. *Science* 282: 1865–1867.
Hutcheon ID, Marhas KK, Krot AN, Goswami JN, and Jones RH (2009) ^{26}Al in plagioclase-rich chondrules in carbonaceous chondrites: Evidence for an extended duration of chondrule formation. *Geochimica et Cosmochimica Acta* 73: 5080–5099.
Hutcheon ID and Phinney DL (1996) Radiogenic ^{53}Cr* in Orgueil carbonates: Chronology of aqueous activity on the CI parent body. *Lunar and Planetary Science* 27: 577–578.
Hutcheon ID, Weisberg MK, Phinney DL, Zolensky ME, Prinz M, and Ivanov AV (1999a) Radiogenic ^{53}Cr in Kaidun carbonates: Evidence for very early aqueous activity. *Lunar and Planetary Science* 30: #1722.
Ireland TR (1988) Correlated morphological, chemical, and isotopic characteristics of hibonites from the Murchison carbonaceous chondrite. *Geochimica et Cosmochimica Acta* 52: 2827–2839.
Ireland TR (1990) Presolar isotopic and chemical signatures in hibonite-bearing refractory inclusions from the Murchison carbonaceous chondrite. *Geochimica et Cosmochimica Acta* 54: 3219–3237.
Ireland TR, Compston W, and Heydegger HR (1985) Titanium isotopic anomalies in hibonites from the Murchison carbonaceous chondrite. *Geochimica et Cosmochimica Acta* 49: 1989–1993.
Ishii HA, Krot AN, Bradley JP, et al. (2010) Discovery, mineral paragenesis, and origin of wadalite in a meteorite. *American Mineralogist* 95: 440–448.
Ito M, Nagasawa H, and Yurimoto H (2006) A study of Mg and K isotopes in Allende CAIs: Implications to the time scale for the multiple heating processes. *Meteoritics and Planetary Science* 41: 1871–1881.
Jacobsen B, Matzel J, Hutcheon ID, et al. (2011) Formation of the short-lived radionuclide ^{36}Cl in the protoplanetary disk during late-stage irradiation of a volatile-rich reservoir. *The Astrophysical Journal* 731: L28.
Jacobsen B, Yin Q-Z, Moynier F, et al. (2008) ^{26}Al–^{26}Mg and ^{207}Pb–^{206}Pb systematics of Allende CAIs: Canonical solar initial ^{26}Al/^{27}Al reinstated. *Earth and Planetary Science Letters* 272: 353–364.
Jeffery PM and Reynolds JH (1961) Origin of excess Xe^{129} in stone meteorites. *Journal of Geophysical Research* 66: 3582–3583.
Jogo K, Nakamura T, Noguchi T, and Zolotov MY (2009) Fayalite in the Vigarano CV3 carbonaceous chondrite: Occurrences, formation age and conditions. *Earth and Planetary Science Letters* 287: 320–328.
Kaiser T and Wasserburg GJ (1983) The isotopic composition and concentration of Ag in iron meteorites. *Geochimica et Cosmochimica Acta* 47: 43–58.
Kelly WR and Wasserburg GJ (1978) Evidence for the existence of ^{107}Pd in the early solar system. *Geophysical Research Letters* 5: 1079–1082.
Kinoshita N, Paul M, Kashiv Y, et al. (2012) A shorter ^{146}Sm half-life measured and implications for ^{146}Sm–^{142}Nd chronology in the solar system. *Science* 335: 1614–1617.
Kita NT, Huss GR, Tachibana S, Amelin Y, Nyquist LE, and Hutcheon ID (2005) Constraints on the origin of chondrules and CAIs from short-lived and long-lived radionuclides. In: Krot AN, Scott ERD, and Reipurth B (eds.) *Chondrites and the Protoplanetary Disk*. *Astronomical Society of the Pacific Conference Series* 341: pp. 558–587. San Francisco, CA: Astronomical Society of the Pacific.
Kita NT, Nagahara H, Togashi S, and Morishita Y (2000) A short duration of chondrule formation in the solar nebula: Evidence from ^{26}Al in Semarkona ferromagnesian chondrules. *Geochimica et Cosmochimica Acta* 64: 3913–3922.
Kita NT, Ushikubo T, Knight KB, et al. (2012) Internal ^{26}Al–^{26}Mg isotope systematics of a Type B CAI: Remelting of refractory precursor solids. *Geochimica et Cosmochimica Acta* 86: 37–51.
Kleine T, Hans U, Irving AJ, and Bourdon B (2012) Chronology of the angrite parent body and implications for core formation in protoplanets. *Geochimica et Cosmochimica Acta* 84: 186–203.
Kleine T, Mezger K, Palme H, Scherer E, and Münker C (2005a) Early core formation in asteroids and late accretion of chondrite parent bodies: Evidence from ^{182}Hf–^{182}W

in CAIs, metal-rich chondrites, and iron meteorites. *Geochimica et Cosmochimica Acta* 69: 5805–5818.
Kleine T, Münker C, Mezger K, and Palme H (2002) Rapid accretion and early core formation on asteroids and the terrestrial planets from Hf–W chronometry. *Nature* 418: 952–955.
Kleine T, Palme H, Mezger K, and Halliday AN (2005b) Hf–W chronometry of luar metals and the age and early differentiation of the Moon. *Science* 310: 1671–1674.
Kleine T, Touboul M, Bourdon B, et al. (2009) Hf–W chronology of the accretion and early evolution of asteroids and terrestrial planets. *Geochimica et Cosmochimica Acta* 73: 5150–5188.
Korschinek G, Bergmaier A, Faestermann T, et al. (2010) A new value for the half-life of ^{10}Be by heavy-ion elastic recoil detection and liquid scintillation counting. *Nuclear Instruments and Methods in Physics Research Section B* 268: 187–191.
Krot AN, Amelin Y, Bland P, et al. (2009) Origin and chronology of chondritic components: A review. *Geochimica et Cosmochimica Acta* 73: 4963–4997.
Krot AN, Amelin Y, Cassen P, and Meibom A (2005) Young chondrules in CB chondrites from a giant impact in the early solar system. *Nature* 436: 989–992.
Kunihiro T, Rubin AE, McKeegan KD, and Wasson JT (2004) Initial ^{26}Al/^{27}Al in carbonaceous-chondrite chondrules: Too little ^{26}Al to melt asteroids. *Geochimica et Cosmochimica Acta* 68: 2947–2957.
Kurahashi E, Kita NT, Nagahara H, and Morishita Y (2008) ^{26}Al–^{26}Mg systematics of chondrules in a primitive CO chondrite. *Geochimica et Cosmochimica Acta* 72: 3865–3882.
Lachner J, Dillmann I, Faestermann T, et al. (2012) Attempt to detect primordial ^{244}Pu on Earth. *Physical Review C* 85: #015801.
Larsen KA, Trinquier A, Paton C, et al. (2011) Evidence for magnesium isotope heterogeneity in the solar protoplanetary disk. *The Astrophysical Journal* 735: L37.
Lee D-C and Halliday AN (1995) Hafnium–tungsten chronometry and the timing of terrestrial core formation. *Nature* 378: 771–774.
Lee D-C and Halliday AN (1996) Hf–W isotopic evidence for rapid accretion and differentiation in the early solar system. *Science* 274: 1876–1879.
Lee D-C and Halliday AN (2000a) Hf–W internal isochrons for ordinary chondrites and the initial ^{182}Hf/^{180}Hf of the solar system. *Chemical Geology* 169: 35–43.
Lee D-C and Halliday AN (2000b) Accretion of primitive planetesimals: Hf–W isotopic evidence from enstatite chondrites. *Science* 288: 1629–1631.
Lee D-C, Halliday AN, Leya I, Wieler R, and Wiechert U (2002) Cosmogenic tungsten and the origin and earliest differentiation of the Moon. *Earth and Planetary Science Letters* 198: 267–274.
Lee D-C, Halliday AN, Singletary SJ, and Grove TL (2009) ^{182}Hf–^{182}W chronometry and early differentiation of the ureilite parent body. *Earth and Planetary Science Letters* 288: 611–618.
Lee D-C, Halliday AN, Snyder GA, and Taylor LA (1997) Age and origin of the Moon. *Science* 278: 1098–1103.
Lee T (1978) A local proton irradiation model for isotopic anomalies in the solar system. *The Astrophysical Journal* 224: 217–226.
Lee T, Mayeda TK, and Clayton RN (1980) Oxygen isotopic anomalies in Allende inclusion HAL. *Geophysical Research Letters* 7: 493–496.
Lee T and Papanastassiou DA (1974) Mg isotopic anomalies in the Allende meteorite and correlation with O and Sr effects. *Geophysical Research Letters* 1: 225–228.
Lee T, Papanastassiou DA, and Wasserburg GJ (1976) Demonstration of ^{26}Mg excess in Allende and evidence for ^{26}Al. *Geophysical Research Letters* 3: 109–112.
Lee T, Papanastassiou DA, and Wasserburg GJ (1977) Aluminum-26 in the early solar system: Fossil or fuel? *The Astrophysical Journal* 211: L107–L110.
Lee T, Russell WA, and Wasserburg GJ (1978) Calcium isotopic anomalies and the lack of aluminum-26 in an unusual Allende inclusion. *The Astrophysical Journal* 228: L93–L98.
Lee T, Shu FH, Shang H, Glassgold AE, and Rehm KE (1998) Protostellar cosmic rays and extinct radioactivities in meteorites. *The Astrophysical Journal* 506: 898–912.
Leya I, Halliday AN, and Wieler R (2003) The predictable collateral consequences of nucleosynthesis by spallation reactions in the early solar system. *The Astrophysical Journal* 594: 605–616.
Leya I, Wieler R, and Halliday AN (2000) Cosmic-ray production of tungsten isotopes in lunar samples and meteorites and its implications for Hf–W cosmochemistry. *Earth and Planetary Science Letters* 175: 1–12.
Lin Y, Guan Y, Leshin LA, Ouyang Z, and Daode W (2005) Short-lived chlorine-36 in a Ca- and Al-rich inclusion from the Ningqiang carbonaceous chondrite. *Proceedings of the National Academy of Sciences* 102: 1306–1311.
Liu M-C, Chaussidon M, Göpel C, and Lee T (2012a) A heterogeneous solar nebula as sampled by CM hibonite grains. *Earth and Planetary Science Letters* 327–328: 75–83.
Liu M-C, Chaussidon M, Srinivasan G, and McKeegan KD (2012b) A lower initial abundance of short-lived 41Ca in the early solar system and its implications for solar system formation. *The Astrophysics Journal* 761: 137 (7 pp).
Liu M-C, McKeegan KD, and Davis AM (2006) Magnesium isotopic compositions of CM hibonite grains. *Lunar and Planetary Science* 37: #2428.
Liu M-C, McKeegan KD, Davis AM, and Ireland TR (2008) Reevaluation of calcium-41 in CM and CV refractory inclusions. *Lunar and Planetary Science* 39: #1895.
Liu M-C, McKeegan KD, Goswami JN, et al. (2009) Isotopic records in CM hibonites: Implications for timescales of mixing of isotope reservoirs in the solar nebula. *Geochimica et Cosmochimica Acta* 73: 5051–5079.
Liu M-C, Nittler LR, Alexander CMO'D, and Lee T (2010) Lithium–beryllium–boron isotopic compositions in meteoritic hibonite: Implications for the origin of ^{10}Be and early solar system irradiation. *The Astrophysical Journal* 719: L99–L103.
Lugmair GW and Galer SJG (1992) Age and isotopic relationships among the angrites Lewis Cliff 86010 and Angra dos Reis. *Geochimica et Cosmochimica Acta* 56: 1673–1694.
Lugmair GW, Shimamura T, Lewis RS, and Anders E (1983) Samarium-146 in the early solar system: Evidence from neodymium in the Allende meteorite. *Science* 222: 1015–1018.
Lugmair GW and Shukolyukov A (1998) Early solar system timescales according to ^{53}Mn–^{53}Cr systematics. *Geochimica et Cosmochimica Acta* 62: 2863–2886.
Lugmair GW and Shukolyukov A (2001) Early solar system events and timescales. *Meteoritics and Planetary Science* 36: 1017–1026.
MacPherson GJ, Bullock ES, Janney PE, et al. (2010) Early solar nebula condensates with canonical, not supracanonical initial ^{26}Al/^{27}Al ratios. *The Astrophysical Journal* 711: L117–L121.
MacPherson GJ, Davis AM, and Zinner EK (1995) The distribution of aluminum-26 in the early solar system – A reappraisal. *Meteoritics* 30: 365–386.
MacPherson GJ, Huss GR, and Davis AM (2003) Extinct ^{10}Be in type A calcium–aluminum-rich inclusions from CV chondrites. *Geochimica et Cosmochimica Acta* 67: 3165–3179.
MacPherson GJ, Kita NT, Ushikubo T, Bullock ES, and Davis AM (2012) Well-resolved variations in the formation ages for Ca–Al-rich inclusions in the early solar system. *Earth and Planetary Science Letters* 331–332: 43–54.
Makide K, Nagashima K, Krot AN, Huss GR, Hutcheon ID, and Bischoff A (2009) Oxygen- and magnesium-isotope compositions of calcium–aluminum-rich inclusions from CR2 carbonaceous chondrites. *Geochimica et Cosmochimica Acta* 73: 5018–5050.
Makide K, Nagashima K, Krot AN, et al. (2011) Heterogeneous distribution of ^{26}Al at the birth of the solar system. *The Astrophysical Journal* 733: L31 (5 pp).
Marhas KK and Goswami JN (2003) Be–B systematics in CM and CV hibonites: Implications for solar energetic particle production of short-lived nuclides in the early solar system. *Lunar and Planetary Science* 34: #1303.
Marhas KK, Goswami JN, and Davis AM (2002) Short-lived nuclides in hibonite grains from Murchison: Evidence for solar system evolution. *Science* 298: 2182–2185.
Markowski A, Leya I, Quitté G, Ammon K, Halliday AN, and Wieler R (2006a) Correlated helium-3 and tungsten isotopes in iron meteorites: Quantitative cosmogenic corrections and planetesimal formation times. *Earth and Planetary Science Letters* 250: 104–115.
Markowski A, Quitté G, Halliday AN, and Kleine T (2006b) Tungsten isotopic compositions of iron meteorites: Chronological constraints vs. cosmogenic effects. *Earth and Planetary Science Letters* 242: 1–15.
Markowski A, Quitté G, Kleine T, Halliday AN, Bizzarro M, and Irving AJ (2007) Hafnium–tungsten chronometry of angrites and the earliest evolution planetary objects. *Earth and Planetary Science Letters* 262: 214–229.
McKeegan KD, Chaussidon M, and Robert F (2000a) Incorporation of short-lived Be-10 in a calcium–aluminum-rich inclusion from the Allende meteorite. *Science* 289: 1334–1337.
McKeegan KD, Greenwood JP, Leshin LA, and Cosarinsky M (2000b) Abundance of ^{26}Al in ferromagnesian chondrules of unequilibrated ordinary chondrites. *Lunar and Planetary Science* 31: #2009.
Meyer B and Clayton DD (2000) Short-lived radioactivities and the birth of the Sun. *Space Science Review* 92: 133–152.
Mishra RK, Goswami JN, Tachibana S, Huss GR, and Rudraswami NG (2010) ^{60}Fe and ^{26}Al in chondrules from unequilibrated chondrites: Implications for early solar system processes. *The Astrophysical Journal* 714: L217–L221.
Mostefaoui S, Kita NT, Togashi S, Tachibana S, Nagahara H, and Morishita Y (2002) The relative formation ages of ferromagnesian chondrules inferred from their initial aluminum-26/aluminum-27 ratios. *Meteoritics and Planetary Science* 37: 421–438.
Mostefaoui S, Lugmair GW, and Hoppe P (2005) ^{60}Fe: A heat source for planetary differentiation from a nearby supernova explosion. *The Astrophysical Journal* 625: 271–277.

Moynier F, Day JMD, Okui W, et al. (2012) Planetary-scale strontium isotopic heterogeneity and the age of volatile depletion of early solar system materials. *The Astrophysical Journal* 758: 45.

Moynier F, Yin Q-Z, and Jacobsen B (2007) Dating the first stage of planet formation. *The Astrophysical Journal* 671: L181–L183.

Münker C, Weyer S, Mezger K, Rehkämper M, Wombacher F, and Bischoff A (2000) ^{92}Nb–^{92}Zr and the early differentiation history of planetary bodies. *Science* 289: 1538–1542.

Murty SVS, Goswami JN, and Shukolyukov YA (1997) Excess Ar-36 in the Efremovka meteorite: A strong hint for the presence of Cl-36 in the early solar system. *The Astrophysical Journal* 475: L65–L68.

Niederer FR, Papanastassiou DA, and Wasserburg GJ (1980) Endemic isotopic anomalies in titanium. *The Astrophysical Journal* 240: L73–L77.

Nielsen SG, Rehkämper M, and Halliday AN (2006) Large thallium isotopic variations in iron meteorites and evidence for lead-205 in the early solar system. *Geochimica et Cosmochimica Acta* 70: 2643–2657.

Niemeyer S and Lugmair GW (1981) Ubiquitous isotopic anomalies in Ti from normal Allende inclusions. *Earth and Planetary Science Letters* 53: 211–225.

Nimmo F and Kleine T (2007) How rapidly did Mars accrete? Uncertainties in the Hf-W timing of core formation. *Icarus* 191: 497–504.

Nyquist LE, Kleine T, Shih C-Y, and Reese YD (2009) The distribution of short-lived radioisotopes in the early solar system and the chronology of asteroid accretion, differentiation, and secondary alteration. *Geochimica et Cosmochimica Acta* 73: 5115–5136.

Nyquist L, Lindstrom D, Mittlefehldt D, et al. (2001) Manganese–chromium formation intervals for chondrules from the Bishunpur and Chainpur meteorites. *Meteoritics and Planetary Science* 36: 911–938.

Nyquist LE, Reese Y, Wiesmann H, Shih C-Y, and Takeda H (2003) Fossil ^{26}Al and ^{53}Mn in the Asuka 881394 eucrite: evidence of the earliest crust on asteroids 4 Vesta. *Earth and Planetary Science Letters* 214: 11–25.

Ogliore RC, Huss GR, and Nagashima K (2011) Ratio estimation in SIMS analysis. *Nuclear Instruments and Methods in Physics Research Section B* 269: 1910–1918.

Papanastassiou DA (1986) Chromium isotopic anomalies in the Allende meteorite. *The Astrophysical Journal* 308: L27–L30.

Papanastassiou DA, Bogdanovski O, and Wasserburg GJ (2002) ^{53}Mn–^{53}Cr systematics in Allende refractory inclusions. *Meteoritics and Planetary Science* 37: A114.

Papanastassiou DA and Wasserburg GJ (1969) Initial strontium isotopic abundances and the resolution of small time differences in the formation of planetary objects. *Earth and Planetary Science Letters* 5: 361–376.

Pellas P, Fiéni C, Trieloff M, and Jessberger EK (1997) The cooling history of the Acapulco meteorite as recorded by the ^{244}Pu and ^{40}Ar–^{39}Ar chronometers. *Geochimica et Cosmochimica Acta* 61: 3477–3501.

Pellas P and Storzer D (1981) ^{244}Pu fission track thermometry and its application to stony meteorites. *Proceedings of the Royal Society of London* A374: 253–270.

Petaev MI and Jacobsen SB (2009) Petrologic study of SJ101, a new forsterite-bearing CAI from the Allende CV3 meteorite. *Geochimica et Cosmochimica Acta* 73: 5100–5114.

Petitat M, Birck J-L, Luu TH, and Gounelle M (2011a) The chromium isotopic composition of the ungrouped carbonaceous chondrite Tagish Lake. *The Astrophysical Journal* 736: 23 (8 pp).

Petitat M, Marrocchi Y, McKeegan KD, et al. (2011b) ^{53}Mn–^{53}Cr ages of Kaidun carbonates. *Meteoritics and Planetary Science* 46: 275–283.

Podosek FA and Cassen P (1994) Theoretical, observational, and isotopic estimates of the lifetime of the solar nebula. *Meteoritics* 29: 6–25.

Podosek FA and Nichols RH Jr. (1997) Short-lived radionuclides in the solar nebula. In: Bernatowicz TJ and Zinner E (eds.) *Astrophysical Implications of the Laboratory Study of Presolar Materials*, pp. 617–647. Woodbury: American Institute of Physics.

Podosek FA, Ott U, Brannon JC, et al. (1997) Thoroughly anomalous chromium in Orgueil. *Meteoritics and Planetary Science* 32: 617–627.

Podosek FA and Swindle TD (1988) Extinct radionuclides. In: Kerridge JF and Matthews MS (eds.) *Meteorites and the Early Solar System*, pp. 1093–1113. Tucson, AZ: University of Arizona Press.

Podosek FA, Zinner E, MacPherson GJ, Lundberg LL, Brannon JC, and Fahey AJ (1991) Correlated study of initial ^{87}Sr/^{86}Sr and Al–Mg isotopic systematics and petrologic properties in a suite of refractory inclusions from the Allende meteorite. *Geochimica et Cosmochimica Acta* 55: 1083–1110.

Preibisch T, Kim YC, Favata F, et al. (2005) The origin of T Tauri X-ray emission: New insights from the Chandra Orion Ultradeep Project. *The Astrophysics of Journal Supplement* 160: 401–422.

Prinzhofer A, Papanastassiou DA, and Wasserburg GJ (1989) The presence of ^{146}Sm in the early solar system and implications for its nucleosynthesis. *The Astrophysical Journal* 344: 81–84.

Qin L, Alexander CMO'D, Carlson RW, Horan MF, and Yokoyama T (2010a) Contributors to chromium isotope variation of meteorites. *Geochimica et Cosmochimica Acta* 74: 1122–1145.

Qin L, Carlson RW, and Alexander CMO'D (2011) Correlated nucleosynthetic isotopic variability in Cr, Sr, Ba, Sm, Nd and Hf in Murchison and QUE 97008. *Geochimica et Cosmochimica Acta* 75: 7806–7828.

Qin L, Dauphas N, Wadhwa M, Mazarik J, and Janney PE (2008a) Rapid accretion and differentiation of iron meteorite parent bodies inferred from ^{182}Hf–^{182}W chronometry and thermal modeling. *Earth and Planetary Science Letters* 273: 94–104.

Qin L, Dauphas N, Wadhwa M, et al. (2008b) Tungsten nuclear anomalies in planetesimal cores. *The Astrophysical Journal* 674: 1234–1241.

Qin L, Rumble D, Alexander CMO'D, Carlson RW, Jenniskens P, and Shaddad MH (2010b) The chromium isotopic composition of Almahatta Sitta. *Meteoritics and Planetary Science* 45: 1771–1777.

Quitté G, Birck J-L, and Allègre CJ (2000) ^{182}Hf–^{182}W systematics in eucrites: The puzzle of iron segregation in the early solar system. *Earth and Planetary Science Letters* 184: 16–25.

Quitté G, Birck J-L, and Allègre CJ (2005) Stony-iron meteorites: History of the metal phase according to tungsten isotopes. *Geochimica et Cosmochimica Acta* 69: 1321–1332.

Quitté G, Halliday AN, Meyer BS, Markowski A, Latkoczy C, and Günther D (2007) Correlated iron 60, nickel 62, and zirconium 96 in refractory inclusions and the origin of the solar system. *The Astrophysical Journal* 655: 678–684.

Quitté G, Latkoczy C, Schönbächler M, Halliday AN, and Günther D (2011) ^{60}Fe–^{60}Ni systematics in the eucrite parent body: A case study of Bouvante and Juvinas. *Geochimica et Cosmochimica Acta* 75: 7698–7706.

Quitté G, Markowski A, Latkoczy C, Gabriel A, and Pack A (2010) Iron-60 heterogeneity and incomplete isotope mixing in the early solar system. *The Astrophysical Journal* 720: 1215–1224.

Quitté G, Meier M, Latkoczy C, Halliday AN, and Günther D (2006) Nickel isotopes in iron meteorites – Nucleosynthetic anomalies in sulphides with no effects in metals and no trace of ^{60}Fe. *Earth and Planetary Science Letters* 242: 16–25.

Regelous M, Elliott T, and Coath CD (2008) Nickel isotope heterogeneity in the early solar system. *Earth and Planetary Science Letters* 272: 330–338.

Richter FM, Davis AM, DePaolo DJ, and Watson EB (2003) Isotope fractionation by chemical diffusion between molten basalt and rhyolite. *Geochimica et Cosmochimica Acta* 67: 3905–3923.

Richter FM, Davis AM, Ebel DS, and Hashimoto A (2002) Elemental and isotopic fractionation of Type B calcium-, aluminum-rich inclusions: Experiments, theoretical considerations, and constraints on their thermal evolution. *Geochimica et Cosmochimica Acta* 66: 521–540.

Richter S, Eykens R, Kühn H, Aregbe Y, Verbruggen A, and Weyer S (2010) New average values for the n(^{238}U)/n(^{235}U) isotope ratios of natural uranium standards. *International Journal of Mass Spectrometry* 295: 94–97.

Richter FM, Janney PE, Mendybaev RA, Davis AM, and Wadhwa M (2007) Elemental and isotopic fractionation of Type B CAI-like liquids by evaporation. *Geochimica et Cosmochimica Acta* 71: 5544–5564.

Rotaru M, Birck J-L, and Allègre CJ (1992) Clues to early solar system history from chromium isotopes in carbonaceous chondrites. *Nature* 358: 465–470.

Rudraswami NG and Goswami JN (2007) ^{26}Al in chondrules from unequilibrated L chondrites: Onset and duration of chondrule formation in the early solar system. *Earth and Planetary Science Letters* 257: 231–244.

Rudraswami NG, Goswami JN, Chattopadhyay B, Sengupta SK, and Thapliyal AP (2008) ^{26}Al records in chondrules from unequilibrated ordinary chondrites: II. Duration of chondrule formation and parent body thermal metamorphism. *Earth and Planetary Science Letters* 274: 93–102.

Rugel G, Faestermann T, Knie K, et al. (2009) New measurement of the ^{60}Fe half-life. *Physical Review Letters* 103: 072502.

Russell SS, Hartmann L, Cuzzi J, Krot AN, Gounelle M, and Weidenschilling S (2006) Timescales of the solar protoplanetary disk. In: Lauretta DS and McSween HY Jr. (eds.) *Meteorites and the Early Solar System II*, pp. 233–251. Tucson, AZ: University of Arizona Press.

Russell SS, Srinivasan G, Huss GR, Wasserburg GJ, and MacPherson GJ (1996) Evidence for widespread ^{26}Al in the solar nebula and constraints for nebula timescales. *Science* 273: 757–762.

Sahijpal S and Goswami JN (1998) Refractory phases in primitive meteorites devoid of ^{26}Al and ^{41}Ca: Representative samples of first solar system solids? *The Astrophysical Journal* 509: L137–L140.

Sahijpal S, Goswami JN, and Davis AM (2000) K, Mg, Ti, and Ca isotopic compositions and refractory trace element abundances in hibonites from CM and CV meteorites: Implications for early solar system processes. *Geochimica et Cosmochimica Acta* 64: 1989–2005.

Sahijpal S, Goswami JN, Davis AM, Grossman L, and Lewis RS (1998) A stellar origin for the short-lived nuclides in the early solar system. *Nature* 391: 559–561.
Sahijpal S and Soni P (2007) Numerical simulations of the production of extinct short-lived nuclides by magnetic flaring in the early solar system. *Meteoritics and Planetary Science* 42: 1005–1027.
Sanloup C, Blicher-Toft J, Télouk P, Gillet P, and Albarède F (2000) Zr isotope anomalies in chondrites and the presence of ^{92}Nb in the early solar system. *Earth and Planetary Science Letters* 184: 75–81.
Scherstén A, Elliott T, Hawkesworth C, Russell S, and Masarik J (2006) Hf–W evidence for rapid differentiation of iron meteorite parent bodies. *Earth and Planetary Science Letters* 241: 530–542.
Schiller M, Baker JA, and Bizzarro M (2010) ^{26}Al–^{26}Mg dating of asteroidal magmatism in the young solar system. *Geochimica et Cosmochimica Acta* 74: 4844–4864.
Schiller M, Baker J, Creech J, et al. (2011) Rapid timescales for magma ocean crystallization of the howardite-eucrite-diogenite parent body. *The Astrophysical Journal* 740: L22 (6 pp).
Schoenberg R, Kamber BS, Collerson KD, and Eugster O (2002) New W-isotope evidence for rapid terrestrial accretion and very early core formation. *Geochimica et Cosmochimica Acta* 66: 3151–3160.
Schönbächler J, Carlson RW, Horan MF, Mock TD, and Hauri E (2008) Silver isotope variations in chondrites: Volatile depletion and the initial ^{107}Pd abundance of the solar system. *Geochimica et Cosmochimica Acta* 72: 5330–5341.
Schönbächler M, Rehkämper M, Halliday AN, et al. (2002) Niobium–zirconium chronometry and early solar system development. *Science* 295: 1705–1708.
Schramm DN, Tera F, and Wasserburg GJ (1970) The isotopic abundance of ^{26}Mg and limits on ^{26}Al in the early solar system. *Earth and Planetary Science Letters* 10: 44–59.
Schulz T, Münker C, Mezger K, and Palme H (2010) Hf–W chronometry of primitive achondrites. *Geochimica et Cosmochimica Acta* 74: 1706–1718.
Schulz T, Münker C, Palme H, and Mezger K (2009) Hf–W chronometry of the IAB iron meteorite parent body. *Earth and Planetary Science Letters* 280: 185–193.
Schulz T, Upadhyay D, Münker C, and Mezger K (2012) Formation and exposure history of non-magmatic iron meteorites and winonaites: Clues from Sm and W isotopes. *Geochimica et Cosmochimica Acta* 85: 200–212.
Scott ERD and Sanders IS (2009) Implications of the carbonaceous chondrites Mn–Cr isochron for the formation of early refractory planetesimals and chondrules. *Geochimica et Cosmochimica Acta* 73: 5137–5149.
Shu FH, Adams FC, and Lizano S (1987) Star formation in molecular clouds: Observation and theory. *Annual Review of Astronomy and Astrophysics* 25: 23–81.
Shukolyukov A and Lugmair GW (1993a) Fe-60 in eucrites. *Earth and Planetary Science Letters* 119: 159–166.
Shukolyukov A and Lugmair GW (1993b) Live iron-60 in the early solar system. *Science* 259: 1138–1142.
Shukolyukov A and Lugmair GW (1998) Isotopic evidence for the Cretaceous-Tertiary impactor and its type. *Science* 282: 927–929.
Shukolyukov A and Lugmair GW (2006) Manganese-chromium isotope systematics of carbonaceous chondrites. *Earth and Planetary Science Letters* 250: 200–213.
Simon JI and Young ED (2011) Resetting, errorchrons and the meaning of canonical CAI initial ^{26}Al/^{27}Al values. *Earth and Planetary Science Letters* 304: 468–482.
Snyder GA, Lee D-C, Ruzicka AM, Prinz M, Taylor LA, and Halliday AN (2001) Hf–W, Sm–Nd, and Rb–Sr isotopic evidence of late impact fractionation and mixing of silicates on iron meteorite parent bodies. *Earth and Planetary Science Letters* 186: 311–324.
Spivak-Birndorf L, Wadhwa M, and Janney P (2009) ^{26}Al–^{26}Mg systematics in D'Orbigny and Sahara 99555 angrites: Implications for high-resolution chronology using extinct chronometers. *Geochimica et Cosmochimica Acta* 73: 5202–5211.
Spivak-Birndorf L, Wadhwa M, and Janney P (2011) ^{60}Fe–^{60}Ni chronology of the D'Orbigny angrite: Implications for the initial solar system abundance of ^{60}Fe. *Lunar and Planetary Science* 42: #2281.
Spivak-Birndorf L, Wadhwa M, and Janney P (2012) ^{60}Fe–^{60}Ni systematics of Chainpur chondrules and the plutonic angrites Northwest Africa 4590 and 4801. *Lunar and Planetary Science* 43: #2861.
Srinivasan G (2001) Be–B isotope systematics in CAI E65 from Efremovka CV3 chondrite. *Meteoritics and Planetary Science* 36: A195–A196.
Srinivasan G, Goswami JN, and Bhandari N (1999) Al-26 in eucrite Piplia Kalan: Plausible heat source and formation chronology. *Science* 284: 1348–1350.
Srinivasan G, Sahijpal S, Ulyanov AA, and Goswami JN (1996) Ion microprobe studies of Efremovka CAIs: Potassium isotope composition and ^{41}Ca in the early solar system. *Geochimica et Cosmochimica Acta* 60: 1823–1835.
Srinivasan G, Ulyanov AA, and Goswami JN (1994) ^{41}Ca in the early solar system. *The Astrophysical Journal* 431: L67–L70.
Srinivasan G, Whitehouse MJ, Weber I, and Yamaguchi A (2007) The crystallization age of eucrite zircon. *Science* 317: 345–347.
Stewart BW, Papanastassiou DA, and Wasserburg GJ (1994) Sm–Nd chronology and petrogenesis of mesosiderites. *Geochimica et Cosmochimica Acta* 58: 3487–3509.
Sugiura N and Krot AN (2007) ^{26}Al–^{26}Mg systematics of Ca–Al-rich inclusions, amoeboid olivine aggregates, and chondrules from the ungrouped carbonaceous chondrites Acfer 094. *Meteoritics and Planetary Science* 42: 1183–1195.
Sugiura N, Shuzou Y, and Ulyanov A (2001) Beryllium–boron and aluminum–magnesium chronology of calcium–aluminum-rich inclusions in CV chondrites. *Meteoritics and Planetary Science* 36: 1397–1408.
Swindle TD, Caffee MW, Hohenberg CM, Lindstrom MM, and Taylor GJ (1991) Iodine–xenon studies of petrographically and chemically characterized Chainpur chondrules. *Geochimica et Cosmochimica Acta* 55: 861–880.
Swindle TD, Davis AM, Hohenberg CM, MacPherson GJ, and Nyquist LE (1996) Isotopic constraints on the timing of the formation of solids in the solar nebula. In: Hewins RH, Jones RH, and Scott ERD (eds.) *Chondrules and the Protoplanetary Disk*, pp. 77–86. Cambridge: Cambridge University Press.
Tachibana S and Huss GR (2003) The initial abundance of ^{60}Fe in the solar system. *The Astrophysical Journal* 588: L41–L44.
Tachibana S, Huss GR, Kita NT, Shimoda G, and Morishita Y (2006) ^{60}Fe in chondrites: Debris from a nearby supernova in the early solar system? *The Astrophysical Journal* 639: L87–L90.
Tang H and Dauphas N (2011) Constraints from achondrites on the initial ^{60}Fe/^{56}Fe ratio of the solar system. *Lunar and Planetary Science* 42: #1068.
Tang H and Dauphas N (2012) Abundance, distribution, and origin of ^{60}Fe in the solar protoplanetary disk. *Earth and Planetary Science Letters* 359–360: 248–263.
Telus M, Huss GR, Nagashima K, Ogliore RC, and Tachibana S (2012) Reevaluating our understanding of the ^{60}Fe–^{60}Ni system in chondrites. *Lunar and Planetary Science* 43: #2733.
Tera F and Carlson RW (1999) Assessment of the Pb–Pb and U–Pb chronometry of the early solar system. *Geochimica et Cosmochimica Acta* 63: 1877–1889.
Tera F and Wasserburg GJ (1972) U–Th–Pb systematics in three Apollo 14 basalts and the problem of initial lead in lunar rocks. *Earth and Planetary Science Letters* 14: 281–304.
Theis KJ, Schönbächler M, Benedix GK, Rehkämper M, Andreasen R, and Davies C (2013) Palladium-silver chronology of IAB iron meteorites. *Earth and Planetary Science Letters* 361: 402–411.
Thrane K, Bizzarro M, and Baker JA (2006) Extremely brief formation interval for refractory inclusions and uniform distribution of ^{26}Al in the early solar system. *The Astrophysical Journal* 646: L159–L162.
Tilton GR (1988) Age of the solar system. In: Kerridge JF and Matthews MS (eds.) *Meteorites and the Early Solar System*, pp. 259–275. Tucson, AZ: University of Arizona Press.
Touboul M, Kleine T, and Bourdon B (2008) Hf–W systematics of cumulate eucrites and the chronology of the eucrite parent body. *Lunar and Planetary Science* 39: #2336.
Touboul M, Kleine T, Bourdon B, Palme H, and Wieler R (2007) Late formation and prolonged differentiation of the Moon inferred from W isotopes in lunar metals. *Nature* 450: 1206–1209.
Touboul M, Kleine T, Bourdon B, Palme H, and Wieler R (2009a) Tungsten isotopes in ferroan anorthosites: Implications for the age of the Moon and lifetime of its magma ocean. *Icarus* 199: 245–249.
Touboul M, Kleine T, Bourdon B, Van Orman JA, Maden C, and Zipfel J (2009b) Hf–W thermochronometry: II. Accretion and thermal history of the acapulcoite-lodranite parent body. *Earth and Planetary Science Letters* 284: 168–178.
Touboul M, Puchtel IS, and Walker RJ (2012) ^{182}W evidence for long-term preservation of early mantle differentiation products. *Science* 335: 1065–1069.
Trinquier A, Birck J-L, and Allègre CJ (2007) Widespread ^{54}Cr heterogeneity in the inner solar system. *The Astrophysical Journal* 655: 1179–1185.
Trinquier A, Birck J-L, Allègre CJ, Göpel C, and Ulfbeck D (2008) ^{53}Mn–^{53}Cr systematics of the early solar system revisited. *Geochimica et Cosmochimica Acta* 72: 5146–5163.
Trinquier A, Elliott T, Ulfbeck D, Coath C, Krot AN, and Bizzarro M (2009) Origin of nucleosynthetic isotope heterogeneity in the solar protoplanetary disk. *Science* 324: 374–376.
Villeneuve J, Chaussidon M, and Libourel G (2009) Homogeneous distribution of ^{26}Al in the solar system from the Mg isotopic composition of chondrules. *Science* 325: 985–988.
Villeneuve J, Chaussidon M, and Libourel G (2011) Magnesium isotopes constraints on the origin of Mg-rich olivines from the Allende chondrite: Nebular versus planetary? *Earth and Planetary Science Letters* 301: 107–116.
Wadhwa M, Amelin Y, Bogdanovski O, Shukoluyukov A, Lugmair GW, and Janney P (2009) Ancient relative and absolute ages for a basaltic meteorite: Implications for timescales of planetesimals accretion and differentiation. *Geochimica et Cosmochimica Acta* 73: 5189–5201.
Wadhwa M, Amelin Y, Davis AM, et al. (2006a) From dust to planetesimals: Implications for the solar protoplanetary disk from short-lived radionuclides.

In: Reipurth B, Jewitt D, and Keil K (eds.) *Protostars and Planets V*, pp. 835–848. Tucson, AZ: University of Arizona Press.
Wadhwa M and Lugmair GW (1996) Age of the eucrite 'Caldera' from convergence of long-lived and short-lived chronometers. *Geochimica et Cosmochimica Acta* 60: 4889–4893.
Wadhwa M and Russell SS (2000) Timescales of accretion and differentiation in the early solar system: The meteoritic evidence. In: Mannings V, Boss AP, and Russell SS (eds.) *Protostars and Planets IV*, pp. 995–1018. Tucson, AZ: University of Arizona Press.
Wadhwa M, Srinivasan G, and Carlson RW (2006b) Timescales of planetary differentiation in the early solar system. In: Lauretta DS and McSween HY Jr. (eds.) *Meteorites and the Early Solar System II*, pp. 715–731. Tucson, AZ: University of Arizona Press.
Wadhwa M, Zinner EK, and Crozaz G (1997) Manganese–chromium systematics in sulfides of unequilibrated enstatite chondrites. *Meteoritics and Planetary Science* 32: 281–292.
Wasserburg GJ (1985) Short-lived nuclei in the early solar system. In: Black DC and Matthews MS (eds.) *Protostars and Planets II*, pp. 703–737. Tucson, AZ: University of Arizona Press.
Wasserburg GJ, Busso M, and Gallino R (1996) Abundances of actinides and short-lived nonactinides in the interstellar medium: Diverse supernova sources for the r-processes. *The Astrophysical Journal* 466: L109–L113.
Wasserburg GJ, Busso M, Gallino R, and Nollett KM (2006) Short-lived nuclei in the early solar system: Possible AGB sources. *Nuclear Physics A* 77: 5–69.
Wasserburg GJ, Busso M, Gallino R, and Raiteri CM (1994) Asymptotic giant branch stars as a source of short-lived radioactive nuclei in the solar nebula. *The Astrophysical Journal* 424: 412–428.
Wasserburg GJ and Papanastassiou DA (1982) Some short-lived nuclides in the early solar system – A connection with the placental ISM. In: Schramm DN (ed.) *Essays in Nuclear Astrophysics*, pp. 77–140. Cambridge: Cambridge University Press.
Wasserburg GJ, Wimpenny J, and Yin Q-Z (2011) Mg isotopic heterogeneity, Al–Mg isochrons, and canonical $^{26}Al/^{27}Al$ in the early solar system. In: *Formation of the First Solids in the Solar System*. Houston, TX: The Lunar and Planetary Institute LPI Contribution No. 1639, #9038.
Wetherill GW (1956) Discordant uranium-lead ages. *Transactions, American Geophysical Union* 37: 320–326.
Weyer S, Anbar AD, Gerdes A, Gordon GW, Algeo TJ, and Boyle EA (2008) Natural fractionation of $^{238}U/^{235}U$. *Geochimica et Cosmochimica Acta* 72: 345–359.
Whitby J, Burgess R, Turner G, Gilmour J, and Bridges J (2000) Extinct ^{129}I in halite from a primitive meteorite: Evidence for evaporite formation in the early solar system. *Science* 288: 1819–1821.
Whitby J, Gilmour J, Turner G, Prinz M, and Ash RD (2001) Iodine–xenon dating of chondrules from the Quinzhen and Kota Kota enstatite chondrites. *Geochimica et Cosmochimica Acta* 66: 347–359.
Wiechert U, Halliday AN, Lee D-C, Snyder GA, Taylor LA, and Rumble D (2001) Oxygen isotopes and the Moon-forming giant impact. *Science* 294: 345–348.
Wielandt D, Nagashima K, Krot AN, Huss GR, Ivanova MA, and Bizzarro M (2012) Evidence for multiple sources of ^{10}Be in the early solar system. *The Astrophysical Journal* 748: L25.
Willbold M, Elliott T, and Moorbath S (2011) The tungsten isotopic composition of the Earth's mantle before the terminal bombardment. *Nature* 477: 195–198.
Williams JP and Cieza LA (2011) Protoplanetary disks and their evolution. *Annual Review of Astronomy and Astrophysics* 49: 67–117.
Yamakawa A, Yamashita K, Makishima A, and Nakamura E (2010) Chromium isotope systematics of achondrites: Chronology and isotopic heterogeneity of the inner solar system bodies. *The Astrophysical Journal* 720: 150–154.
Yamashita K, Maruyama S, Yamakawa A, and Nakamura E (2010) ^{53}Mn–^{53}Cr chronometry of CB chondrite: Evidence for uniform distribution of ^{53}Mn in the early solar system. *The Astrophysical Journal* 723: 20–24.
Yin Q-Z, Jacobsen SB, McDonough WF, and Horn I (2000) Supernova sources and the ^{92}Nb–^{92}Zr *p*-process chronometer. *The Astrophysical Journal* 535: L49–L53.
Yin Q-Z, Jacobsen B, Moynier F, and Hutcheon ID (2007) Toward consistent chronology in the early solar system: High-resolution ^{53}Mn–^{53}Cr chronometry for chondrules. *The Astrophysical Journal* 662: L43–L46.
Yin Q-Z, Jacobsen SB, Yamashita K, Blichert-Toft J, Télouk P, and Albarède F (2002) A short timescale for terrestrial planet formation from Hf–W chronometry of meteorites. *Nature* 418: 949–952.
Young ED and Galy A (2004) The isotope geochemistry and cosmochemistry of magnesium. *Reviews in Mineralogy and Geochemistry* 55: 197–230.
Young ED, Galy A, and Nagahara H (2002) Kinetic and equilibrium mass-dependent isotope fractionation laws in nature and their geochemical and cosmochemical significance. *Geochimica et Cosmochimica Acta* 66: 1095–1104.
Young ED, Simon JI, Galy A, Russell SS, Tonui E, and Lovera O (2005) Supra-canonical $^{26}Al/^{27}Al$ and the residence time of CAIs in the solar protoplanetary disk. *Science* 308: 223–227.
Yurimoto H and Wasson JT (2002) Extremely rapid cooling of a carbonaceous-chondrite chondrule containing very ^{16}O-rich olivine and a ^{26}Mg-excess. *Geochimica et Cosmochimica Acta* 66: 4355–4363.
Zhang J, Dauphas N, Davis AM, Leya I, and Fedkin A (2012) The proto-Earth as a significant source of lunar material. *Nature Geoscience* 5: 251–255.
Zinner E (1998) Stellar nucleosynthesis and the isotopic composition of presolar grains from primitive meteorites. *Annual Review of Earth and Planetary Science* 26: 147–188.
Zinner E, Fahey AJ, Goswami JN, Ireland TR, and McKeegan KD (1986) Large ^{48}Ca anomalies are associated with ^{50}Ti anomalies in Murchison and Murray hibonites. *The Astrophysical Journal* 311: L103–L107.